

QA: QA

**VALIDATION TEST PLAN (VTP)  
for the  
FEHM Application Version 2.21**

**STN: 10086-2.21-00**

**REV. NO. 00**

**DOCUMENT ID: 10086-VTP-2.21-00**

**August 2003**

**Effective date**

**Prepared by:**

\_\_\_\_\_  
**Zora V. Dash**

**Los Alamos National Laboratory, EES-6**

\_\_\_\_\_  
**Date**

**Verified by:**

\_\_\_\_\_  
**Myles Fitzgerald**

**Los Alamos National Laboratory, EES-9**

\_\_\_\_\_  
**Date**

\_\_\_\_\_  
**Fred Pollock**

**Bechtel SAIC, LLC**

**Software Independent Verification & Validation**

\_\_\_\_\_  
**Date**

**Los Alamos National Laboratory**

*Copyright, 2003, The Regents of the University of California.*

*This program was prepared by the Regents of the University of California at Los Alamos National Laboratory (the University) under contract No. W-7405-ENG-36 with the U.S. Department of Energy (DOE). All rights in the program are reserved by the DOE and the University. Permission is granted to the public to copy and use this software without charge, provided that this Notice and any statement of authorship are reproduced on all copies. Neither the U.S. Government nor the University makes any warranty, express or implied, or assumes any liability or responsibility for the use of this software.*

**CHANGE HISTORY**

<b><u>Revision Number</u></b>	<b><u>Effective Date</u></b>	<b><u>Description of and Reason for Revision</u></b>
00	8/19/03	Initial revision, based on AP-SI.1Q.

## TABLE OF CONTENTS

LIST OF FIGURES .....	8
LIST OF TABLES.....	10
1.0 OVERVIEW of REQUIREMENTS.....	12
1.1 PURPOSE .....	12
1.2 FUNCTIONAL DESCRIPTION.....	12
1.3 ASSUMPTIONS AND LIMITATIONS .....	17
2.0 TEST STEP DESCRIPTION.....	18
2.1 Testing of Thermodynamic Functions .....	21
2.1.1 Purpose .....	21
2.1.2 Functional Description .....	21
2.1.3 Assumptions and Limitations .....	21
2.1.4 Summary of Test Cases .....	22
2.2 Test of Heat Conduction.....	25
2.2.1 Purpose .....	25
2.2.2 Functional Description .....	25
2.2.3 Assumptions and Limitations .....	25
2.2.4 Summary of Test Cases .....	27
2.3 Test of Temperature in a Wellbore.....	30
2.3.1 Purpose .....	30
2.3.2 Functional Description .....	30
2.3.3 Assumptions and Limitations .....	30
2.3.4 Summary of Test Cases .....	30
2.4 Test of Hydraulic Head.....	33
2.4.1 Purpose .....	33
2.4.2 Functional Description .....	33
2.4.3 Assumptions and Limitations .....	33
2.4.4 Summary of Test Cases .....	34
2.4.5 Acknowledgement .....	35
2.5 Test of Pressure Transient Analysis.....	36
2.5.1 Purpose .....	36
2.5.2 Functional Description .....	36
2.5.3 Assumptions and Limitations .....	36
2.5.4 Summary of Test Cases .....	37
2.6 Test of Simplified Water Table Calculations.....	39
2.6.1 Purpose .....	39
2.6.2 Functional Description .....	39
2.6.3 Assumptions and Limitations .....	39
2.6.4 Summary of Test Cases .....	39

2.7	Test of Infiltration into a One-Dimensional, Layered, Unsaturated Fractured Medium . . . . .	42
2.7.1	Purpose . . . . .	42
2.7.2	Functional Description . . . . .	42
2.7.3	Assumptions and Limitations . . . . .	42
2.7.4	Summary of Test Cases . . . . .	45
2.8	Test of Vapor Extraction from an Unsaturated Reservoir . . . . .	47
2.8.1	Purpose . . . . .	47
2.8.2	Functional Description . . . . .	47
2.8.3	Assumptions and Limitations . . . . .	47
2.8.4	Summary of Test Cases . . . . .	49
2.9	Test of Barometric Pumping Mechanisms . . . . .	51
2.9.1	Purpose . . . . .	51
2.9.2	Functional Description . . . . .	51
2.9.3	Assumptions and Limitations . . . . .	51
2.9.4	Summary of Test Cases . . . . .	54
2.9.5	Acknowledgement . . . . .	55
2.10	Test of Dual Porosity . . . . .	56
2.10.1	Purpose . . . . .	56
2.10.2	Functional Description . . . . .	56
2.10.3	Assumptions and Limitations . . . . .	56
2.10.4	Summary of Test Cases . . . . .	58
2.11	Test of Heat and Mass Transfer in Porous Media . . . . .	60
2.11.1	Purpose . . . . .	60
2.11.2	Functional Description . . . . .	60
2.11.3	Assumptions and Limitations . . . . .	60
2.11.4	Summary of Test Cases . . . . .	61
2.12	Test of Free Convection . . . . .	63
2.12.1	Purpose . . . . .	63
2.12.2	Functional Description . . . . .	63
2.12.3	Assumptions and Limitations . . . . .	63
2.12.4	Summary of Test Cases . . . . .	64
2.12.5	Acknowledgement . . . . .	65
2.13	Test of Toronyi Two-Phase Problem . . . . .	67
2.13.1	Purpose . . . . .	67
2.13.2	Functional Description . . . . .	67
2.13.3	Assumptions and Limitations . . . . .	67
2.13.4	Summary of Test Cases . . . . .	67
2.14	Test of DOE Code Comparison Project Problem Five, Case A . . . . .	70
2.14.1	Purpose . . . . .	70
2.14.2	Functional Description . . . . .	70
2.14.3	Assumptions and Limitations . . . . .	70
2.14.4	Summary of Test Cases . . . . .	70
2.15	Test of Heat Pipe . . . . .	73
2.15.1	Purpose . . . . .	73
2.15.2	Functional Description . . . . .	73

2.15.3	Assumptions and Limitations . . . . .	73
2.15.4	Summary of Test Cases . . . . .	73
2.16	Test of Dry-Out of a Partially Saturated Medium . . . . .	76
2.16.1	Purpose . . . . .	76
2.16.2	Functional Description . . . . .	76
2.16.3	Assumptions and Limitations . . . . .	76
2.16.4	Summary of Test Cases . . . . .	78
2.17	Test of One Dimensional Reactive Solute Transport . . . . .	80
2.17.1	Purpose . . . . .	80
2.17.2	Functional Description . . . . .	80
2.17.3	Assumptions and Limitations . . . . .	80
2.17.4	Summary of Test Cases . . . . .	80
2.18	Test of Henry's Law Species . . . . .	83
2.18.1	Purpose . . . . .	83
2.18.2	Functional Description . . . . .	83
2.18.3	Assumptions and Limitations . . . . .	83
2.18.4	Summary of Test Cases . . . . .	83
2.19	Test of Fracture Transport with Matrix Diffusion . . . . .	87
2.19.1	Purpose . . . . .	87
2.19.2	Functional Description . . . . .	87
2.19.3	Assumptions and Limitations . . . . .	87
2.19.4	Summary of Test Cases . . . . .	89
2.20	Test of the Movement of a Dissolved Mineral Front . . . . .	93
2.20.1	Purpose . . . . .	93
2.20.2	Functional Description . . . . .	93
2.20.3	Assumptions and Limitations . . . . .	93
2.20.4	Summary of Test Cases . . . . .	94
2.21	Test of Multi-Solute Transport with Chemical Reaction . . . . .	96
2.21.1	Purpose . . . . .	96
2.21.2	Functional Description . . . . .	96
2.21.3	Assumptions and Limitations . . . . .	96
2.21.4	Summary of Test Cases . . . . .	97
2.22	Test of Three-Dimensional Radionuclide Transport . . . . .	99
2.22.1	Purpose . . . . .	99
2.22.2	Functional Description . . . . .	99
2.22.3	Assumptions and Limitations . . . . .	99
2.22.4	Summary of Test Cases . . . . .	99
2.23	Test of Streamline Particle Tracking Model . . . . .	102
2.23.1	Purpose . . . . .	102
2.23.2	Functional Description . . . . .	102
2.23.3	Assumptions and Limitations . . . . .	103
2.23.4	Summary of Test Cases . . . . .	109
2.24	Test of Cell-Based Particle Tracking Model . . . . .	114
2.24.1	Purpose . . . . .	114
2.24.2	Functional Description . . . . .	114

2.24.3	Assumptions and Limitations . . . . .	114
2.24.4	Summary of Test Cases . . . . .	115
3.0	INSTRUCTIONS for EXECUTION of TEST CASES. . . . .	122
4.0	REFERENCES . . . . .	125
APPENDIX: FEHM VALIDATION SCRIPTS . . . . .		128
A.	Description of Scripts . . . . .	128
B.	Installation . . . . .	131
C.	Customization of Scripts for Local Environment. . . . .	131
D.	Using the Validation Scripts . . . . .	132
E.	Assumptions and Limitations . . . . .	132
F.	FEHM_VVSECT.pl . . . . .	133
G.	Example of Run Comparison Script . . . . .	138
H.	Execution Log. . . . .	139
I.	Summary Report . . . . .	140
J.	List of Files in the Verification Archive . . . . .	142

**LIST OF FIGURES**

Figure 1.	Schematic diagrams of 2-D and 3-D heat conduction problems. . . . .	26
Figure 2.	Geometric configurations tested by the 2-D heat conduction problem. . . . .	27
Figure 3.	Geometric elements tested by the 3-D heat conduction problem. . . . .	29
Figure 4.	Schematic drawing of the problem geometry and boundary conditions for the temperature in a wellbore problem. . . . .	31
Figure 5.	Schematic drawing of the problem geometry and boundary conditions for the head pressure problem. . . . .	33
Figure 6.	Schematic drawing of the problem geometry and boundary conditions for the transient pressure problem. . . . .	36
Figure 7.	Schematic drawing of the problem geometry and boundary conditions for the simplified water table problem. . . . .	40
Figure 8.	Schematic drawing of the problem geometry for the one-dimensional infiltration test problem. . . . .	43
Figure 9.	Schematic diagram of the geometry and boundary conditions for the vapor extraction problem. . . . .	48
Figure 10.	Schematic diagram of pore-scale velocity (1a) and contaminant transport (1b) verification models. . . . .	52
Figure 11.	Schematic diagram of the geometry and boundary conditions for the dual porosity problem. . . . .	57
Figure 12.	Schematic diagram of the Avdonin problem geometry. . . . .	61
Figure 13.	Schematic diagram of 2-D free convection problems. . . . .	63
Figure 14.	Plot of Nu vs Ra for air and water from FEHM simulations for determination of Rac . . . . .	65
Figure 15.	Solution domain and saturation results for the Toronyi problem. . . . .	68
Figure 16.	Schematic diagram of the geometry and boundary conditions for the DOE code comparison project problem. . . . .	71
Figure 17.	Schematic diagram of the geometry and boundary conditions for the Heat Pipe Problem. . . . .	74



Figure 18. Schematic drawing of the geometry and boundary conditions for the Dry-Out Simulations. . . . .	77
Figure 19. Schematic drawing of the geometry and boundary conditions for the 1-D reactive tracer transport problem. . . . .	80
Figure 20. Schematic drawing of the geometry and boundary conditions for the Henry's Law species tests. . . . .	83
Figure 21. Schematic drawing of the geometry and boundary conditions for the fracture transport problem. . . . .	89
Figure 22. Schematic drawing of the geometry and boundary conditions for the calcite dissolution problem. . . . .	93
Figure 23. Aqueous and mineral front profiles modeled by the analytical solution. . . .	94
Figure 24. Schematic drawing of the geometry and boundary conditions for the cobalt transport problem. . . . .	96
Figure 25. Model domain and flow boundary conditions for the radionuclide transport test problem. . . . .	100
Figure 26. Model domain and flow boundary conditions for the streamline particle tracking standard dispersion model test problems. . . . .	103
Figure 27. Model domain and flow boundary conditions for the streamline particle tracking reverse tracking model test problems. . . . .	104
Figure 28. Model domain and flow boundary conditions for the streamline particle tracking test of the divergence of the dispersion tensor model. . . . .	105
Figure 29. Model domain and flow boundary conditions for the cell-based particle tracking test problems. . . . .	115
Figure 30. FEHM solution for cumulative breakthrough concentration versus time. .	121
Figure 31. Illustration of code execution and terminal output for the Avdonin test problem . . . . .	122
Figure 32. Diagram of verification directory structure . . . . .	130

**LIST OF TABLES**

Table I.	Functional Requirements of the FEHM Application . . . . .	12
Table II.	FEHM Macro Control Statements Used by Test Problems . . . . .	14
Table III.	Test Results Log. . . . .	19
Table IV.	Input Parameters for the 2-D and 3-D Heat Conduction Problems . . . . .	26
Table V.	Input Parameters for the Temperature in a Wellbore Problem. . . . .	32
Table VI.	Input Parameters for the Head Pressure Problem . . . . .	34
Table VII.	Input Parameters for the Transient Pressure Problem. . . . .	37
Table VIII.	Input Parameters for the Simplified Water Table Problem . . . . .	41
Table IX.	Input Parameters for the One-dimensional Infiltration Problem . . . . .	43
Table X.	Input Parameters for the Vapor Extraction Problem. . . . .	48
Table XI.	Input Parameters for the Barometric Pumping Problem. . . . .	53
Table XII.	Input Parameters for the Dual Porosity Problems . . . . .	57
Table XIII.	Input Parameters for the Avdonin Problem . . . . .	62
Table XIV.	Input Parameters for the 2-D Free Convection Problem . . . . .	66
Table XV.	Input Parameters for the Toronyi Two-Phase Problem . . . . .	69
Table XVI.	Input Parameters for the DOE Code Comparison Project, Problem 5, Case A 72	
Table XVII.	Input Parameters for the Heat Pipe Problem . . . . .	75
Table XVIII.	Input Parameters for the Dry-Out Simulations . . . . .	77
Table XIX.	Input Parameters for the 1-D Reactive Tracer Transport Problem. . . . .	81
Table XX.	Adsorption Parameters for the Reactive Tracer Transport Problem . . . . .	81
Table XXI.	Input Parameters for the Henry's Law Species Tests . . . . .	84
Table XXII.	Adsorption, Henry's Law, and Reaction Parameters for the Henry's Law Species Tests. . . . .	85

Table XXIII. Input Parameters for the Fracture Transport with Matrix Diffusion Test Problem . . . . .	90
Table XXIV. Adsorption Parameters for the Fracture Transport Problem . . . . .	91
Table XXV. Input Parameters for the Calcite Dissolution Problem . . . . .	95
Table XXVI. Input Parameters for the Multi-Solute Reactive Transport Test Problem . .	98
Table XXVII. Input Parameters and Conditions for the Radionuclide Transport Test Problem . . . . .	101
Table XXVIII. Input Parameters and Conditions for the Streamline Particle Tracking Test Problems . . . . .	106
Table XXIX. Analytical Values for Standard Deviation at $6.949 \times 10^8$ days . . . . .	111
Table XXX. Input Parameters and Conditions for the Cell-Based Particle Tracking Test Problems . . . . .	116
Table XXXI. Scripts and Support Programs for Verification Operations. . . . .	128

## 1.0 OVERVIEW of REQUIREMENTS

### 1.1 PURPOSE

The goal of this validation effort is to test the options and features of the FEHM application that satisfy the requirements specified in the Software Requirements Document for the FEHM Application Version 2.21 (FEHM RD, 10086-RD-2.21-00). This document details the test cases to be performed, many of which were developed for prior versions of FEHM (Zyvoloski, et al., 1992, Zyvoloski and Dash, 1991), and lists the acceptance criteria that must be satisfied.

### 1.2 FUNCTIONAL DESCRIPTION

The overall validation effort for the **FEHM** application consists of rigorous and complete testing of the model, whenever possible, against known analytical solutions of the same problem. An alternative approach for more complex test cases for which no analytical solution exists is to benchmark the code against the results of other numerical models. Thermodynamic properties will be compared with tables maintained by the National Bureau of Standards (Harr et al., 1984).

These simulations will encompass the options and features of FEHM that will be used in actual simulations of flow and transport in the unsaturated zone, and in modeling and interpreting pressure transient tests, temperature logs, and tracer tests (both conservative and reactive tracers) performed in the saturated zone. The overall verification of FEHM will be accomplished by comparison of results with the published analytical solutions and results from other codes. Because of the nonlinear nature of the water and steam properties, additional verification of the thermodynamics package is included.

The verification test cases in Section 2.0 are organized in groups based on the functions and features being tested, and include: testing of the thermodynamic functions (Section 2.1); heat transfer tests (Sections 2.2 and 2.3); isothermal fluid flow tests (Sections 2.4 - 2.10); combined heat and mass transfer tests (Sections 2.11 - 2.16); and solute transport tests (Sections 2.17 - 2.24). Table I provides a summary of the FEHM requirements and a listing of which problems test them.

**Table I. Functional Requirements of the FEHM Application**

Requirement	RD Section	Tested by (VTP Section <sup>†</sup> )
Finite-Element Coefficient Generation	2.2	2.2, 2.3, 2.4, 2.5, 2.6, 2.7, 2.8, 2.9, 2.10, 2.11, 2.12, 2.13, 2.14, 2.15, 2.16, 2.17, 2.18, 2.19, 2.20, 2.21, 2.22, 2.23, 2.24
Formulate Transient Equations	2.3	
Heat-conduction equations	2.3.1	2.2
Heat- and mass-transfer equations	2.3.2	2.3, 2.4, 2.5, 2.6, 2.7, 2.10, 2.11, 2.12, 2.13, 2.14, 2.15
Noncondensable gas flow equations	2.3.3	2.8, 2.9, 2.12, 2.16
Solute-transport equations	2.3.4	2.9, 2.17, 2.18, 2.19, 2.20, 2.21, 2.22
Cell-based particle-tracking module	2.3.5	2.24

**Table I. Functional Requirements of the FEHM Application (Continued)**

Requirement	RD Section	Tested by (VTP Section <sup>†</sup> )
Streamline particle-tracking module	2.3.6	2.23
Sources and sinks	2.3.7	2.3, 2.4, 2.5, 2.6, 2.7, 2.8, 2.9, 2.10, 2.11, 2.13, 2.14, 2.16, 2.17, 2.18, 2.19, 2.20, 2.21, 2.22, 2.23, 2.24
Apply Constitutive Relationships	2.4	
Pressure- and temperature-dependent water properties	2.4.1	2.1, 2.3, 2.4, 2.5, 2.10, 2.11, 2.12, 2.13, 2.14, 2.15
Properties of air and air/water vapor mixtures	2.4.2	2.6, 2.8, 2.9, 2.12, 2.15, 2.16
Equation-of-state models	2.4.3	2.9
Relative-permeability and capillary-pressure functions	2.4.4	2.6, 2.7, 2.8, 2.9, 2.12, 2.13, 2.14, 2.15, 2.16, 2.18, 2.22
Adsorbing solutes	2.4.5	2.17, 2.18, 2.19, 2.23, 2.24
Multiple, interacting solutes	2.4.6	2.18, 2.20, 2.21, 2.22, 2.24
Dual-porosity formulation	2.4.7	2.10
Generalized dual-porosity formulation	2.4.8	2.19
Double-porosity/double-permeability formulation	2.4.9	2.7
Stress-dependent properties	2.4.10	To be developed
Variable thermal conductivity	2.4.11	To be developed
Mass transport at interfaces	2.4.12	To be developed
Compute Solution to Transient Equations	2.5	2.2, 2.3, 2.4, 2.5, 2.6, 2.7, 2.8, 2.9, 2.10, 2.11, 2.12, 2.13, 2.14, 2.15, 2.16, 2.17, 2.18, 2.19, 2.20, 2.21, 2.22, 2.23, 2.24
Implement time-step mechanism	2.5.1	
Solve nonlinear equation set at each time step	2.5.2	
Provide Input/Output Data Files	2.6	2.2, 2.3, 2.4, 2.5, 2.6, 2.7, 2.8, 2.9, 2.10, 2.11, 2.12, 2.13, 2.14, 2.15, 2.16, 2.17, 2.18, 2.19, 2.20, 2.21, 2.22, 2.23, 2.24
Inputs	2.6.2	
Outputs	2.6.4	
Provide Restart Capability	2.7	
Write information needed for restart to output file	2.7.1	2.22, 2.23, 2.24
Read information needed for restart from restart file	2.7.2	2.14, 2.22, 2.23, 2.24
Resume the calculation	2.7.3	2.14, 2.22, 2.23, 2.24

**Table I. Functional Requirements of the FEHM Application (Continued)**

Requirement	RD Section	Tested by (VTP Section <sup>‡</sup> )
Provide Multiple Realization Option	2.8	2.9 (Done in conjunction with automated testing)
Interface with GoldSim	2.9	2.24 (Windows only)
INPUT AND OUTPUT REQUIREMENTS	3.0	See “Provide Input/Output Data Files”, “Inputs”, and “Outputs” above.

<sup>‡</sup>VTP Sections

- 2.1 Testing of Thermodynamic Functions
- 2.2 Test of Heat Conduction
- 2.3 Test of Temperature in a Wellbore
- 2.4 Test of Hydraulic Head
- 2.5 Test of Pressure Transient Analysis
- 2.6 Test of Simplified Water Table Calculations
- 2.7 Test of Infiltration into a One-Dimensional, Layered, Unsaturated Fractured Medium
- 2.8 Test of Vapor Extraction from an Unsaturated Reservoir
- 2.9 Test of Barometric Pumping Mechanisms
- 2.10 Test of Dual Porosity
- 2.11 Test of Heat and Mass Transfer in Porous Media
- 2.12 Test of Free Convection
- 2.13 Test of Toronyi Two-Phase Problem
- 2.14 Test of DOE Code Comparison Project Problem Five, Case A
- 2.15 Test of Heat Pipe
- 2.16 Test of Dry-Out of a Partially Saturated Medium
- 2.17 Test of One Dimensional Reactive Solute Transport
- 2.18 Test of Henry's Law Species
- 2.19 Test of Fracture Transport with Matrix Diffusion
- 2.20 Test of the Movement of a Dissolved Mineral Front
- 2.21 Test of Multi-Solute Transport with Chemical Reaction
- 2.22 Test of Three-Dimensional Radionuclide Transport
- 2.23 Test of Streamline Particle Tracking Model
- 2.24 Test of Cell-Based Particle Tracking Model

Table II summarizes the input design elements (macro control statements) that are tested by the simulations. A cross-reference to the users manual where the macros are fully described is also provided.

**Table II. FEHM Macro Control Statements Used by Test Problems**

Control Statement	UM Section	Used by (VTP Section)
<b>file</b>	6.2.4	2.23.4.4, 2.24
<b>adif</b>	6.2.5	2.15
<b>airwater</b>	6.2.6	2.4, 2.6, 2.7, 2.8, 2.9, 2.18, 2.22, 2.23.4.4
<b>boun</b>	6.2.7	2.6, 2.7.4.2, 2.9, 2.12

**Table II. FEHM Macro Control Statements Used by Test Problems (Continued)**

Control Statement	UM Section	Used by (VTP Section)
<b>bous</b>	6.2.8	2.23.4.4, use of " <b>head</b> " (2.4, 2.6) also enables this option
<b>cden</b>	6.2.9	Not used
<b>cond</b>	6.2.10	2.2, 2.3, 2.5, 2.10, 2.11, 2.12, 2.13, 2.14, 2.15, 2.16, 2.17, 2.18, 2.19, 2.20, 2.21, 2.22, 2.23, 2.24
<b>cont</b>	6.2.11	2.2, 2.3, 2.4, 2.5, 2.6, 2.7, 2.8, 2.9, 2.11, 2.12, 2.13, 2.14, 2.16, 2.18, 2.20
<b>coor</b>	6.2.12	2.2, 2.3, 2.4, 2.5, 2.7, 2.8, 2.9, 2.10, 2.11, 2.12, 2.13, 2.14, 2.15, 2.16, 2.17, 2.18, 2.19, 2.20, 2.21, 2.22, 2.23, 2.24
<b>ctrl</b>	6.2.13	2.2, 2.3, 2.4, 2.5, 2.6, 2.7, 2.8, 2.9, 2.10, 2.11, 2.12, 2.13, 2.14, 2.15, 2.16, 2.17, 2.18, 2.19, 2.20, 2.21, 2.22, 2.23, 2.24
<b>dpdp</b>	6.2.14	2.7
<b>dual</b>	6.2.15	2.10
<b>dvel</b>	6.2.16	Not used
<b>elem</b>	6.2.17	2.2, 2.3, 2.4, 2.5, 2.7, 2.8, 2.9, 2.10, 2.11, 2.12, 2.13, 2.14, 2.15, 2.16, 2.17, 2.18, 2.19, 2.20, 2.21, 2.22, 2.23, 2.24
<b>eos</b>	6.2.18	2.9
<b>exrl</b>	6.2.19	Not used
<b>fdm</b>	6.2.20	2.6, 2.13, 2.15
<b>finv</b>	6.2.21	2.2.4.2
<b>flow</b>	6.2.22	2.2, 2.3, 2.4, 2.5, 2.6, 2.7, 2.8, 2.10, 2.11, 2.13, 2.14, 2.16, 2.17, 2.18, 2.19, 2.20, 2.21, 2.22, 2.23, 2.24
<b>flo2</b>	6.2.23	Not used
<b>flo3</b>	6.2.24	2.6
<b>floa</b>	6.2.25	Not used
<b>flxo</b>	6.2.26	2.9, 2.15
<b>flxz</b>	6.2.27	2.6
<b>fper</b>	6.2.28	Not used
<b>frlp</b>	6.2.29	Not used
<b>gdpm</b>	6.2.30	2.19.4.4
<b>grad</b>	6.2.31	2.12, 2.15
<b>head</b>	6.2.32	2.4, 2.6, 2.23.4.4
<b>hflx</b>	6.2.33	2.12, 2.15, 2.16

**Table II. FEHM Macro Control Statements Used by Test Problems (Continued)**

Control Statement	UM Section	Used by (VTP Section)
<b>hyco</b>	6.2.34	Not used
<b>ice or meth</b>	6.2.35	Not used
<b>impf</b>	6.2.36	Not used
<b>init</b>	6.2.37	2.2, 2.3, 2.5, 2.10, 2.11, 2.13, 2.14, 2.17, 2.19, 2.20, 2.21, 2.22, 2.24
<b>isot</b>	6.2.38	2.23.4.4
<b>iter</b>	6.2.39	2.4, 2.6, 2.7, 2.8, 2.9, 2.10, 2.12, 2.15, 2.16, 2.20, 2.21, 2.22, 2.23
<b>itfc</b>	6.2.40	Not used
<b>itup</b>	6.2.41	2.6, 2.16, 2.22
<b>iupk</b>	6.2.42	Not used
<b>mdnode</b>	6.2.43	Not used
<b>mptr</b>	6.2.44	2.24.4.3, 2.24.4.5
<b>ngas</b>	6.2.45	2.12, 2.15, 2.16
<b>nobr</b>	6.2.46	Not used
<b>node</b>	6.2.47	2.2, 2.3, 2.5, 2.6, 2.7, 2.8, 2.9, 2.10, 2.11, 2.12, 2.13, 2.14, 2.15, 2.16, 2.17, 2.18, 2.19, 2.20, 2.21, 2.22, 2.23, 2.24
<b>nod2</b>	6.2.48	Not used
<b>nod3</b>	6.2.49	Not used
<b>perm</b>	6.2.50	2.2, 2.3, 2.4, 2.5, 2.6, 2.7, 2.8, 2.9, 2.10, 2.11, 2.12, 2.13, 2.14, 2.15, 2.16, 2.17, 2.18, 2.19, 2.20, 2.21, 2.22, 2.23, 2.24
<b>pest</b>	6.2.51	Not used
<b>ppor</b>	6.2.52	Not used
<b>pres</b>	6.2.53	2.4, 2.6, 2.7, 2.8, 2.9, 2.12, 2.13, 2.15, 2.16, 2.18, 2.22, 2.23
<b>ptrk</b>	6.2.54	2.24.4.1
<b>renu</b>	6.2.55	Not used
<b>rflo</b>	6.2.56	Not used
<b>rlp</b>	6.2.57	2.6, 2.7, 2.8, 2.9, 2.12, 2.13, 2.14, 2.15, 2.16, 2.18, 2.22
<b>rock</b>	6.2.58	2.2, 2.3, 2.4, 2.5, 2.6, 2.7, 2.8, 2.9, 2.10, 2.11, 2.12, 2.13, 2.14, 2.15, 2.16, 2.17, 2.18, 2.19, 2.20, 2.21, 2.22, 2.23, 2.24
<b>rxn</b>	6.2.59	2.20, 2.21, 2.22
<b>sol</b>	6.2.60	2.2, 2.3, 2.4, 2.5, 2.6, 2.7, 2.8, 2.9, 2.10, 2.11, 2.12, 2.13, 2.14, 2.15, 2.16, 2.17, 2.18, 2.19, 2.20, 2.21, 2.22, 2.23, 2.24



**Table II. FEHM Macro Control Statements Used by Test Problems (Continued)**

Control Statement	UM Section	Used by (VTP Section)
<b>sptr</b>	6.2.61	2.23
<b>stop</b>	6.2.62	2.2, 2.3, 2.4, 2.5, 2.6, 2.7, 2.8, 2.10, 2.11, 2.12, 2.13, 2.14, 2.15, 2.16, 2.17, 2.18, 2.19, 2.20, 2.21, 2.22, 2.23, 2.24
<b>subm</b>	6.2.63	Not used
<b>svar</b>	6.2.64	Not used
<b>szna or napl</b>	6.2.65	Not used
<b>text</b>	6.2.66	2.7, 2.12, 2.15, 2.22
<b>thic</b>	6.2.67	Not used
<b>time</b>	6.2.68	2.2, 2.3, 2.4, 2.5, 2.6, 2.7, 2.8, 2.9, 2.10, 2.11, 2.12, 2.13, 2.14, 2.15, 2.16, 2.17, 2.18, 2.19, 2.20, 2.21, 2.22, 2.23, 2.24
<b>trac</b>	6.2.69	2.9.4.2, 2.17, 2.18, 2.19, 2.20, 2.21, 2.22
<b>user</b>	6.2.70	Not used
<b>vapl</b>	6.2.71	2.16
<b>vcon</b>	6.2.72	Not used
<b>wtsi</b>	6.2.73	2.6
<b>zone</b>	6.2.73	2.2, 2.3, 2.4, 2.6, 2.7, 2.11, 2.12, 2.13, 2.15, 2.22, 2.23
<b>zonn</b>	6.2.75	Not used

### 1.3 ASSUMPTIONS AND LIMITATIONS

The validation effort assumes that the FEHM application is installed on Sun Ultra SPARCstations running running Solaris 7 or later (UNIX) and PC platforms running Windows 2000 or later or Linux 2.4.18 or later and that dynamic memory allocation is supported.

In completing the validation testing of FEHM results from FEHM are compared to results obtained from analytical solutions and several alternate flow and transport codes. We do not rerun those alternate codes or recompute analytical solutions when verifying the newest version of FEHM but instead use results (data tables) obtained from them when the test problems were first developed. Data tables from alternate flow and transport codes are used for 2.7 Test of Infiltration into a One-Dimensional, Layered, Unsaturated Fractured Medium (TOUGH2), 2.17 Test of One Dimensional Reactive Solute Transport (SORBEQ), 2.21 Test of Multi-Solute Transport with Chemical Reaction (PDREACT), 2.22 Test of Three-Dimensional Radionuclide Transport (TRACRN), and 2.24 Test of Cell-Based Particle Tracking Model (CHAIN).

When comparing against an analytical solution or other code, it is assumed that close agreement between FEHM and the analytical solution or alternate model results constitutes a verification of both. Different mathematical procedures

giving the same result is what is expected and desired, but only if the code is performing properly. Fortuitous agreement between models using entirely different mathematical solution procedures is judged to be extremely unlikely.

The acceptance criteria are based on maximum error, percent error, or root mean square (RMS) error. These are standard error measures used in mathematics and physical sciences. The RMS error indicates average error over the solution domain, while the maximum and percent errors represent the largest errors in the domain. The maximum error is defined to be the absolute value of the maximum difference (error) between the values of the FEHM solution ( $FS$ ) and the analytical or alternate model solution ( $AS$ ) where the error between each point is computed as  $Error = abs(AS - FS)$ . The percent error ( $PE$ ) is defined as the error divided by the the analytical or alternate model solution times 100 and is computed for each point using  $PE = abs\left(\frac{AS - FS}{AS}\right) \times 100$ . The  $RMS$  error is calculated using the

following  $RMS = \sqrt{\sum \left(\frac{AS - FS}{AS}\right)^2} / \text{Number of points compared}$ .

## 2.0 TEST STEP DESCRIPTION

The tests outlined in this section will apply in their entirety to any version of the code, no matter what platform is being used. In general, the results from different platforms/compilers should be identical to within three significant digits, since differences in machine precision should be the only differences in the versions. The results for problems using random functions (i.e., streamline particle tracking simulations) may vary to a greater extent due to differences in implementation of random number generators, but will still meet the specified acceptance criteria. Table III provides a log for tracking test status when executing the test suite.

<b>Table III. Test Results Log</b>			
Test Identifier and Description	Pass	Fail	Initial & Date
2.1 Testing of Thermodynamic Functions Enthalpy Density Compressibility Viscosity Saturation Pressure and Temperature			
2.2 Test of Heat Conduction 2-D Heat Conduction 3-D Heat Conduction			
2.3 Test of Temperature in a Wellbore Injection into a Wellbore			
2.4 Test of Hydraulic Head Head Pressure			
2.5 Test of Pressure Transient Analysis Radial Flow from a Well			
2.6 Test of Simplified Water Table Calculations Simplified Water Table			
2.7 Test of Infiltration into a One-Dimensional, Layered, Unsaturated Fractured Medium Infiltration using ECM Infiltration using DKM			
2.8 Test of Vapor Extraction from an Unsaturated Reservoir Vapor Extraction			
2.9 Test of Barometric Pumping Mechanisms Pore-scale Velocity Contaminant Mass Transfer			
2.10 Test of Dual Porosity Dual Porosity			
2.11 Test of Heat and Mass Transfer in Porous Media Heat and Mass Transfer			
2.12 Test of Free Convection 2-D Free Convection in a Square			
2.13 Test of Toronyi Two-Phase Problem Toronyi Two-Phase			
2.14 Test of DOE Code Comparison Project Problem Five, Case A DOE Code Comparison			
2.15 Test of Heat Pipe Thermal Hydrologic Heat Pipe Problem			

Table III. Test Results Log			
Test Identifier and Description	Pass	Fail	Initial & Date
2.16 Test of Dry-Out of a Partially Saturated Medium Dry-Out Without Vapor Pressure Lowering Dry-Out With Vapor Pressure Lowering			
2.17 Test of One Dimensional Reactive Solute Transport Reactive Tracer Transport			
2.18 Test of Henry's Law Species Air Movement Water Movement			
2.19 Test of Fracture Transport with Matrix Diffusion Transport with Matrix Diffusion, No Sorption Transport with Matrix Diffusion, Sorption in the Matrix Transport with Matrix Diffusion, Sorption in the Fracture and Matrix Generalized Dual Porosity			
2.20 Test of the Movement of a Dissolved Mineral Front Calcite Dissolution			
2.21 Test of Multi-Solute Transport with Chemical Reaction Cobalt Transport			
2.22 Test of Three-Dimensional Radionuclide Transport Decay Chain Transport			
2.23 Test of Streamline Particle Tracking Model Breakthrough Curve In Situ Concentration Profile Generalized Dispersion Tensor Reverse Tracking Model Particle Capture Model Divergence of Dispersion Tensor Model			
2.24 Test of Cell-Based Particle Tracking Model Breakthrough Curve Breakthrough Curve, Dual Permeability Model Breakthrough Curves for Decay-Chain GoldSim/FEHM Interface Breakthrough Curve, Dual Permeability Mode, Multispecies			

## 2.1 Testing of Thermodynamic Functions

### 2.1.1 Purpose

Density, viscosity, and enthalpy are strong functions of pressure ( $P$ ) and temperature ( $T$ ). Because FEHM is an implicit code which uses a Newton-Raphson iteration, derivatives of the thermodynamic functions with respect to  $P$  and  $T$  are also required. The equations for all water properties listed in Section 2.1.4 will be evaluated over the range of pressure and temperature for which they were created.

The equation for the saturation line is important for the determination of the phase state of the liquid vapor system. The saturation functions will also be evaluated over the range of pressure and temperature for which they were created.

### 2.1.2 Functional Description

The test suite consists of a set of simple programs that call the FEHM thermodynamic functions with pressures and temperatures in the prescribed ranges. An agreement of FEHM and the National Bureau of Standards Steam Tables (Harr et al., 1984), with a deviation of less than 2%, over the entire range of temperatures and pressures tested, will constitute a verification of the FEHM thermodynamics functions.

### 2.1.3 Assumptions and Limitations

The FEHM thermodynamics functions were created for a specific range of temperatures and pressures, and the tests are conducted only within the stipulated range. Valid ranges for testing of each function are given below under Required Inputs. The FEHM code, however, will function over the entire range of pressures ( $0.001 \leq P \leq 110.0$  MPa) and temperatures ( $0.001 \leq T \leq 360$  °C) specified in the FEHM RD (10086-RD-2.21-00). If more precision is required than attainable with the builtin functions, the code provides an option for user defined equation of state data.

It is not practical to validate the functions for all pressures and temperatures in the specified ranges, so the testing was restricted to the following values of pressure and temperature for the thermodynamic functions:  $P = 0.001, 1, 5 - 100$  in increments of 5, and 110 MPa,  $T = 20 - 360$  in increments of 20 °C. Testing of the compressibility functions was restricted to the following values of pressure and temperature:

$P = 0.001, 5 - 105$  in increments of 5 MPa,  $T = 20.0, 100.0, 200, 360$  °C. Testing of the saturation functions were restricted to the following values of pressure and temperature:  $P = 0.122813\text{e-}02, 0.233883\text{e-}02, 0.424550\text{e-}02, 0.738139\text{e-}02, 0.123445\text{e-}01, 0.199322\text{e-}01, 0.311758\text{e-}01, 0.473731\text{e-}01, 0.701172\text{e-}01, 0.101322, 0.143241, 0.198483, 0.270020, 0.475717, 1.00193, 1.90617, 3.34467, 5.49987, 8.58378, 12.8525, 14.5941$ MPa,  $T = 10 - 340$  in increments of 10 °C.

The thermodynamics functions are being tested independently of the FEHM code so do not test code response when Pressures or Temperatures are out of range. For further discussion of code behavior in these cases see the "Models and Methods Summary" and "Software Design Document" of the FEHM Application (Zyvoloski et al. 1999).

## 2.1.4 Summary of Test Cases

### 2.1.4.1 Enthalpy

2.1.4.1.1 Function Tested. This test verifies that the rational polynomial expression implemented in FEHM correctly computes the enthalpy as a function of pressure and temperature.

2.1.4.1.2 Test Scope. This test is a verification test.

2.1.4.1.3 Requirements Tested. Requirement 2.4.1, "Pressure- and temperature-dependent water properties," of the FEHM RD is verified by this test.

2.1.4.1.4 Required Inputs. The pressures ( $P$ ) and temperatures ( $T$ ) at which to calculate enthalpy are required: for liquid enthalpies, the range of  $0.001 \leq P \leq 110.0$  MPa and  $15 \leq T \leq 360$  °C, for vapor enthalpies, the range of  $0.001 \leq P \leq 20.0$  MPa and  $15 \leq T \leq 360$  °C.

2.1.4.1.5 Expected Outputs. Values for enthalpy from the FEHM thermodynamics functions will be output and compared to values obtained from the National Bureau of Standards Steam Tables. Values within 2% of the Steam Tables data will be considered acceptable.

Required output files for these tests are the:

- FEHM thermodynamics function values files  
(*thermo\_liq.fehm*, *thermo\_vap.fehm*)

### 2.1.4.2 Density

2.1.4.2.1 Function Tested. This test verifies that the rational polynomial expression implemented in FEHM correctly computes the density as a function of pressure and temperature.

2.1.4.2.2 Test Scope. This test is a verification test.

2.1.4.2.3 Requirements Tested. Requirement 2.4.1, "Pressure- and temperature-dependent water properties," of the FEHM RD is verified by this test.

2.1.4.2.4 Required Inputs. The pressures ( $P$ ) and temperatures ( $T$ ) at which to calculate density are required: for liquid densities, the range of  $0.001 \leq P \leq 110.0$  MPa and  $15 \leq T \leq 360$  °C, for vapor densities, the range of  $0.001 \leq P \leq 20.0$  MPa and  $15 \leq T \leq 360$  °C.

2.1.4.2.5 Expected Outputs. Values for density from the FEHM thermodynamics functions will be output and compared to values obtained from the National Bureau of Standards Steam Tables. Values within 2% of the Steam Tables data will be considered acceptable.

Required output files for these tests are the:

- FEHM thermodynamics function values files  
(*thermo\_liq.fehm*, *thermo\_vap.fehm*)

### 2.1.4.3 Compressibility (Derivative of Density with Respect to Pressure)

2.1.4.3.1 Function Tested. This test verifies that the rational polynomial expression implemented in FEHM correctly computes the compressibility (derivative of density with respect to pressure) as a function of pressure and temperature.

2.1.4.3.2 Test Scope. This test is a verification test.

2.1.4.3.3 Requirements Tested. Requirement 2.4.1, "Pressure- and temperature-dependent water properties," of the FEHM RD is verified by this test.

2.1.4.3.4 Required Inputs. The pressures ( $P$ ) and temperatures ( $T$ ) at which to calculate compressibility are required: for liquid compressibilities, the range of  $0.001 \leq P \leq 110.0$  MPa and  $15 \leq T \leq 360$  °C, for vapor compressibilities, the range of  $0.001 \leq P \leq 20.0$  MPa and  $15 \leq T \leq 360$  °C.

2.1.4.3.5 Expected Outputs. Values for compressibility from the FEHM thermodynamics functions will be output and compared to values obtained from the National Bureau of Standards Steam Tables. Compressibility is a commonly used property of the fluid but does not appear directly in the equations that are solved and does not affect the solution. The compressibility is not directly derived from the Steam Tables data, but is computed from the derivative of the density function. Therefore, a root mean square error of the difference between the FEHM thermodynamics function data and the National Bureau of Standards Steam Table data less than or equal to 0.02 will be considered acceptable.

Required output files for these tests are the:

- FEHM thermodynamics function values files  
(*compress\_liq.fehm*, *compress\_vap.fehm*)

### 2.1.4.4 Viscosity

2.1.4.4.1 Function Tested. This test verifies that the rational polynomial expression implemented in FEHM correctly computes the viscosity as a function of pressure and temperature.

2.1.4.4.2 Test Scope. This test is a verification test.

2.1.4.4.3 Requirements Tested. Requirement 2.4.1, "Pressure- and temperature-dependent water properties," of the FEHM RD is verified by this test.

2.1.4.4.4 Required Inputs. The pressures ( $P$ ) and temperatures ( $T$ ) at which to calculate viscosity are required: for liquid viscosities, the range of  $0.001 \leq P \leq 110.0$  MPa and  $15 \leq T \leq 360$  °C, for vapor viscosities, the range of  $0.001 \leq P \leq 20.0$  MPa and  $15 \leq T \leq 360$  °C.

2.1.4.4.5 Expected Outputs. Values for viscosity from the FEHM thermodynamics functions will be output and compared to values obtained from the National Bureau of Standards Steam

Tables. Values within 2% of the Steam Tables data will be considered acceptable.

Required output files for these tests are the:

- FEHM thermodynamics function values files  
(*thermo\_liq.fehm*, *thermo\_vap.fehm*)

#### **2.1.4.5 Saturation Pressure and Temperature**

**2.1.4.5.1 Function Tested.** This test verifies that the rational polynomial expression implemented in FEHM correctly computes the pressure as a function of saturation temperature and temperature as a function of saturation pressure.

**2.1.4.5.2 Test Scope.** This test is a verification test.

**2.1.4.5.3 Requirements Tested.** Requirement 2.4.2, "Properties of air and air/water vapor mixtures," of the FEHM RD is verified by this test.

**2.1.4.5.4 Required Inputs.** The temperatures ( $T$ ) at which to calculate saturation pressure and pressure ( $P$ ) for which to calculate saturation temperature, in the range of  $0.00123 \leq P \leq 14.59410$  MPa and  $10 \leq T \leq 340$  °C.

**2.1.4.5.5 Expected Outputs.** Values for saturation pressure and temperature from the FEHM saturation functions will be output and compared to values obtained from the National Bureau of Standards Steam Tables. Values within 2% of the Steam Tables data will be considered acceptable.

Required output files for these tests are the:

- FEHM saturation function value files (*sat\_pressures.fehm*, *sat\_temperatures.fehm*)



## 2.2 Test of Heat Conduction

### 2.2.1 Purpose

Though simple heat conduction simulations without flow are not used in the modeling studies of Yucca Mountain, heat transfer is an important process in many calculations, including potential repository heating calculations. Furthermore, it is convenient to use the analytical solutions available for 2-D and 3-D heat conduction in solids. The solutions give an excellent check on the purely geometric aspects of the code as well as the finite element representation of second order partial differential equations.

The code will be checked against both 2-D and 3-D analytical solutions with regular grid spacing for triangular, rectangular, prism, brick, tetrahedral, and mixed elements. All solutions will be for linear (constant parameter) problems.

### 2.2.2 Functional Description

The test suite consists of a set of simulations with heat conduction only that model the same problem using different finite element meshes. In addition to demonstrating that the heat conduction problem has been correctly formulated, it will demonstrate that the various element types have been correctly implemented.

### 2.2.3 Assumptions and Limitations

The analytical solutions for 2-D and 3-D Heat Conduction are provided by Carslaw and Jaeger (1959). For 2-dimensional heat conduction in a rectangle the analytical solution takes the form

$$T = T_s + \frac{16(T_0 - T_s)}{\pi^2} \left( \sum_{m=0}^{\infty} \sum_{n=0}^{\infty} \frac{(-1)^{m+n}}{(2m+1)(2n+1)} \cos \frac{(2m+1)\pi x}{2a} \cos \frac{(2n+1)\pi y}{2b} e^{-\alpha_{m,n} t} \right)$$

where  $\alpha_{m,n} = \frac{\kappa\pi^2}{4} \left[ \frac{(2m+1)^2}{a^2} + \frac{(2n+1)^2}{b^2} \right]$  and

the region is taken to be  $-a < x < a, -b < y < b$ .

Extended to 3-dimensional heat conduction in a cube

$$T = T_s + \frac{64(T_0 - T_s)}{\pi^3} \left( \sum_{l=0}^{\infty} \sum_{m=0}^{\infty} \sum_{n=0}^{\infty} \frac{(-1)^{l+m+n}}{(2l+1)(2m+1)(2n+1)} \cos \frac{(2l+1)\pi x}{2a} \cos \frac{(2m+1)\pi y}{2b} \cos \frac{(2n+1)\pi z}{2c} e^{-\alpha_{l,m,n} t} \right)$$

where  $\alpha_{l,m,n} = \frac{\kappa\pi^2}{4} \left[ \frac{(2l+1)^2}{a^2} + \frac{(2m+1)^2}{b^2} + \frac{(2n+1)^2}{c^2} \right]$  and

the rectangular region is taken to be  $-a < x < a, -b < y < b, -c < z < c$ .

A sensitivity study of the number of terms required for the solution to achieve a precision of  $10^{-3}$  °C shows that up to 30 terms ( $l, m, n$ ) are needed when  $t < 2000$  s, and that no more than 10 terms are needed for  $t \geq 2000$  s.

Heat conduction in a solid 1 meter square/cube with an initial temperature,  $T_0 = 200^\circ\text{C}$ , is modeled after a temperature,  $T_s = 100^\circ\text{C}$ , is imposed on all surfaces at time,  $t = 0$ . Due to symmetry only a quarter of the square, or an eighth of the cube (0.5 meters on a side) needs to be modeled (see Fig. 1).

Table IV summarizes the rock properties and problem dimensions used for the heat conduction problem.

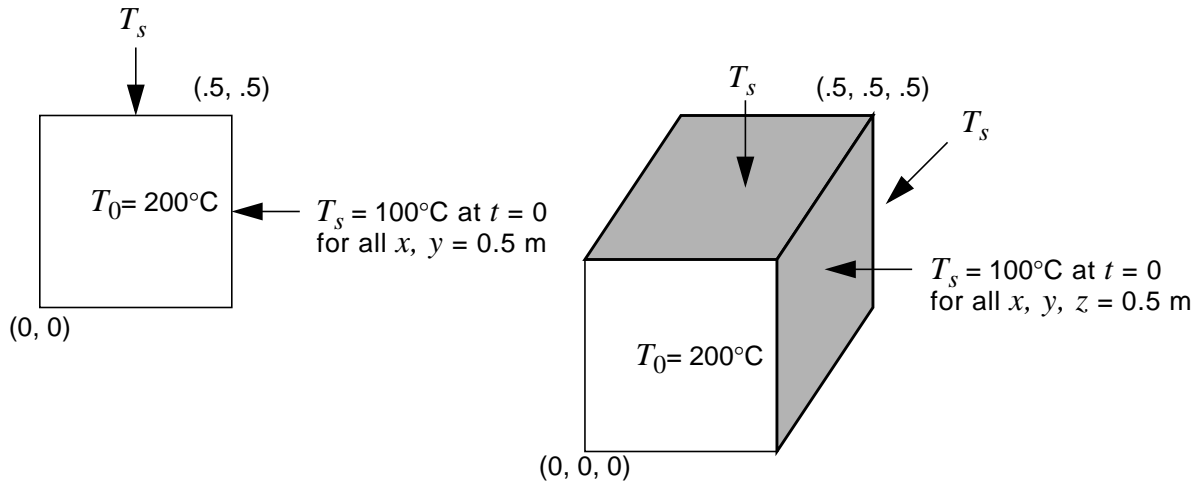


**Figure 1. Schematic diagrams of 2-D and 3-D heat conduction problems.**

**Table IV. Input Parameters for the 2-D and 3-D Heat Conduction Problems**

Parameter	Symbol	Value
Rock thermal conductivity	$\kappa_r$	$2.7 \frac{\text{W}}{\text{m} \cdot \text{K}}$
Rock density	$\rho_r$	$2700 \text{ kg/m}^3$
Rock specific heat	$C_r$	$1000 \frac{\text{J}}{\text{kg} \cdot \text{K}}$
Rock thermal diffusivity	$\kappa = \frac{\kappa_r}{\rho_r C_r}$	$10^{-6} \text{ m}^2/\text{s}$
Width	$a$	0.5 m
Length	$b$	0.5 m
Height	$c$	0.5 m
Node spacing	$\Delta x, \Delta y, \Delta z$	0.05 m
Time step	$\Delta t$	0.005 days
Total elapsed time	$t$	4 days (2-D) 3 days (3-D)
Initial temperature	$T_0$	200 °C
Boundary conditions: At $x, y, z = 0.5$ m, $T_s(t) = 100^\circ\text{C}$		

## 2.2.4 Summary of Test Cases

### 2.2.4.1 2-D Heat Conduction in a Square

2.2.4.1.1 Function Tested. This test verifies that FEHM correctly models 2-dimensional heat conduction. It also verifies that the finite element representation of 2-D 3-node triangles (triangular element meshes), 4-node quadrilaterals (rectangular element meshes), mixed element meshes (containing both triangular and rectangular elements), and refined element meshes (containing rectangular and trapezoidal elements) have been correctly implemented (see Fig. 2).

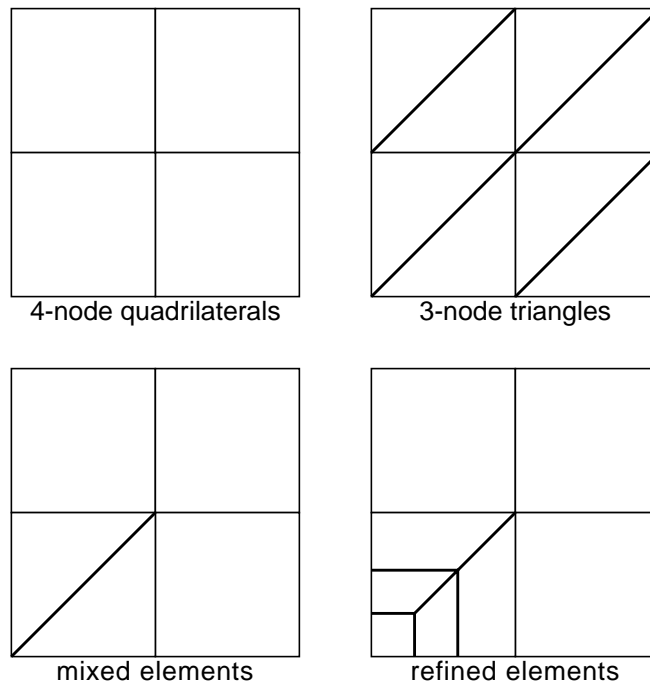


**Figure 2. Geometric configurations tested by the 2-D heat conduction problem.**

2.2.4.1.2 Test Scope. This test case is a verification test.

2.2.4.1.3 Requirements Tested. Requirements 2.2, “Finite-Element Coefficient Generation,” 2.3, “Formulate Transient Equations,” specifically Section 2.3.1, 2.5, “Compute Solution to Transient Equations,” and 2.6, “Provide Input/Output Data Files,” of the FEHM RD are verified by this test.

2.2.4.1.4 Required Inputs. Input is provided in the following files:

- *heat2d.in*: Basic input data file used in conjunction with the following geometry data files
- *heat2d.geom.2d\_tri*: 3-node triangles (121 nodes, 200 elements),
- *heat2d.geom.2d\_quad*: 4-node quadrilaterals (121 nodes, 100 elements),

- *heat2d.geom.2d\_mix*: mixed elements, 3-node triangles and 4-node quadrilaterals (121 nodes, 104 elements), or
- *heat2d.geom.2d\_ref*: refined elements, 4-node quadrilaterals with refinement about the node at  $x = y = 0$  m (127 nodes, 104 elements).

2.2.4.1.5 Expected Outputs. Values from FEHM for temperature change versus time at the center of the square ( $x = y = 0$  m) and values for temperature versus position ( $x = y$ ) at a specified time (time = 0.25 days) will be output and compared to the analytical solution. Values within 5% of the analytical solution will be considered acceptable.

Required output files for these tests are the:

- History data plot files (*2d\_mix.his*, *2d\_quad.his*, *2d\_ref.his*, *2d\_tri.his*), and
- AVS contour data plot files for  $t = 0.25$  days (*2d\_mix.10002\_sca\_node*, *2d\_quad.10002\_sca\_node*, *2d\_ref.10002\_sca\_node*, *2d\_tri.10002\_sca\_node*).

## 2.2.4.2 3-D Heat Conduction in a Cube

2.2.4.2.1 Function Tested. This test verifies that FEHM correctly models 3-dimensional heat conduction. It also verifies that the finite element representation of 3-D, 6-node triangular prisms (prism elements), 8-node quadrilateral polyhedrons (brick elements), 4-node tetrahedrals, mixed element meshes (containing both triangular prisms and quadrilateral polyhedrons), and refined element meshes (containing quadrilateral polyhedrons and trapezoidal polyhedrons) have been correctly implemented (see Fig. 3). In addition, the finite volume option, in which the code subdivides brick elements into tetrahedrals, is tested.

2.2.4.2.2 Test Scope. This test case is a verification test.

2.2.4.2.3 Requirements Tested. Requirements 2.2, "Finite-Element Coefficient Generation," 2.3, "Formulate Transient Equations," specifically Section 2.3.1, 2.5, "Compute Solution to Transient Equations," and 2.6, "Provide Input/Output Data Files," of the FEHM RD are verified by this test

2.2.4.2.4 Required Inputs. Problem input is provided in the following files:

- *heat3d.in*: Basic input data file used in conjunction with the following geometry data files
- *heat3d.geom.3d\_tri*: 6-node triangular prisms (1331 nodes, 2000 elements),
- *heat3d.geom.3d\_quad*: 8-node quadrilateral polyhedrons (1331 nodes, 1000 elements),
- *heat3d.geom.3d\_tets*: 4-node tetrahedrals (1331 nodes, 6000 elements),
- *heat3d.geom.3d\_mix*: mixed elements, 6-node triangular prisms and 8-node quadrilateral polyhedrons (1331 nodes, 1020 elements), or

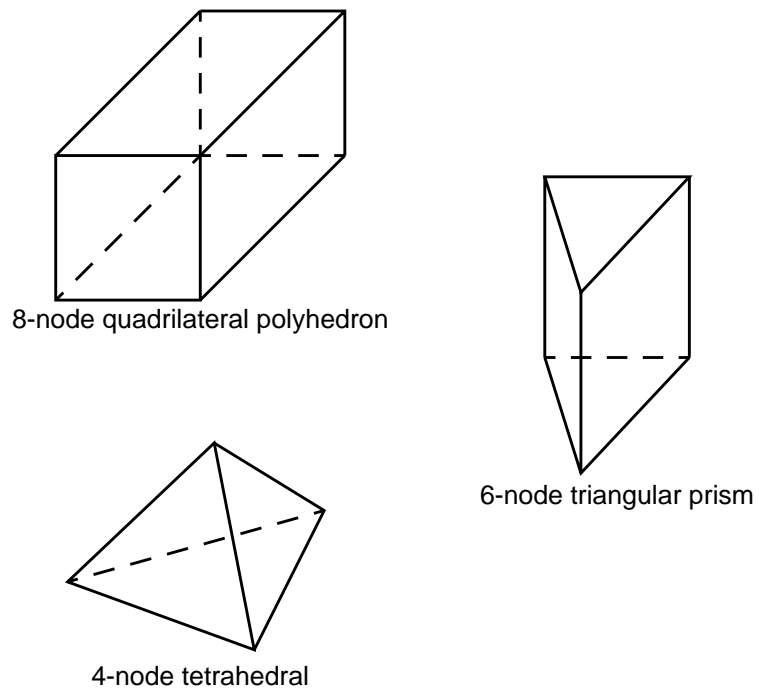


**Figure 3. Geometric elements tested by the 3-D heat conduction problem.**

- *heat3d.geom.3d\_ref*: refined elements, 8-node quadrilateral polyhedrons with refinement about node at  $x = y = 0$  m for  $z = 0$ . to 0.5 m (1364 nodes, 1020 elements); and
- *heat3d.finv.in*: Basic input data file using the finite volume option in conjunction with the following geometry data files
- *heat3d.geom.3d\_quad*, or
- *heat3d.geom.3d\_ref*

**2.2.4.2.5 Expected Outputs.** Values from FEHM for temperature change versus time at the center of the cube ( $x = y = z = 0$  m) and values for temperature versus position ( $x = y = z$ ) at a specified time (time = 0.25 days) will be output and compared to the analytical solution. Values within 5% of the analytical solution will be considered acceptable.

Required output files for these tests are the:

- History data plot files (*3d\_mix.his*, *3d\_quad.his*, *3d\_ref.his*, *3d\_tets.his*, *3d\_tri.his*, *3d\_quad.finv.his*, *3d\_ref.finv.his*), and
- AVS contour data plot files for  $t = 0.25$  days (*3d\_mix.10002\_sca\_node*, *3d\_quad.10002\_sca\_node*, *3d\_ref.10002\_sca\_node*, *3d\_tets.10002\_sca\_node*, *3d\_tri.10002\_sca\_node*, *3d\_quad.finv.10002\_sca\_node*, *3d\_ref.finv.10002\_sca\_node*).

## 2.3 Test of Temperature in a Wellbore

### 2.3.1 Purpose

The ability to model temperature changes in a wellbore is important to the interpretation of temperature surveys. Ramey (1962) has developed a semi-analytical technique for predicting the thermal drawdown in a wellbore. Comparison with this solution will help verify that the code is capable of analyzing temperature logs, and, more generally, of handling a thermal conduction problem coupled to advective heat transport.

### 2.3.2 Functional Description

The test suite consists of a simulation of fluid injection into a wellbore. In addition to demonstrating that the heat and mass transfer problem has been correctly formulated, it will demonstrate that the 2-D radial geometry has been correctly implemented.

### 2.3.3 Assumptions and Limitations

Fluid injection at constant temperature,  $T_{inj}$ , into a wellbore is modeled (Fig. 4). Flow is confined to the wellbore, i.e., there is no flow between the wellbore and the surrounding rock. Table V defines the input parameters used for FEHM and the Ramey analytical solution. The semi-analytical solution is given by

$$T_f(z,t) = b + az - aA + (T_{inj} - b + aA)e^{-\frac{z}{A}}$$

where  $A = \frac{qcf(t)}{2\pi\kappa}$  and  $f(t) = \frac{1}{\frac{4}{\pi^2} \int_0^\infty \frac{e^{-\alpha u^2 t} du}{u(J_0^2(r_w u) + Y_0^2(r_w u))}$ .

$J_0$  and  $Y_0$  are Bessel functions of the first and second kind, of order 0, respectively. The initial temperature distribution in the medium is given by a linear geothermal gradient  $T_r = b + az$  where  $b$  is the surface rock

temperature and  $a$  is the geothermal gradient. Although the Ramey solution models a semi-infinite reservoir in the radial direction, for the FEHM model the reservoir radius has been set to 40 m.

### 2.3.4 Summary of Test Cases

#### 2.3.4.1 Constant Temperature Injection into a Wellbore

2.3.4.1.1 Function Tested. This test verifies that FEHM has correctly implemented the heat and mass transfer problem and 2-D radial geometry.

2.3.4.1.2 Test Scope. This test case is a verification test.

2.3.4.1.3 Requirements Tested. Requirements 2.2, "Finite-Element Coefficient Generation," 2.3, "Formulate Transient Equations," specifically Section 2.3.2 and Section 2.3.7, 2.4, "Apply Constitutive Relationships," specifically Section 2.4.1, 2.5, "Compute Solution to Transient Equations," and 2.6, "Provide Input/Output Data Files," of the FEHM RD are verified by this test.

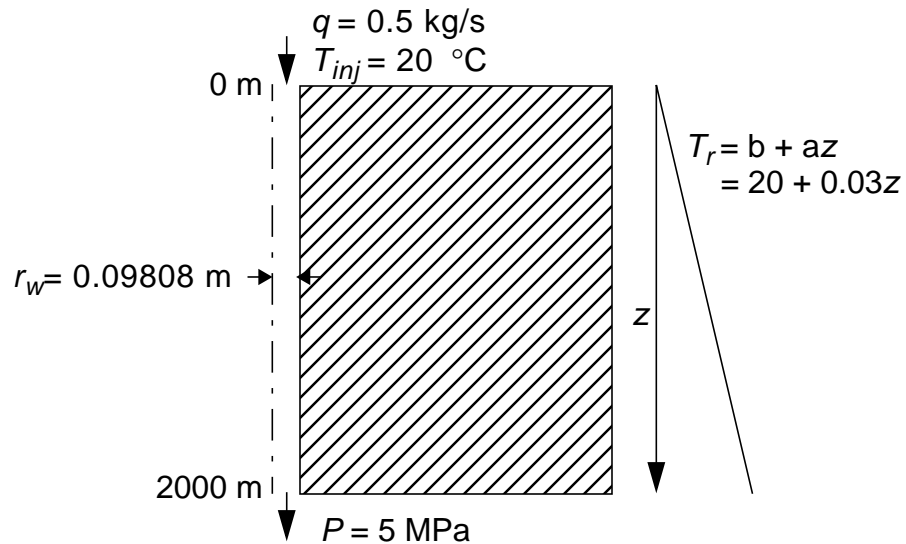


**Figure 4. Schematic drawing of the problem geometry and boundary conditions for the temperature in a wellbore problem.**

2.3.4.1.4 Required Inputs. Problem input is provided in the following files:

- *ramey.in*: Basic input data,
- *ramey.geom*: Geometry data (1010 nodes, 900 elements).

2.3.4.1.5 Expected Outputs. Values from FEHM for temperature versus time at fixed depth ( $d = 1000$  and  $2000$  m), and values for temperature versus depth ( $d = 0 - 2000$  m) at a specified time ( $t = 25$  days) will be output and compared to the analytical solution. Values within 5% of the analytical solution will be considered acceptable.

Required output files for this test are the:

- History data plot file (*ramey.his*), and
- AVS contour data plot file for  $t = 25$  days (*ramey.10002\_sca\_node*).

**Table V. Input Parameters for the Temperature in a Wellbore Problem**

Parameter	Symbol	Value
Rock thermal conductivity	$\kappa_r$	$2.7 \frac{\text{W}}{\text{m} \cdot \text{K}}$
Rock density	$\rho_r$	$2700 \text{ kg/m}^3$
Rock specific heat	$C_r$	$1000 \frac{\text{J}}{\text{kg} \cdot \text{K}}$
Rock thermal diffusivity	$\alpha_r = \frac{\kappa_r}{\rho_r C_r}$	$10^{-6} \text{ m}^2/\text{s}$
Rock (matrix) permeability	$k$	$10^{-20} \text{ m}^2$
Porosity	$f$	0
Fluid heat capacity	$C_f$	$4200 \frac{\text{J}}{\text{kg} \cdot \text{K}}$
Wellbore radius	$r_w$	0.09808 m
Radial extent	$r$	40 m
Node spacing (radial)	$\Delta r$	0.19616 - 17.25495 m
Well depth	$z$	2000 m
Node spacing (vertical)	$\Delta z$	20 m
Surface rock temperature	$b$	20 °C
Geothermal gradient	$a$	0.03 °C/m
Injection rate	$q$	0.5 kg/s
Injection temperature	$T_{inj}$	20 °C
Time step	$\Delta t$	0.001 - 1 days
Total elapsed time	$t$	25 days
Initial Temperature distribution ( $T$ in °C, $z$ in m): $T(z) = 20 + 0.03 z$ for $r = 0 - 40 \text{ m}$		
Boundary conditions: At $r = 0 \text{ m}$ , $z = 0 \text{ m}$ , $q = 0.5 \text{ kg/s}$ , $T_{inj} = 20 \text{ °C}$ At $r = 0 \text{ m}$ , $z = 2000 \text{ m}$ , $P(t) = 5 \text{ MPa}$		



## 2.4 Test of Hydraulic Head

### 2.4.1 Purpose

This test verifies that head and pressure formulations for a saturated problem yield the same solution for the same problem.

### 2.4.2 Functional Description

The test suite consists of simulations of a 3-D saturated reservoir where the hydraulic head is held constant. In addition to demonstrating that the pressure equation has been correctly formulated, it will demonstrate that solutions generated using a hydraulic head formulation yield the same results as those generated using a pressure formulation.

### 2.4.3 Assumptions and Limitations

A 3-D saturated reservoir is modeled, where a hydrostatic problem is solved by running FEHM after imposing a forced pressure on the top of the solution domain. A steady-state solution is obtained for the problems by solving for 1 year. For the pressure solution, head ( $H$ ) is calculated from

pressure ( $P$ ) as  $H = z + \frac{P}{\rho g}$ , where  $z$  is height,  $\rho$  is density, and  $g$  is the

gravity constant. A gravity constant of  $9.81 \text{ m/s}^2$  and a density of  $995.41044 \text{ kg/m}^3$  (value at  $T = 30^\circ\text{C}$ ,  $P = 0.1 \text{ MPA}$ ) are used. It should be noted that within FEHM when the head formulation is used, the head calculation is modified as follows to include the reference pressure

$$H = z + \frac{P - P_{ref}}{\rho g}.$$

Figure 5 shows the problem geometry and boundary conditions. This problem is isothermal. Input parameters defining the problem are given in Table VI.

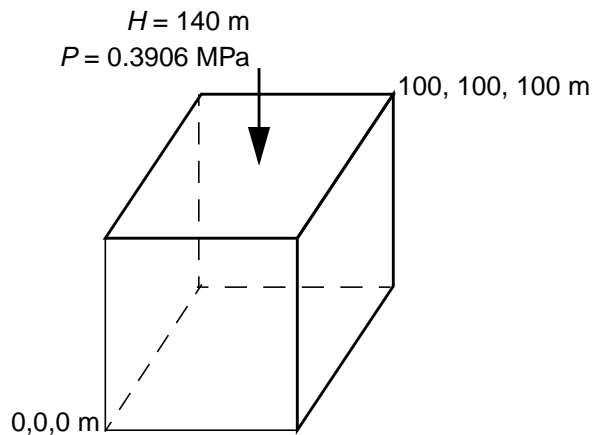


**Figure 5. Schematic drawing of the problem geometry and boundary conditions for the head pressure problem.**

**Table VI. Input Parameters for the Head Pressure Problem**

Parameter	Symbol	Value
Reservoir permeability in horizontal direction	$k$	$10^{-13} \text{ m}^2$
Reservoir permeability in vertical direction	$k$	$10^{-14} \text{ m}^2$
Reservoir porosity	$f$	0.1
Fluid compressibility	$c$	$5.4 \cdot 10^{-4} \text{ MPa}^{-1}$
Fluid density	$\rho$	$995.41044 \text{ kg/m}^3$
Fluid viscosity	$\mu$	$8.0 \cdot 10^{-4} \text{ Pa}\cdot\text{s}$
Reservoir dimensions	$x, y, z$	100 m
Node spacing	$\Delta x, \Delta y, \Delta z$	25 m
Initial Pressure (pressure formulation)	$P_i$	0.48825 MPa
Initial Hydraulic Head (head formulation)	$H$	150 m
Reference pressure	$P_{ref}$	0.1 MPa
Temperature (isothermal)	$T$	30 °C
Time step	$\Delta t$	0.001 - 100 days
Total elapsed time	$t$	1 year
Boundary conditions: At $t = 0, z = 100 \text{ m}$		
Head formulation: $H = 140 \text{ m}$		
Pressure formulation: $P = 0.3906 \text{ MPa}$		

## 2.4.4 Summary of Test Cases

### 2.4.4.1 Head Pressure Problem

2.4.4.1.1 Function Tested. This test verifies that FEHM has correctly implemented the pressure equations, i.e., the conservation of mass with Darcy's law.

2.4.4.1.2 Test Scope. This test case is a verification test.

2.4.4.1.3 Requirements Tested. Requirements 2.2, "Finite-Element Coefficient Generation," 2.3, "Formulate Transient Equations," specifically Section 2.3.2 and Section 2.3.7, 2.5, "Compute Solution to Transient Equations," and 2.6, "Provide Input/Output Data Files," of the FEHM RD are verified by this test.

2.4.4.1.4 Required Inputs. Problem input is provided in the following file:

- *head.dat*: Basic input for head formulation;
- *pres.dat*: Basic input for pressure formulation; and
- *head3D.grid*: Geometry data (3-D block, 125 nodes, 64 elements).

2.4.4.1.5 Expected Outputs. Values from FEHM, for pressure versus depth, at a specified time ( $t = 1$  year), will be output and compared. Values of pressure within 0.05 % of each other will be considered acceptable.

Required output files for this test are the:

- AVS contour data plot files for  $t = 1$  year  
(*head.10002\_sca\_node*, *pres.10002\_sca\_node*).

## 2.4.5 Acknowledgement

This test suite was developed by Lee G. Glascoe, a Postdoctoral Research Associate with the Los Alamos Geoanalysis Group (EES-5) of the Earth and Environmental Science Division, and incorporated into the Validation Test Plan in March 2000.

## 2.5 Test of Pressure Transient Analysis

### 2.5.1 Purpose

Properties of underground reservoirs are often determined by pressure tests. Theis (1935) developed a solution for radial flow to a well in the form of pressure as a function of time and the spatial coordinates. Comparison with this solution will help demonstrate that the pressure equation (the conservation of mass with Darcy's law) is implemented correctly.

### 2.5.2 Functional Description

The test suite consists of a simulation of 1-D radial flow into an infinite aquifer. In addition to demonstrating that the transient pressure equation has been correctly formulated, it will demonstrate that the radial geometry has been correctly implemented.

### 2.5.3 Assumptions and Limitations

Injection into a centrally located well at a constant volumetric rate,  $q$ , is modeled. The well (modeled as a line source) is assumed to be situated in a porous medium of infinite radial extent. The analytical solution (from Matthews and Russell, 1967) is given by

$$p(r,t) = p_i - \frac{q\mu}{2\pi kh} \left[ -\frac{1}{2} Ei \left( -\frac{\phi\mu cr^2}{4kt} \right) \right]$$

where the exponential integral function is  $-Ei(-x) = \int_x^\infty \frac{e^{-u}}{u} du$ .

Figure 6 shows the problem geometry and boundary conditions. This problem is isothermal. Input parameters defining the problem are given in Table VII.

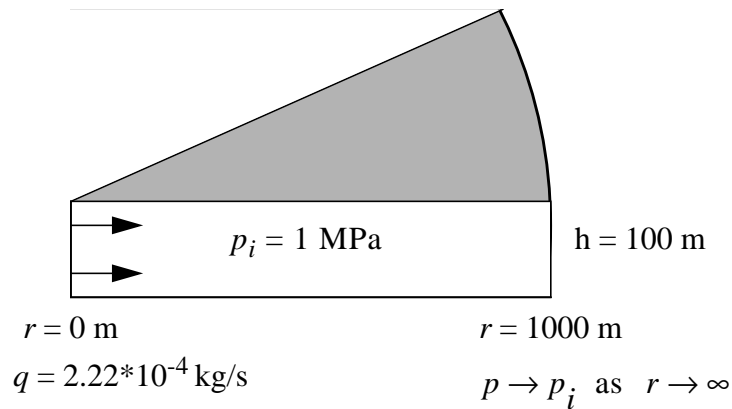


**Figure 6. Schematic drawing of the problem geometry and boundary conditions for the transient pressure problem.**

**Table VII. Input Parameters for the Transient Pressure Problem**

Parameter	Symbol	Value
Reservoir permeability in radial direction	$k$	$10^{-14} \text{ m}^2$
Reservoir porosity	$\phi$	0.4
Fluid compressibility	$c$	$5.06 \cdot 10^{-4} \text{ MPa}^{-1}$
Fluid viscosity	$\mu$	$5.48 \cdot 10^{-4} \text{ Pa}\cdot\text{s}$
Reservoir thickness	$h$	100 m
Node spacing (vertical)	$\Delta h$	100 m
Reservoir length (radial)	$r$	0 - 1000 m
Node spacing (radial)	$\Delta r$	0.00144 - 107 m
Flow rate	$q$	$2.22 \cdot 10^{-4} \text{ kg/s}$
Initial Pressure	$p_i$	1 MPa
Temperature (isothermal)	$T$	50 °C
Time step	$\Delta t$	300 s
Total elapsed time	$t$	1 day

Boundary conditions:  $p \rightarrow p_i$  as  $r \rightarrow \infty$

$$\lim_{r \rightarrow 0} r \frac{\partial p}{\partial r} = \frac{q\mu}{2\pi kh} \quad (\text{Constant flow at } r = 0, \text{ line source})$$

## 2.5.4 Summary of Test Cases

### 2.5.4.1 Radial Flow from a Well

2.5.4.1.1 Function Tested. This test verifies that FEHM has correctly implemented the pressure equations, i.e., the conservation of mass with Darcy's law.

2.5.4.1.2 Test Scope. This test case is a verification test.

2.5.4.1.3 Requirements Tested. Requirements 2.2, "Finite-Element Coefficient Generation," 2.3, "Formulate Transient Equations," specifically Section 2.3.2 and Section 2.3.7, 2.5, "Compute Solution to Transient Equations," and 2.6, "Provide Input/Output Data Files," of the FEHM RD are verified by this test.

2.5.4.1.4 Required Inputs. Problem input is provided in the following file:

- *theis.in*: Basic input and geometry data (202 nodes, 100 elements).

2.5.4.1.5 Expected Outputs. Values from FEHM, for pressure versus time, at fixed radii ( $r = 0.00144$  and  $3.44825$  m), and values for pressure versus radius ( $r = 0 - 1000$  m), at a specified time ( $t = 1$  day), will be output and compared to the analytical solution. Values of pressure within 5% of the analytical solution will be considered acceptable.

Required output files for this test are the:

- History data plot file (*theis.his*), and
- AVS contour data plot file for  $t = 1$  day (*theis.10002\_sca\_node*).

## 2.6 Test of Simplified Water Table Calculations

### 2.6.1 Purpose

The simplified water table calculations are important in basin scale problems where the amount of water in the aquifer is important. The test example compares the wtsi solution with that of a full unsaturated zone solution. This tests the accuracy of the water budget in the wtsi solution as well as the accuracy of the calculated position of the water table in the wtsi solution. For Yucca Mountain this capability is important for calculating future climate water table positions. The simplified water table test problem exercises the new macro wtsi. This macro, used in conjunction with the head macro is useful in large-scale simulations where the water table position is needed but unsaturated zone information is not.

### 2.6.2 Functional Description

The test suite consists of a simulation of water flux and injection into a system with a constant pressure boundary. This problem tests the following processes in FEHM:

- The simplified water table approximation;
- The head solution; and
- The seepage face boundary condition.

### 2.6.3 Assumptions and Limitations

The problem consists of a 2-D grid that has a specified flux on the left boundary, a well source, and a constant head on the right boundary. Other boundaries are no-flow (Figure 7). The problem is compared to an unsaturated zone problem with the same boundary conditions. While we do not expect an exact match, we do expect the water table position and total water budget to be close. Input parameters defining the problem are given in Table VIII.

### 2.6.4 Summary of Test Cases

#### 2.6.4.1 Simplified Water Table Problem

2.6.4.1.1 Function Tested. This test verifies that FEHM has correctly implemented the pressure equations, i.e., the conservation of mass with Darcy's law.

2.6.4.1.2 Test Scope. This test case is a verification test.

2.6.4.1.3 Requirements Tested. Requirements 2.2, "Finite-Element Coefficient Generation," 2.3, "Formulate Transient Equations," specifically Section 2.3.2 and Section 2.3.7, 2.5, "Compute Solution to Transient Equations," and 2.6, "Provide Input/Output Data Files," of the FEHM RD are verified by this test.

2.6.4.1.4 Required Inputs. Problem input is provided in the following file:

- *2d\_heter\_uz.in*: Basic input.
- *2d\_heter\_wtsi.in*: Basic input.
- *.fdm\_2d\_heter\_100\_17.grid*: Geometry file containing fdm grid definition.

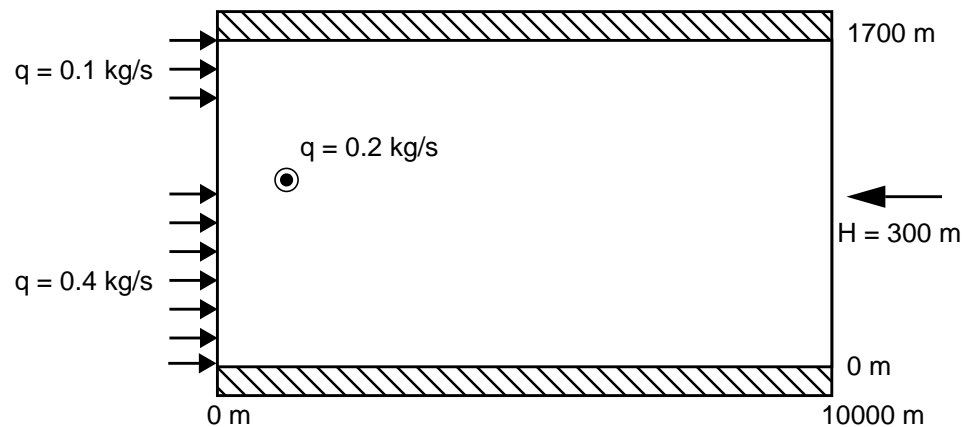


**Figure 7. Schematic drawing of the problem geometry and boundary conditions for the simplified water table problem.**

**2.6.4.1.5 Expected Outputs.** Values from FEHM for saturation at steady state ( $t = 365.25 \times 10^6$  days) will be output for both the UZ and WTSI simulations and used to calculate the water table position. Values with an RMS error less than 0.05 will be considered acceptable. In addition the total water budget for each simulation will be compared and will be considered acceptable if within 5 %.

Required output files for this test are the:

- FEHM generalized summary output files (*2d\_heter\_uz.out*, *2d\_heter\_wtsi.out*), and
- AVS contour data plot file for  $t = 365.25 \times 10^6$  days (*2d\_heter\_uz.10002\_sca\_node*, *2d\_heter\_wtsi.10002\_sca\_node*).



**Table VIII. Input Parameters for the Simplified Water Table Problem**

Parameter	Symbol	Value
Reservoir permeability	$k$	$10^{-12} \text{ m}^2$
Reservoir porosity	$\phi$	0.2
Reservoir height	$z$	1700 m
Node spacing (vertical)	$\Delta z$	100 m
Reservoir length	$x$	0 - 10000 m
Node spacing	$\Delta x$	100 m
Reference pressure	$P_r$	0.1 MPa
Reference temperature	$T_r$	20 °C
Residual saturation Liquid Vapor	$S_r$	0.0
Maximum saturation Liquid Vapor	$S_{max}$	1.0
Capillary pressure at zero saturation	$P_{capmax}$	0.1 MPa
Saturation at which capillary pressure goes to zero	$S_{lmax}$	1.0
Time step	$\Delta t$	0.1 - 1.e8 days
Total elapsed time	$t$	$365.25 \cdot 10^6$ days
Boundary conditions:		
At $x = 0 \text{ m}$ , $z = 1400 - 1700 \text{ m}$	$q = 0.1 \text{ kg/s}$	
At $x = 0 \text{ m}$ , $z = 0 - 950 \text{ m}$	$q = 0.4 \text{ kg/s}$	
At $x = 950 \text{ m}$ , $z = 550 \text{ m}$	$q = 0.2 \text{ kg/s}$ (well source)	
At $x = 10000 \text{ m}$ , $z = 0 - 1700 \text{ m}$	$H = 300 \text{ m}$	

## **2.7 Test of Infiltration into a One-Dimensional, Layered, Unsaturated Fractured Medium**

### **2.7.1 Purpose**

Modeling infiltration into an unsaturated fractured medium can be performed by implementing either the equivalent continuum method (ECM) or the double porosity/double permeability method (DKM). The ECM provides a lumped set of properties for the material which are derived from the separate matrix and fracture properties along with hydrologic conditions such as saturation and pressure. The DKM considers the fractures as a continuous medium and the matrix as another continuous medium and provides for conductance between the two. See Section 7.2 on page 30 of the "Models and Methods Summary" of the FEHM Application (Zyvoloski et al. 1999) for more details of the double porosity/double permeability method. The DKM requires twice as many finite element nodes and hence takes longer to run than the ECM. Both methods utilize the same set of van Genuchten capillary pressure model parameters to describe the hydrologic properties. The two methods are often compared with each other to assess whether the additional computational burden associated with the DKM is necessary to capture behavior such as fast flow paths in fractures, which are smoothed out in the composite property model of the ECM. This set of tests verify that each method, the ECM and the DKM, are implemented properly.

### **2.7.2 Functional Description**

The test problem, described by Ho (1995), consists of simulations of infiltration into a one-dimensional column. The column is a transect through a system of four stratigraphic units each characterized by a unique set of parameters describing the matrix and fracture properties. The stratigraphic system is a representation of the lithologic layering at Yucca Mountain. The four units are the Tiva Canyon welded tuff (TCw), the Paintbrush nonwelded tuff (PTn), the Topopah Springs welded tuff (TSw), and the Calico Hills nonwelded vitrophere (CHnv). A schematic of the thicknesses and layering of the four units considered is shown in Fig. 8. The properties for these four units were taken from TSPA-93 (Wilson, 1994) and are located in the required input files. Key aspects of this data set include matrix intrinsic permeabilities and matrix residual saturations each of which span four orders of magnitude over the various units.

The test will demonstrate that the equivalent continuum method and the double porosity/double permeability method have been correctly implemented through comparison with simulations performed with TOUGH2, another well documented model capable of solving this problem (Pruess, 1991).

### **2.7.3 Assumptions and Limitations**

Infiltration of 4 mm/yr is applied at the top of the system. For the DKM simulations, it is applied to the fracture nodes only. The bottom boundary for all tests is assumed to be the water table, so full saturation is set there. The TOUGH2 simulations with which FEHM will be compared were run at Sandia National Laboratory using TOUGH2 - version 1.1 (April 1993). This is an isothermal air-water problem. Input parameters defining the problem are given in Table IX.

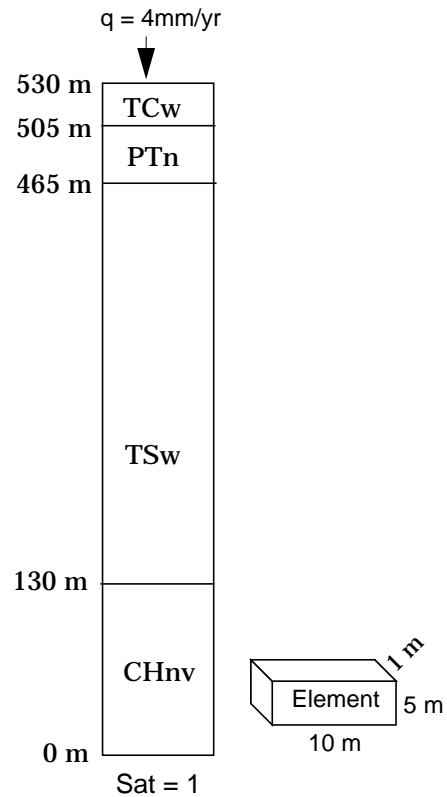


**Figure 8. Schematic drawing of the problem geometry for the one-dimensional infiltration test problem.**

**Table IX. Input Parameters for the One-dimensional Infiltration Problem**

Parameter	Symbol	Value
Fracture Permeability		
TCw	$k_f$	$4.06 \cdot 10^{-9} \text{ m}^2$
PTn		$7.14 \cdot 10^{-9} \text{ m}^2$
TSw		$4.57 \cdot 10^{-9} \text{ m}^2$
CHnv		$6.53 \cdot 10^{-9} \text{ m}^2$
Matrix Permeability		
TCw	$k_m$	$2.04 \cdot 10^{-18} \text{ m}^2$
PTn		$2.51 \cdot 10^{-14} \text{ m}^2$
TSw		$2.09 \cdot 10^{-18} \text{ m}^2$
CHnv		$1.10 \cdot 10^{-16} \text{ m}^2$

**Table IX. Input Parameters for the One-dimensional Infiltration Problem (Continued)**

Parameter	Symbol	Value
Fracture porosity (Volume fraction for fracture node)		
TCw	$\phi_f$ ( $V_f$ )	$2.93 \cdot 10^{-4}$
PTn		$9.27 \cdot 10^{-5}$
TSw		$2.43 \cdot 10^{-4}$
CHnv		$1.11 \cdot 10^{-4}$
Matrix porosity		
TCw	$\phi_m$	0.087
PTn		0.421
TSw		0.139
CHnv		0.331
Matrix node length scale		
TCw	$L_{fI}$	0.18 m
PTn		0.64 m
TSw		0.21 m
CHnv		0.46 m
Column width	$w$	10 m
Node spacing (horizontal)	$\Delta w$	10 m
Column height (elevation)	$h$	530 m
Node spacing (vertical) <sup>†</sup>	$\Delta h$	5 m
Reference pressure	$P_r$	0.1 MPa
Reference temperature	$T_r$	20 °C
Maximum saturation	$S_{lmax}$	1.0
Fracture residual saturation	$S_{lr,f}$	0.03
Matrix residual saturation		
TCw	$S_{lr,m}$	0.0212
PTn		0.154
TSw		0.0453
CHnv		0.0968
van Genuchten model parameters for the fracture		
Inverse of air entry head		
TCw	$\alpha_{G,f}$	$12.05 \text{ m}^{-1}$
PTn		$2.5 \text{ m}^{-1}$
TSw		$11.96 \text{ m}^{-1}$
CHnv		$2.5 \text{ m}^{-1}$

**Table IX. Input Parameters for the One-dimensional Infiltration Problem (Continued)**

Parameter	Symbol	Value
Power in formula		
TCw	$n_f$	3.0
PTn		3.0
TSw		3.0
CHnv		3.0
van Genuchten model parameters for the matrix		
Inverse of air entry head		
TCw	$\alpha_{G,m}$	0.00715 m <sup>-1</sup>
PTn		0.371 m <sup>-1</sup>
TSw		0.0133 m <sup>-1</sup>
CHnv		0.0273 m <sup>-1</sup>
Power in formula		
TCw	$n_m$	1.62
PTn		2.37
TSw		1.8
CHnv		2.46
Initial fracture saturation	$S_{I0,f}$	0.5
Initial matrix saturation		
TCw	$S_{I0,m}$	0.95
PTn		0.31
TSw		0.95
CHnv		0.85
Time step	$\Delta t$	1 - 1*10 <sup>8</sup> days
Total elapsed time	$t$	1*10 <sup>9</sup> days
Boundary conditions:	At $h = 530$ m At $h = 0$ m	$q = 4$ mm/yr $S = 1.0$

‡ For the FEHM simulation an additional node was added at each material interface to facilitate comparison with TOUGH2 which uses cell centered elements whereas FEHM uses node centered elements.

## 2.7.4 Summary of Test Cases

### 2.7.4.1 Test of infiltration into a one-dimensional, layered, unsaturated medium using the equivalent continuum method (ECM)

2.7.4.1.1 Function Tested. This test verifies that FEHM has correctly implemented for simulations of infiltration into a one-dimensional, layered, unsaturated medium using ECM.

2.7.4.1.2 Test Scope. This test case is a verification test.

2.7.4.1.3 Requirements Tested. Requirements 2.2, "Finite-Element Coefficient Generation," 2.3, "Formulate Transient Equations,"

specifically Section 2.3.2 and Section 2.3.7, 2.4, “Apply Constitutive Relationships,” specifically Section 2.4.4, 2.5, “Compute Solution to Transient Equations,” and 2.6, “Provide Input/Output Data Files,” of the FEHM RD are verified by this test.

2.7.4.1.4 Required Inputs. Problem input is provided in the following files:

- *infiltration.ecm.in*: Basic input data, case 1;
- *infiltration.geom*: Geometry data used for the above cases.

2.7.4.1.5 Expected Outputs. Values from FEHM for saturation vs. elevation will be output, nondimensionalized, and compared to the TOUGH2 solution. A root mean square error of the difference between the two simulations less than or equal to 0.05 will be considered acceptable.

The required output file for this test is the:

- AVS contour data plot file for  $t = 1.e9$  days (*infiltration.ecm.10002\_sca\_node*).

#### **2.7.4.2 Test of infiltration into a one-dimensional, layered, unsaturated medium using the double porosity/double permeability method (DKM)**

2.7.4.2.1 Function Tested. This test verifies that FEHM has been correctly implemented for simulations of infiltration into a one-dimensional, layered, unsaturated medium using DKM.

2.7.4.2.2 Test Scope. This test case is a verification test.

2.7.4.2.3 Requirements Tested. Requirements 2.2, “Finite-Element Coefficient Generation,” 2.3, “Formulate Transient Equations,” specifically Section 2.3.2 and Section 2.3.7, 2.4, “Apply Constitutive Relationships,” specifically Section 2.4.4 and Section 2.4.9, 2.5, “Compute Solution to Transient Equations,” and 2.6, “Provide Input/Output Data Files,” of the FEHM RD are verified by this test.

2.7.4.2.4 Required Inputs. Problem input is provided in the following files:

- *infiltration.dpm.in*: Basic input data, case 2;
- *infiltration.geom*: Geometry data used for the above cases.

2.7.4.2.5 Expected Outputs. Values from FEHM for saturation vs. elevation will be output, nondimensionalized, and compared to the TOUGH2 solution. A root mean square error of the difference between the two simulations less than or equal to 0.05 will be considered acceptable.

Required output files for this test are the:

- AVS contour data plot file for  $t = 1.e9$  days [fracture solution] (*infiltration.dpm.10002\_sca\_node*), and
- AVS dual contour data plot file for  $t = 1.e9$  days [matrix solution] (*infiltration.dpm.10002\_sca\_dual\_node*).

## 2.8 Test of Vapor Extraction from an Unsaturated Reservoir

### 2.8.1 Purpose

The ability to model vapor/gas transport in unsaturated media is important to the design of vapor extraction systems and interpretation of their performance. Analytical solutions of steady state gas flow to a soil vapor extraction well in the unsaturated zone have been described by Shan et al. (1992). Comparison with this solution will help verify that vapor/gas transport has been correctly implemented in FEHM.

### 2.8.2 Functional Description

The test suite consists of two simulations of steady, 2-D radial soil-vapor flow to a well in an unsaturated reservoir. The first case uses an isotropic permeability model while the second case models an anisotropic reservoir. In addition to demonstrating that the gas flow problem has been correctly formulated for isotropic and anisotropic permeability models, it will demonstrate that the 2-D radial coordinate geometry has been correctly implemented.

### 2.8.3 Assumptions and Limitations

The analytical solution for pressure for this test case is expressed as an infinite series:

$$P = \frac{\bar{q}}{4\pi\alpha_r} \left[ \ln \left( \frac{a-z + [\hat{r}^2 + (a-z)^2]^{-1/2}}{b-z + [\hat{r}^2 + (b-z)^2]^{-1/2}} \cdot \frac{b+z + [\hat{r}^2 + (b+z)^2]^{-1/2}}{a+z + [\hat{r}^2 + (a+z)^2]^{-1/2}} \right) - \sum_{n=1}^{\infty} (-1)^n \ln \left( \frac{a+z+2nh + [\hat{r}^2 + (a+z+2nh)^2]^{-1/2}}{b+z+2nh + [\hat{r}^2 + (b+z+2nh)^2]^{-1/2}} \cdot \frac{a+z-2nh + [\hat{r}^2 + (a+z-2nh)^2]^{-1/2}}{b+z-2nh + [\hat{r}^2 + (b+z-2nh)^2]^{-1/2}} \cdot \frac{-a+z+2nh + [\hat{r}^2 + (-a+z+2nh)^2]^{-1/2}}{-b+z+2nh + [\hat{r}^2 + (-b+z+2nh)^2]^{-1/2}} \cdot \frac{-a+z-2nh + [\hat{r}^2 + (-a+z-2nh)^2]^{-1/2}}{-b+z-2nh + [\hat{r}^2 + (-b+z-2nh)^2]^{-1/2}} \right) \right]$$

$$\text{where } \bar{q} = \frac{2P_a q_m}{(a-b)\phi\rho_g}, \alpha_r = \frac{k_r P_a}{\phi\mu_g}, \hat{r} = \left(\frac{k_z}{k_r}\right)^{1/2} r,$$

$r$  is the radial distance,  $z$  the vertical distance,  $h$  is the depth to the water table (impermeable boundary), and  $a$  and  $b$  are the depths to the bottom and top of the open well bore interval, respectively. A sensitivity study of

the number of terms required for the solution to achieve a precision of  $10^{-3}$  Pa shows that no more than 50 terms are needed. The analytical solution is calculated for each node of the FEHM grid where  $0.0001 \leq r \leq 30$  m, and  $0 \leq z \leq 10$  m.

The geometry and boundary conditions are shown in Fig. 9. The upper surface is at atmospheric pressure and the remaining edges are impermeable, no flow boundaries with the exception of the extraction wellbore. The problem is isothermal. Values of the analytical solution are inaccurate in the region surrounding the extraction wellbore ( $r \leq 0.05$  m,  $2.8 \leq z \leq 7.2$  m) so they are excluded from the results used for comparison. Table X lists the input parameters for the vapor extraction problem. The solution is verified by comparison of FEHM results to the analytical solution (for  $n = 1$  to 50) over the problem domain.

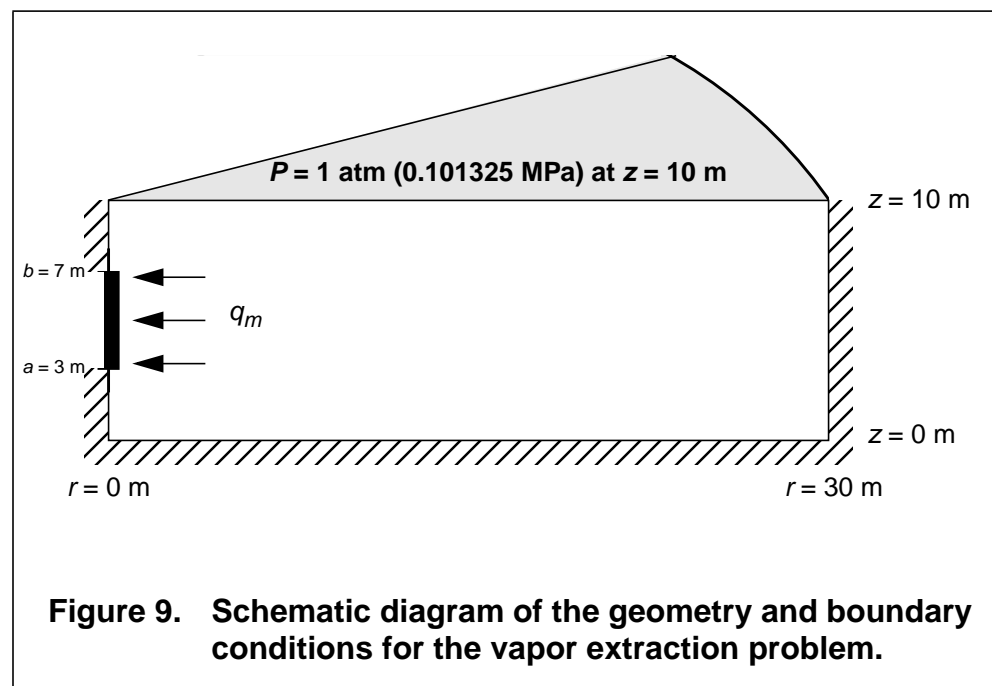


**Table X. Input Parameters for the Vapor Extraction Problem**

Parameter	Symbol	Value
Reservoir permeability		
Isotropic case	$k_r, k_z$	$10^{-11} \text{ m}^2$
Anisotropic case -radial	$k_r$	$10^{-11} \text{ m}^2$
Anisotropic case -vertical	$k_z$	$10^{-12} \text{ m}^2$
Reservoir porosity	$\phi$	0.4
Reservoir length	$r$	30 m
Node spacing (radial)	$\Delta r$	0.0001 - 1 m



**Table X. Input Parameters for the Vapor Extraction Problem (Continued)**

Reservoir thickness (elevation)	$h$	10 m
Node spacing (vertical)	$\Delta h$	0.5 m
Extraction interval, bottom	$a$	3 m
Extraction interval, top	$b$	7 m
Ambient (reference) temperature	$T_a$	10 °C
Ambient pressure	$P_a$	0.101325 MPa
Initial pressure	$P_0$	0.101325 MPa
Initial saturation	$S_0$	0.05
Residual liquid saturation	$S_{lr}$	0.10
Maximum liquid saturation	$S_{lmax}$	0.99
van Genuchten model parameters		
Inverse of air entry head	$\alpha_G$	0.005 m <sup>-1</sup>
Power in formula	$n$	1.8
Gas density	$\rho_g$	1.24 kg/m <sup>3</sup>
Gas viscosity	$\mu_g$	1.76 x 10 <sup>-5</sup> Pa•s
Extraction rate		
Isotropic case	$q_m$	0.0825 kg/s
Anisotropic case		0.05 kg/s
Time step	$\Delta t$	0.001 - 75 days
Total elapsed time		
Isotropic case	$t$	365 days
Anisotropic case		730 days
Boundary conditions: At $z = 10$ m $P = 0.101325$ MPa, $S = 0.05$		
At $r = 0$ m, $3 \leq z \leq 7$ m $q = q_m$		
(Line sink wellbore, $z$ positive upwards)		

## 2.8.4 Summary of Test Cases

### 2.8.4.1 Vapor Extraction from an Unsaturated Reservoir

2.8.4.1.1 Function Tested. This test verifies that FEHM has correctly implemented the gas flow option of the code for radial flow.

2.8.4.1.2 Test Scope. This test case is a verification test.

2.8.4.1.3 Requirements Tested. Requirements 2.2, "Finite-Element Coefficient Generation," 2.3, "Formulate Transient Equations,"

specifically Section 2.3.3 and Section 2.3.7, 2.4, “Apply Constitutive Relationships,” specifically Section 2.4.2 and Section 2.4.4, 2.5, “Compute Solution to Transient Equations,” and 2.6, “Provide Input/Output Data Files,” of the FEHM RD are verified by this test.

2.8.4.1.4 Required Inputs. Problem input is provided in the following files:

- *vapextract\_iso.in*: Basic input data, isotropic case;
- *vapextract\_aniso.in*: Basic input data, anisotropic case;
- *vapextract.geom*: Geometry data used for the above cases.

2.8.4.1.5 Expected Outputs. Values from FEHM, for the steady state vapor pressure at each node, (reached after 365 days for the isotropic case, 730 days for the anisotropic case), will be output and compared to the analytical solution from Shan et al. (1992) for  $n = 1$  to 50. Values within 5% of the analytical solution or a root mean square error of the difference between the two simulations less than or equal to 0.01 will be considered acceptable.

Required output files for these tests are the:

- AVS contour data plot file for  $t = 365$  days [isotropic solution] (*vapextract\_iso.10002\_sca\_node*), and
- AVS contour data plot file for  $t = 730$  days [anisotropic solution] (*vapextract\_aniso.10002\_sca\_node*).

## 2.9 Test of Barometric Pumping Mechanisms

### 2.9.1 Purpose

Air pressure gradients driven by atmospheric pressure fluctuations can provide potential increases in the mass transport mechanisms of volatile contaminants. Testing FEHM's ability to solve simple and complex vapor transport problems involving the effects of barometric pumping is important to understanding the sensitivity of this transport process. Auer et al. (1996) developed a one-dimensional semi-analytical and analytical solution that determines the effects of barometric pumping on pore-scale velocity and volatile mass transfer in a homogeneous porous medium. Comparison with this solution will determine FEHM's capabilities to analyze the effects of barometric pumping on the transport of volatile components.

### 2.9.2 Functional Description

This test suite, consisting of four simulations, verifies the one-dimensional flow solution for air under an imposed cyclic boundary condition and the resulting transport solution for a volatile component. One test is designed to verify pore-scale air velocity in a homogeneous medium at four different times (1.75, 3.5, 5.25, and 7.0 days) during a seven-day barometric cycle. The other test verifies volatile contaminant mass transfer in a system with three different dispersivity values ( $\alpha = 0.0, 0.1, \text{ and } 0.2 \text{ m}$ ) in a porous homogeneous medium. Volatile transport rates are driven by the magnitude of the velocity dependent dispersion term. These tests will demonstrate the capabilities of FEHM for solving volatile transport problems under the effects of barometric pumping.

### 2.9.3 Assumptions and Limitations

Auer et al.'s (1996) determination of pore-scale velocity is defined by a modified version of Darcy's law. They use an analytic solution described by Carslaw and Jaeger (1959), Weeks (1978), and Nilson et al. (1991) to describe the motion of gas through a porous medium during a sinusously varying barometric cycle

$$V = -Re\left(\Delta P \frac{K}{\phi \mu} k \frac{\sinh(k\sqrt{i}(z-L))}{\cosh(k\sqrt{i}L)} \exp(i\omega t)\right)$$

with  $\omega = (2\pi)/T$  and  $k^2 = (\mu\phi 2\pi)/(KP_0T)$ , where  $\phi$  is porosity;  $T$  is the period;  $K$  is the permeability;  $\mu$  is the viscosity;  $\Delta P$  is the pressure perturbation;  $z$  is the depth;  $t$  is time; and  $P_0$  is the average surface pressure. This analysis demonstrates the effects that barometric perturbations at the surface have on subsurface air velocities. In cases where permeability is high [ $K = 10 \text{ Da}$  ( $1 \text{ Da} = 10^{-12} \text{ m}^2$ )], the velocity expression becomes nearly linear with depth. The contributing factor is that  $k^2$  is very small in the case that we are studying. Auer et al. develop a quick estimation of  $k^2$  based on different  $K$  and  $T$  values when  $K$  is in

$$\text{Darcies and } T \text{ is in days as } k^2 = \frac{(5 \times 10^3)}{KT} \text{m}^{-2}.$$

Using a Taylor series expansion it becomes evident that velocity is linearly dependent on  $(\Delta P/P_0)$ ,  $1/T$ , and  $L$  through the following equation

$$V \cong -\frac{(\Delta P)}{P_0}(L-z)\omega \sin(\omega t) .$$

The one-dimensional contaminant transport equation is

$$\frac{\partial C}{\partial t} = -V \frac{d}{dz}(C) + \frac{\partial}{\partial z} \left( D \frac{\partial C}{\partial z} \right)$$

where  $C$  is the concentration per unit volume;  $V$  is the pore-scale velocity; and  $D$  is the coefficient of hydrodynamic dispersion.  $D$  is the sum of intrinsic molecular diffusion and velocity-dependent dispersion.  $D$  is defined as  $D = D_{mol} + \alpha|V|$  where  $\alpha$  is the dispersivity; and  $|V|$  is a positive measure of the air pore velocity (Bear, 1972).  $\alpha$  reflects the complexities of the pore-space connectivity at the scale of interest (i.e. the scale at which  $|V|$  is defined).

This problem assumes one-dimensional, transient flow with fixed saturation. The system is modeled as a column with a no-flow (impermeable) boundary at the bottom and an atmospheric pressure variation at the surface. The atmospheric boundary condition is described by a sine wave with a 0.1 MPa mean, an amplitude of 0.015 MPa and a period of 7 days. The initial pressure in the column is set at 0.1 MPa for the semi-analytic, analytic, and numerical solutions. For the contaminant transport simulation, a concentration of 1.0 is set in the lower half of a 60-m column. Figure 1 shows the problem geometry and boundary conditions. Input parameters defining the problem are given in Table 1.

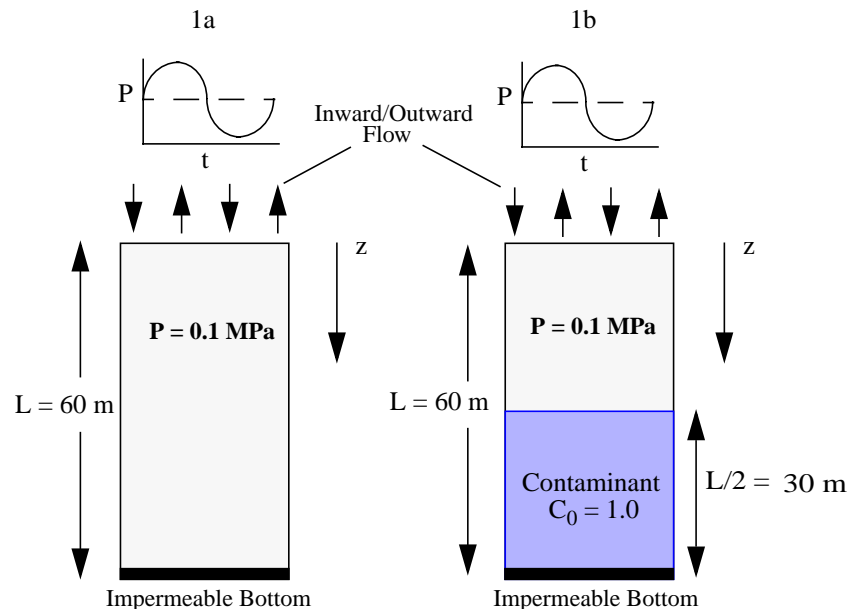


**Figure 10. Schematic diagram of pore-scale velocity (1a) and contaminant transport (1b) verification models.**

**Table XI. Input Parameters for the Barometric Pumping Problem**

Parameter	Symbol	Value
Permeability	$K$	$10^{-11} \text{ m}^2$
Porosity	$\phi$	0.35
Layer thickness	$L$	60 m
Node spacing (vertical)	$\Delta z$	0.5 m
Reference temperature	$T_{ref}$	20 °C
Initial pressure	$P_{ref}$	0.1 MPa
Reference pressure	$P_0$	0.1 MPa
Initial saturation	$S_0$	0.01
Residual liquid saturation	$S_{lr}$	0.0001
Maximum liquid saturation	$S_{lmax}$	1.0
van Genuchten model parameters		
Inverse of air entry head	$\alpha_G$	$3.0 \text{ m}^{-1}$
Power in formula	$n$	3.0
Air density	$\rho$	$1.2 \text{ kg/m}^3$
Air viscosity	$\mu$	$2 \times 10^{-5} \text{ Pa}\cdot\text{s}$
Molecular diffusion coefficient (contaminant transport only)	$D_{mol}$	$7.5 \times 10^{-7} \text{ m}^2/\text{s}$
Dispersivity (contaminant transport only)	$\alpha$	0, 0.1, 0.2 m
Period	$T$	7 days
Relative Pump Amplitude	$\Delta P/P_0$	0.015
Time step		
Pore-scale velocity verification	$\Delta t$	0.001 - 0.002 days
Contaminant transport verification		0.0001 - 0.14 days
Total elapsed time		
Pore-scale velocity verification	$t$	28 days
Contaminant transport verification		10 years
Boundary conditions: At $z = 0 \text{ m}$ $P = 0.1 \pm 0.015 \text{ MPa}$ (sinusoidal, cyclic)		

## 2.9.4 Summary of Test Cases

### 2.9.4.1 Pore-scale velocity in a homogeneous media

2.9.4.1.1Function Tested. This test verifies that FEHM has correctly implemented air motion caused by barometric pumping in one dimension.

2.9.4.1.2Test Scope. This test case is a verification test.

2.9.4.1.3Requirements Tested. Requirements 2.2, "Finite-Element Coefficient Generation," 2.3, "Formulate Transient Equations," specifically Section 2.3.3 and Section 2.3.7, 2.4, "Apply Constitutive Relationships," specifically Section 2.4.2 and Section 2.4.4, 2.5, "Compute Solution to Transient Equations," and 2.6, "Provide Input/Output Data Files," of the FEHM RD are verified by this test.

2.9.4.1.4Required Inputs. Problem input is provided in the following files:

- *baro\_vel.in*: Basic input data for the velocity test;
- *baro.grid*: Geometry data used for the above case [121 x 2 nodes (simulating a 1-D flow system), 120 elements].

2.9.4.1.5Expected Outputs. Values from FEHM, for pore-scale velocity during barometric pumping (7 day period cycle) will be output and compared to the analytical solution from Auer et al. (1996). A root mean square error of the difference between the two simulations less than or equal to 0.01 will be considered acceptable.

Required output files for these tests are the:

- AVS contour data plot files for  $t = 22.75, 24.5, 26.25$  and  $28$  days [corresponding to 1.75, 7.0, 5.25, and 3.5 days within a cycle for the Auer solution] (*baro\_vel.10003\_vec\_node*, *baro\_vel.10004\_vec\_node*, *baro\_vel.10005\_vec\_node*, *baro\_vel.10006\_vec\_node*).

### 2.9.4.2 Contaminant mass transfer of volatile compounds

2.9.4.2.1Function Tested. This test verifies that FEHM has correctly implemented the solute transport solution for a vapor plume migrating under the influence of barometric pumping in one-dimension.

2.9.4.2.2Test Scope. This test case is a verification test.

2.9.4.2.3Requirements Tested. Requirements 2.2, "Finite-Element Coefficient Generation," 2.3, "Formulate Transient Equations," specifically Section 2.3.3 and Section 2.3.7, 2.4, "Apply Constitutive Relationships," specifically Section 2.4.2 and Section 2.4.4, 2.5, "Compute Solution to Transient Equations," and 2.6, "Provide Input/Output Data Files," of the FEHM RD are verified by this test.

2.9.4.2.4Required Inputs. Problem input is provided in the following files:

- *baro\_trans0.in*: Basic input data for contaminant transport, with  $\alpha = 0.0$ ;
- *baro\_trans1.in*: Basic input data for contaminant transport, with  $\alpha = 0.1$ ;

- *baro\_trans2.in*: Basic input data for contaminant transport, with  $\alpha = 0.2$ ;
- *baro.grid*: Geometry data used for the above cases [121 x 2 nodes (simulating a 1-D flow system), 120 elements].
- *baro\_trans.msim*: Multiple simulations input file.

2.9.4.2.5 Expected Outputs. Values from FEHM, for contaminant concentration remaining in the system, will be output and compared to the analytical solution from Auer et al. (1996). A root mean square error of the difference between the two simulations less than or equal to 0.005 will be considered acceptable.

Required output files for these tests are the:

- FEHM generalized summary output files for each  $\alpha$  (*fehmn.out*), which are post-processed to generate data files for contaminant concentration remaining in the system (*baro\_MFR\_0.out*, *baro\_MFR\_1.out*, *baro\_MFR\_2.out*).

## 2.9.5 Acknowledgement

This test suite was developed by Mark P. Haagenstad of the Los Alamos Geoanalysis Group (EES-5) of the Earth and Environmental Science Division, and incorporated into the Validation Test Plan in April 2000. The developer thanks Kay Birdsell for overview and major input on the study; Phil Stauffer who debugged and contributed greatly to the success of the FEHM solution; and Bryan Travis for his mathematical expertise in problem solving and program analysis.

## 2.10 Test of Dual Porosity

### 2.10.1 Purpose

The dual porosity formulation is a computationally efficient way to model flow in a porous medium with high permeability fractures embedded in low permeability matrix material. It has previously been shown by Moench (1984) that dual porosity flow can explain some of the well test data at Yucca Mountain. Warren and Root (1963) provide an analytical solution for dual porosity flow to a wellbore. This test will check the pressure solution for the dual porosity coding in FEHM.

### 2.10.2 Functional Description

The test suite consists of a set of simulations of dual porosity flow to a wellbore. It will demonstrate that the dual porosity formulation has been correctly implemented.

### 2.10.3 Assumptions and Limitations

Warren and Root have defined the dimensionless pressure drop as

$$\psi_f(1, \tau) \approx \frac{1}{2} \left\{ \ln \tau + 0.80908 + Ei \left[ \frac{-\lambda \tau}{\omega(1 - \omega)} \right] - Ei \left[ \frac{-\lambda \tau}{1 - \omega} \right] \right\}$$

$$\text{where } \tau = \frac{\bar{k}_f t}{\phi_m c_m + \phi_f c_f},$$

$$\bar{k}_f = \sqrt{k_{fx} k_{fy}},$$

$$\lambda = \frac{\alpha k_m r_w^2}{\bar{k}_f},$$

$$\omega = \frac{\phi_f c_f}{\phi_m c_m + \phi_f c_f},$$

and  $Ei$  is the exponential integral function (see page 36). In this solution,  $\tau$  is dimensionless time,  $\bar{k}_f$  is the effective permeability of the anisotropic medium,  $\lambda$  is a measure of the size of the matrix region,  $\omega$  represents the strength of coupling between the fracture and the matrix, and  $\alpha$  is a characteristic dimension.

Figure 11 illustrates the problem geometry and boundary conditions. The input parameters are defined in Table XII. The analytical solution uses a steady state approximation for the matrix flow (only one matrix node exists per fracture node) so no transient effects are possible in the matrix. The FEHM dual porosity implementation uses a transient approximation for the matrix material (two matrix nodes exist for each fracture node) so crude transient responses are possible because of flow between two matrix nodes. See Section 7.2 on page 30 of the “Models and Methods Summary” of the FEHM Application (Zyvoloski et al. 1999) for more details and a description of the model parameters ( $L_f$  and  $V_f$ ). The steady state approximation is known to be inaccurate at small times [see Warren and Root (1963), p. 248] and is only valid for  $\tau$  greater than  $\sim 100$ .



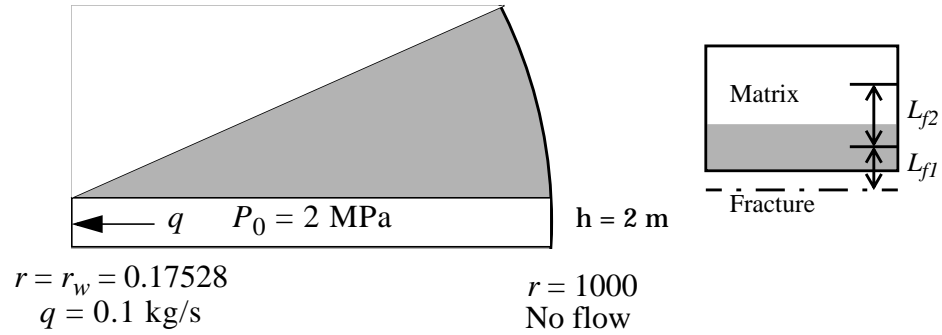


**Figure 11. Schematic diagram of the geometry and boundary conditions for the dual porosity problem.**

**Table XII. Input Parameters for the Dual Porosity Problems**

Parameter	Symbol	Value
Permeability		
fracture	$k_f$	$0.4 \times 10^{-12} \text{ m}^2$
matrix $\left\{ \begin{array}{l} (1) \\ (2) \\ (3) \end{array} \right.$	$k_m$	$1.904 \times 10^{-16} \text{ m}^2$ $1.904 \times 10^{-13} \text{ m}^2$ $1.194 \times 10^{-14} \text{ m}^2$
Porosity		
fracture	$\phi_f$	1.0
matrix $\left\{ \begin{array}{l} (1) \\ (2) \\ (3) \end{array} \right.$	$\phi_m$	0.06081 0.6081 0.47
Volume fraction		
fracture node $\left\{ \begin{array}{l} (1)(2) \\ (3) \end{array} \right.$	$V_f$	0.006711409 0.000476417
first matrix node $\left\{ \begin{array}{l} (1)(2) \\ (3) \end{array} \right.$	$V_{f1}$	0.335570470 0.333492139
Length scale $\left\{ \begin{array}{l} (1)(2) \\ (3) \end{array} \right.$	$L_{f0}$	0.10 0.01
Number in ( ) denotes for which case that value was used.		

**Table XII. Input Parameters for the Dual Porosity Problems (Continued)**

Parameter	Symbol	Value
Compressibility (fracture and matrix)	$c_f c_m$	5.503e-4 MPa <sup>-1</sup>
Flow rate	$q$	0.1 kg/s
Viscosity	$\mu$	1.0021e-3 Pa•s
Reference temperature	$T$	20 °C
Initial pressure	$P_0$	2.0 MPa
Wellbore radius	$r_w$	0.17528 m
Reservoir length	$r$	0 - 1000 m
Node spacing (radial) [average of graded mesh 1.0 m]	$\Delta r$	0.07 - 10 m
Reservoir height	$h$	2 m
Node spacing (vertical)	$\Delta h$	2 m
Time step $\begin{cases} (1) \\ (2)(3) \end{cases}$	$\Delta t$	$1.0 \cdot 10^{-8}$ - 0.01 days $2.0 \cdot 10^{-7}$ - 0.01 days
Total elapsed time $\begin{cases} (1) \\ (2)(3) \end{cases}$	$t$	0.1 days 0.2 days
Boundary conditions: At $r = r_w = 0.17528$ m $q = 0.1$ kg/s At $r = 1000$ m No flow boundary (Sufficiently large to approximate semi-infinite reservoir)		
Number in ( ) denotes for which case that value was used.		

FEHM pressure and time are nondimensionalized using the following formulae for comparison with the Warren and Root solution:

$$P_{non} = \frac{2\pi k_f h \rho}{q \mu} (P_0 - P) \text{ and } \tau = \frac{k_f (t \cdot 86400)}{c \mu r_w^2 [(1 - V_f) \phi_m + V_f \phi_f]}.$$

## 2.10.4 Summary of Test Cases

### 2.10.4.1 Dual Porosity Problem

2.10.4.1.1 Function Tested. This test verifies that FEHM has correctly implemented the dual porosity formulation.

2.10.4.1.2 Test Scope. This test case is a verification test.

2.10.4.1.3 Requirements Tested. Requirements 2.2, “Finite-Element Coefficient Generation,” 2.3, “Formulate Transient Equations,” specifically Section 2.3.2 and Section 2.3.7, 2.4, “Apply Constitutive Relationships,” specifically Section 2.4.1 and Section 2.4.7, 2.5, “Compute Solution to Transient Equations,” and 2.6, “Provide Input/Output Data Files,” of the FEHM RD are verified by this test.

2.10.4.1.4 Required Inputs. Problem input is provided in the following files:

- *dual1.in*: Basic input data, case 1;
- *dual2.in*: Basic input data, case 2;
- *dual3.in*: Basic input data, case 3;
- *dual.geom*: Geometry data used for the above cases.

2.10.4.1.5 Expected Outputs. Values from FEHM for pressure vs. time at the wellbore fracture node,  $r = 0.1398$  (i.e., interior node closest to  $r_w = 0.17528$ ), will be output, nondimensionalized, and compared to the Warren and Root analytical solution. Values within 5% of the analytical solution for  $\tau > 100$  will be considered acceptable.

Required output files for these tests are the:

- History data plot files (*dual1.his*, *dual2.his*, *dual3.his*).

## 2.11 Test of Heat and Mass Transfer in Porous Media

### 2.11.1 Purpose

In some special instances, the flow of a hot fluid in a confined aquifer may be described by an analytical expression. Faust and Mercer (1976) present an analytical solution developed by Avdonin for one-dimensional, radial fluid flow with heat conduction in the orthogonal direction. In addition to testing the coupled heat and mass transfer implementation for a single-phase system, the results will also demonstrate that the radial geometry is correctly implemented with different grid spacings.

### 2.11.2 Functional Description

The test suite consists of a set of simulations of 1-D radial flow into a confined aquifer. The same flow problem is run with the domain divided into 84 nodes (41 elements), 400 nodes (199 elements), and 800 nodes (399 elements). In addition to demonstrating that the heat and mass transfer problem has been correctly formulated, and that the radial geometry has been correctly implemented, this test will assess the impact of finer spatial discretization on accuracy.

### 2.11.3 Assumptions and Limitations

The Avdonin analytical solution presented by Faust and Mercer (1976) takes the form

$$u(\omega, \tau) = \frac{1}{\Gamma(v)} \left( \frac{\omega^2}{4\tau} \right)^v \int_0^1 \exp\left(-\frac{\omega^2}{4\tau s}\right) \operatorname{erfc}\left(\frac{\alpha s \sqrt{\tau}}{2\sqrt{1-s}}\right) \frac{ds}{s^{v+1}}$$

$$\text{where } \omega = \frac{2r}{b},$$

$$\tau = \frac{4\kappa_t t}{c_t \rho_t b^2},$$

$$v = \frac{qc_w \rho_w}{4\pi b \kappa_t},$$

$$\alpha = \left( \frac{\kappa_r c_r \rho_r}{\kappa_t c_t \rho_t} \right)^{1/2},$$

$\operatorname{erfc}$  is the complimentary error function,  $\Gamma$  is the gamma function,  $r$  is the radial coordinate,  $q$  is the injection flow rate,  $u$  is a dimensionless temperature change, and the integration variable  $s$  represents a dimensionless time. The subscripts  $r$ ,  $w$ ,  $t$  refer to rock, water, and total (rock and water) respectively. The temperature is computed using:

$$T = T_0 - u(\omega, \tau) \cdot (T_0 - T_{in}) .$$

This problem assumes one-dimensional, radial, steady-state flow and unsteady heat transport in a single-phase liquid. It simulates the injection of cool water into a geothermal reservoir. Figure 12 shows the problem

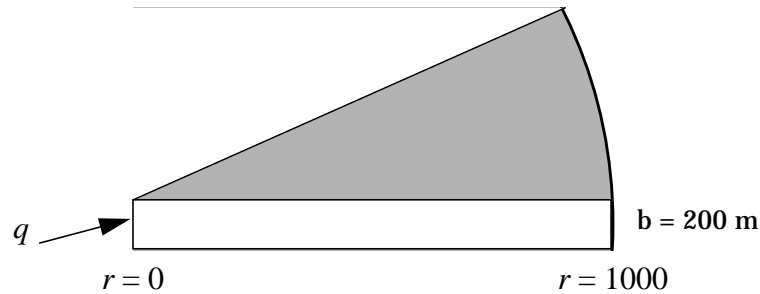


**Figure 12. Schematic diagram of the Avdonin problem geometry.**

geometry with boundary and initial conditions. Input parameters defining the problem are given in Table XIII.

## 2.11.4 Summary of Test Cases

### 2.11.4.1 Heat and Mass Transfer in a 1-D Radial Aquifer

**2.11.4.1.1 Function Tested.** This test verifies that FEHM correctly models 1-dimensional heat and mass transport for radial flow and demonstrates the impact of finer spatial discretization on accuracy.

**2.11.4.1.2 Test Scope.** This test case is a verification test.

**2.11.4.1.3 Requirements Tested.** Requirements 2.2, “Finite-Element Coefficient Generation,” 2.3, “Formulate Transient Equations,” specifically Section 2.3.2 and Section 2.3.7, 2.4, “Apply Constitutive Relationships,” specifically Section 2.4.1, 2.5, “Compute Solution to Transient Equations,” and 2.6, “Provide Input/Output Data Files,” of the FEHM RD are verified by this test.

**2.11.4.1.4 Required Inputs.** Problem input is provided in the following files:

- *avdonin.in*: Basic input data used in conjunction with the following geometry data files
- *avdonin.geom.84* (84 nodes, 42 elements),
- *avdonin.geom.400* (400 nodes, 199 elements), or
- *avdonin.geom.800* (800 nodes, 399 elements).

**2.11.4.1.5 Expected Outputs.** Values from FEHM, for temperature versus time at a fixed radius ( $r = 37.5$  m), and values for temperature versus radius ( $r = 0 - 1000$  m) at a specified time, ( $t = 1.e9$  s) will be output and compared to the analytical solution. Values within 5% of the analytical solution will be considered acceptable.

Required output files for these tests are the:

- History data plot files (*avdonin84.his*, *avdonin400.his*, *avdonin800.his*), and

**Table XIII. Input Parameters for the Avdonin Problem**

Parameter	Symbol	Value
Reservoir permeability	$k$	$10^{-12} \text{ m}^2$
Reservoir porosity	$\phi$	0.2
Rock thermal conductivity	$k_r$	$20 \frac{\text{W}}{\text{m} \cdot \text{K}}$
Rock density	$\rho_r$	$2500 \text{ kg/m}^3$
Rock specific heat	$C_r$	$1000 \frac{\text{J}}{\text{kg} \cdot \text{K}}$
Reservoir thickness	$b$	200 m
Node spacing (vertical)	$\Delta b$	200 m
Reservoir length (radial)	$r$	0 - 1000 m
Node spacing (radial)	$\Delta r$	25 m
84 node domain		0.64 - 12 m
400 node domain		0.32 - 12 m
800 node domain		0.32 - 12 m
Injection rate	$q$	10 kg/s
Injection temperature	$T_{in}$	160 °C
Initial temperature	$T_0$	170 °C
Initial pressure	$P_0$	5 MPa
Time step	$\Delta t$	50 days
Total elapsed time	$t$	$1 \cdot 10^9 \text{ s}$
Boundary conditions:	At $r = r_w = 0 \text{ m}$ ,	$T(t) = 160^\circ\text{C}$ , $q = 10 \text{ kg/s}$
	At $r = 1000 \text{ m}$ ,	$T(t) = 170^\circ\text{C}$ , $P(t) = 5 \text{ MPa}$

- AVS contour data plot files for  $t = 1.e9 \text{ s}$   
(*avdonin84.10002\_sca\_node*, *avdonin400.10002\_sca\_node*,  
*avdonin800.10002\_sca\_node*).

## 2.12 Test of Free Convection

### 2.12.1 Purpose

Free convection in porous media is a well documented phenomenon. Semi analytical techniques (linear stability analysis LSA) have been developed to predict the onset of convection in simple domains for single phase incompressible fluids (Stauffer et al., 1997). LSA coupled with basic scaling analysis provides several ways to check the validity of FEHM in replication of natural convection.

### 2.12.2 Functional Description

The verification consists of a set of simulations that use the same regular grid throughout. A reduced temperature gradient is employed to limit nonlinear effects. Two test cases are provided to give the user a simple way to check that FEHM is running as expected. They will show that FEHM produces flow patterns consistent with experimental results and other computer simulations of free convection.

### 2.12.3 Assumptions and Limitations

Free convection is modeled in a 200 m square/cube. Boundaries are no flow with respect to mass. Top and bottom temperatures are fixed, while the sides are no flow with respect to heat. The initial condition is a linear temperature gradient with depth, keeping the middle of the box fixed at 60°C (Figure 13).

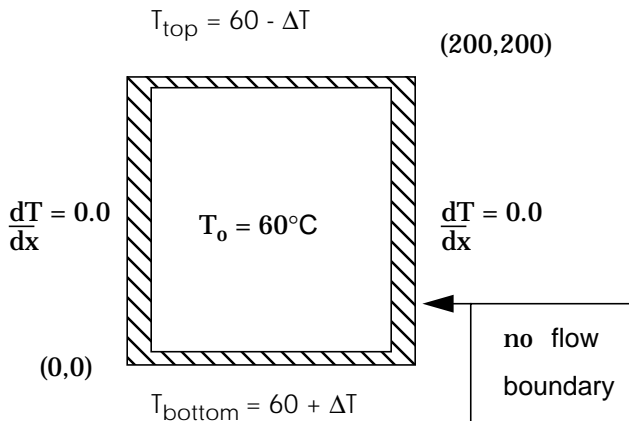


**Figure 13. Schematic diagram of 2-D free convection problems.**

The Rayleigh number  $Ra$  for free convection of an incompressible fluid in a saturated porous media heated from below takes the form:

$$Ra_{(water)} = \frac{\alpha H^2 k g C_p \Gamma \rho^2}{\mu \kappa}$$

where  $\alpha$  is thermal expansivity (1/K),  $H$  is domain height (m),  $k$  is intrinsic permeability (m<sup>2</sup>),  $g$  is gravity (m/s<sup>2</sup>),  $C_p$  is heat capacity [J / (kg

K)],  $\Gamma$  is temperature gradient (K / m),  $\mu$  is viscosity (Pa•s),  $\kappa$  is equivalent thermal conductivity (rock+fluid) [J / (m K)] and  $\rho$  is density (kg/m<sup>3</sup>).

Stauffer et al. (1997) have shown that for a compressible gas (i.e. air)

$$Ra_{(air)} = \frac{\alpha H^2 k g (C_p \Gamma - g) \rho^2}{\mu \kappa} .$$

Free convection is predicted to occur above the critical Rayleigh number ( $Ra_c$ ) which is shown to be  $Ra_c = 4 \cdot \pi^2 = 39.47$  for both single phase air and pure liquid water. Scale analysis of the incompressible system of equations leads to the relation Nusselt number  $Nu = Ra/40$  (Bejan, 1995).

Since the computer is more stable than any natural system, a small perturbation or push is needed to trigger the convective flow. This is accomplished by increasing the lower left or right hand temperature by 2-5 °C for the first time step.

A series of runs were performed to obtain the critical Rayleigh number plot for air and water (Figure 14). Values of Nu computed for the FEHM runs (neglecting velocity) compared (numerically) to the semi-analytical solution had an RMS Error of 0.0307 for air and 0.0141 for water, and were considered acceptable. Due to the complexity of these runs, only two test cases, one for water, and one for air are used for the test suite. When these tests are run, the final steady state temperature profile will be compared to that of the previously generated (check) output (found in *conv2d\_air\_check.10002\_sca\_node* and *conv2d\_water\_check.10002\_sca\_node*) to ensure the continued performance of FEHM. Input parameters defining the problem are given in Table IV .

## 2.12.4 Summary of Test Cases

### 2.12.4.1 2-D Free Convection in a Square

2.12.4.1.1 Function Tested. This test verifies that FEHM correctly models 2-dimensional free convection.

2.12.4.1.2 Test Scope. This test case is a verification test.

2.12.4.1.3 Requirements Tested. Requirements 2.2, "Finite-Element Coefficient Generation," 2.3, "Formulate Transient Equations," specifically Section 2.3.2, Section 2.3.3, and Section 2.3.7, 2.4, "Apply Constitutive Relationships," specifically Section 2.4.1, Section 2.4.2, and Section 2.4.4, 2.5, "Compute Solution to Transient Equations," and 2.6, "Provide Input/Output Data Files," of the FEHM RD are verified by this test.

2.12.4.1.4 Required Inputs. Input is provided in the following files:

- *conv2d\_water.dat*: Basic input and geometry data (2500 nodes, 2401 elements) for the water convection run.
- *conv2d\_air.dat*: Basic input data and geometry data (2500 nodes, 2401 elements) for the air convection run.

2.12.4.1.5 Expected Outputs. When these tests are run, the final steady state temperature and velocity (magnitudes) fields will



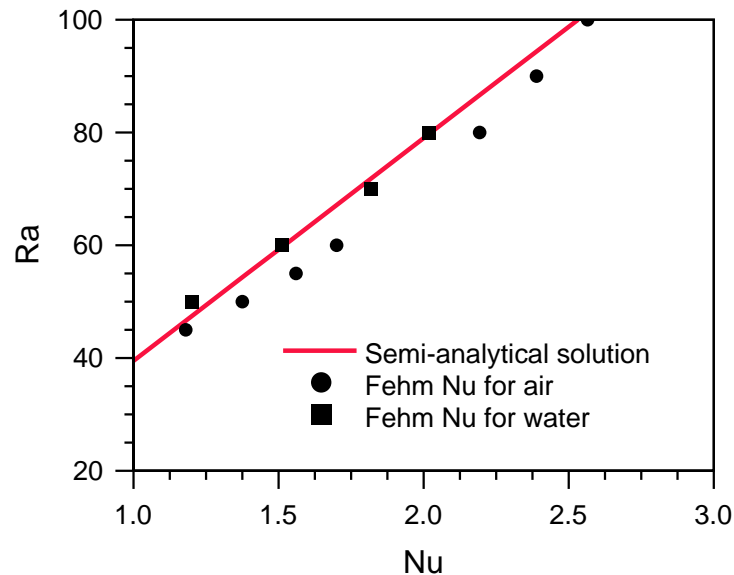


**Figure 14. Plot of Nu vs Ra for air and water from FEHM simulations for determination of  $Ra_c$ .**

be output and compared to that of the check output to ensure the continued performance of FEHM. It is possible due to the nature of the problem for the convection cell to form with a clockwise or counter-clockwise rotation. Values for the temperature field within 0.1% of the check solution will be considered acceptable if the cells are convecting in the same direction. When cells are convecting in opposite directions the maximum errors in the temperature field will be greater than 1% and the magnitude of volume flux will be used for comparison. A root mean square error of the difference between the two simulations volume flux magnitudes less than or equal to 0.001 will be considered acceptable.

Required output files for these tests are the:

- AVS contour data plot files for  $t = 4.e5$  days  
(*conv2d\_air.10002\_sca\_node*, *conv2d\_air.10002\_vec\_node*,  
*conv2d\_water.10002\_sca\_node*,  
*conv2d\_water.10002\_vec\_node*).

### 2.12.5 Acknowledgement

This test suite was developed by Philip H. Stauffer of the Los Alamos Hydrology, Geochemistry, and Geology Group (EES-6) of the Earth and Environmental Science Division, and incorporated into the Validation Test Plan in April 2002.

**Table XIV. Input Parameters for the 2-D Free Convection Problem**

Parameter	Symbol	Value
Fluid thermal conductivity		at 60 °C $\frac{W}{m \cdot K}$
air	$\kappa_f$	0.028
water		0.651
Rock thermal conductivity	$\kappa_r$	$2.7 \frac{W}{m \cdot K}$
Rock density	$\rho_r$	2700 kg/m <sup>3</sup>
Rock specific heat	$C_r$	$1000 \frac{J}{kg \cdot K}$
Porosity		
air	$\phi$	0.5
water		0.2
Initial total pressure		
air	$P_{ini}$	0.1 MPa
water		10. MPa
Intrinsic permeability		
air	$k$	$1.1 \times 10^{-07} m^2$
water		$9.6 \times 10^{-13} m^2$
Height	$H$	200 m
Initial temperature	$T_0$	60 °C
Top boundary temperature		
air	$T_{top}$	58 °C
water		50 °C
Bottom boundary temperature		
air	$T_{bottom}$	62 °C
water		70 °C
Total elapsed time	$t$	$1 \times 10^6$ days
Equivalent thermal conductivity	$\kappa = \kappa_r(1 - \phi) + \kappa_f \cdot \phi$	

## 2.13 Test of Toronyi Two-Phase Problem

### 2.13.1 Purpose

This problem has evolved into a standard test case for checking two-phase heat and mass transfer (Toronyi and Farouq Ali, 1977). Fluid is discharged from a two-phase geothermal reservoir, and the saturation at each node is simulated. There is no analytical solution for this problem; comparisons must be made with other transient heat and mass transfer codes. The problem tests the multiphase capabilities severely, and in doing so, verifies that the liquid and vapor phase transport sub-models of FEHM are working properly.

### 2.13.2 Functional Description

The test suite consists of a simulation of fluid discharge from a two-phase aquifer using both a standard coordinate grid definition and a finite difference model (fdm) grid definition. In addition to demonstrating that the heat and mass transfer problem has been correctly formulated, it will demonstrate that phase partitioning has been correctly implemented. It will also demonstrate that fdm grids have been correctly implemented.

### 2.13.3 Assumptions and Limitations

Fluid is discharged at a constant rate from the two-phase geothermal reservoir until 19% of the original water mass has been removed (78.31 days). There is no flow across the peripheral boundaries. Temperature is controlled by the saturation pressure/temperature curve.

The solution is verified by comparison of FEHM results to those found by Thomas and Pierson (1978). Thomas and Pierson used cell centered elements while FEHM uses node centered, so boundary elements were adjusted to provide matching central nodes using the standard coordinate grid definition. The reservoir model (solution domain) is shown in Fig. 15 along with the node saturations obtained by Thomas and Pierson. The asymmetry in the solution is due to the off-center location of the discharge node and elongated mesh. Table XV lists the input parameters for the Toronyi problem.

### 2.13.4 Summary of Test Cases

#### 2.13.4.1 Toronyi Two-Phase Problem

2.13.4.1.1Function Tested. This test verifies that FEHM has correctly implemented heat and mass transfer and phase partitioning.

2.13.4.1.2Test Scope. This test case is a verification test.

2.13.4.1.3Requirements Tested. Requirements 2.2, "Finite-Element Coefficient Generation," 2.3, "Formulate Transient Equations," specifically Section 2.3.2 and Section 2.3.7, 2.4, "Apply Constitutive Relationships," specifically Section 2.4.1 and Section 2.4.4, 2.5, "Compute Solution to Transient Equations," and 2.6, "Provide Input/Output Data Files," of the FEHM RD are verified by this test.

2.13.4.1.4Required Inputs. Problem input is provided in the following file:

- *toronyi.in*: Basic input and geometry data using the standard coordinate grid definition (64 nodes, 49 elements).

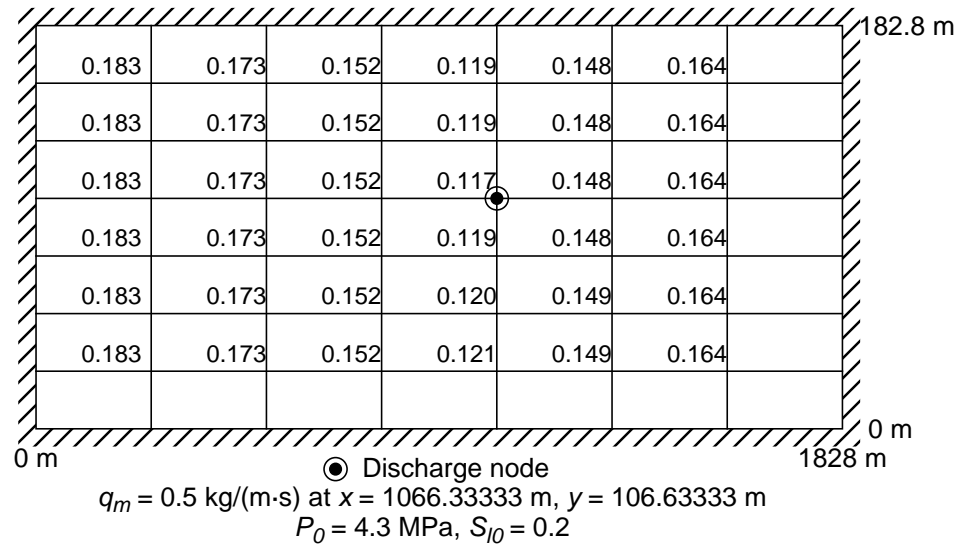


**Figure 15. Solution domain and saturation results for the Toronyi problem.**

- *toronyi\_fdm.in*: Basic input using an fdm grid definition.
- 2.13.4.1.5 Expected Outputs. Values from FEHM, for saturation at each interior node at time  $t = 78.31$  days, will be output and compared to the Thomas and Pierson (1978) saturation data. Values of saturation within 5% of the Thomas and Pierson solution will be considered acceptable.
- Required output file for this test is the:
- AVS contour data plot files for  $t = 78.31$  days  
 (*toronyi.10002\_sca\_node*, *toronyi\_fdm.10002\_sca\_node*).

**Table XV. Input Parameters for the Toronyi Two-Phase Problem**

Parameter	Symbol	Value
Reservoir permeability	$k$	$9.869 \times 10^{-13} \text{ m}^2$
Reservoir porosity	$\phi$	0.05
Rock thermal conductivity	$\kappa_r$	$1.73 \frac{\text{W}}{\text{m} \cdot \text{K}}$
Rock density	$\rho_r$	$2500 \text{ kg/m}^3$
Rock specific heat	$C_r$	$1000 \frac{\text{J}}{\text{kg} \cdot \text{K}}$
Aquifer length	$x$	1828 m
Node spacing ( $x$ ) <sup>‡</sup>	$\Delta x$	304.666
Aquifer width	$y$	182.8 m
Node spacing ( $y$ ) <sup>‡</sup>	$\Delta y$	30.4666
Reference temperature	$T$	250 °C
Initial pressure	$P_0$	4.3 MPa
Initial water saturation	$S_{l0}$	0.2
Residual liquid saturation	$S_{lr}$	0.05
Residual vapor saturation	$S_{lv}$	0.05
Capillary pressure at zero saturation	$P_{capmax}$	1.0 MPa
Saturation at which capillary pressure goes to zero	$S_{lmax}$	1.0
Aquifer discharge	$q_m$	$0.5 \frac{\text{kg}}{\text{m} \cdot \text{s}}$
Initial pressure	$P_0$	4.4816 MPa
Time step	$\Delta t$	10 days
Total elapsed time	$t$	78.31 days
Boundary conditions: At $x = 1066.33333$ , $y = 106.63333$ $q_m = 0.5 \frac{\text{kg}}{\text{m} \cdot \text{s}}$		
No flow across peripheral boundaries		
<sup>‡</sup> For the FEHM simulation node spacing around the periphery is half the general spacing to facilitate comparison with Thomas and Pierson who used cell centered elements whereas FEHM uses node centered elements.		

## 2.14 Test of DOE Code Comparison Project Problem Five, Case A

### 2.14.1 Purpose

This model of a 2-D areal reservoir with multiphase flow was developed as part of a DOE code comparison project (Molloy, 1980). The two-phase (water/water vapor), heat and mass transfer problem is characterized by a moving two-phase boundary. The modeled region has a cold fluid boundary which provides fluid to the system as discharge occurs through a well. Numerical difficulties can occur as nodes go from two-phase to condensed water. This problem is a good test for the two-phase routines, as well as the phase change algorithm. In addition, this problem provides a test of the code restart capabilities as the initial temperature field is input through use of a restart file. There is no analytical solution for this problem, but results from other codes (Pritchett, 1980) are available as a check for FEHM.

### 2.14.2 Functional Description

The test suite consists of a simulation of fluid discharge from a two-phase, 2-D aquifer. Fluid produced at the production well is replaced by cold water recharge over the length of one of the lateral boundaries. In addition to demonstrating that the heat and mass transfer problem has been correctly formulated, it will demonstrate that phase partitioning has been correctly implemented.

### 2.14.3 Assumptions and Limitations

Fluid is discharged from the two-phase geothermal reservoir while cold water recharge occurs over one lateral boundary. The other three boundaries are considered to be impermeable and non-conductive. The geometry and boundary conditions are shown in Fig. 17. Of particular note is the variable initial temperature field and the prescribed pressure and temperature boundary. Table XVI lists the input parameters for the DOE Code Comparison Project problem. A Corey type relative permeability function is used for this model [see the “Models and Methods Summary” of the FEHM Application (Zyvoloski et al. 1999), page 64]. The reader is referred to Pritchett (1980) for a more detailed discussion of this problem and the code comparison. The solution is verified by comparison of FEHM results to those obtained from Pritchett.

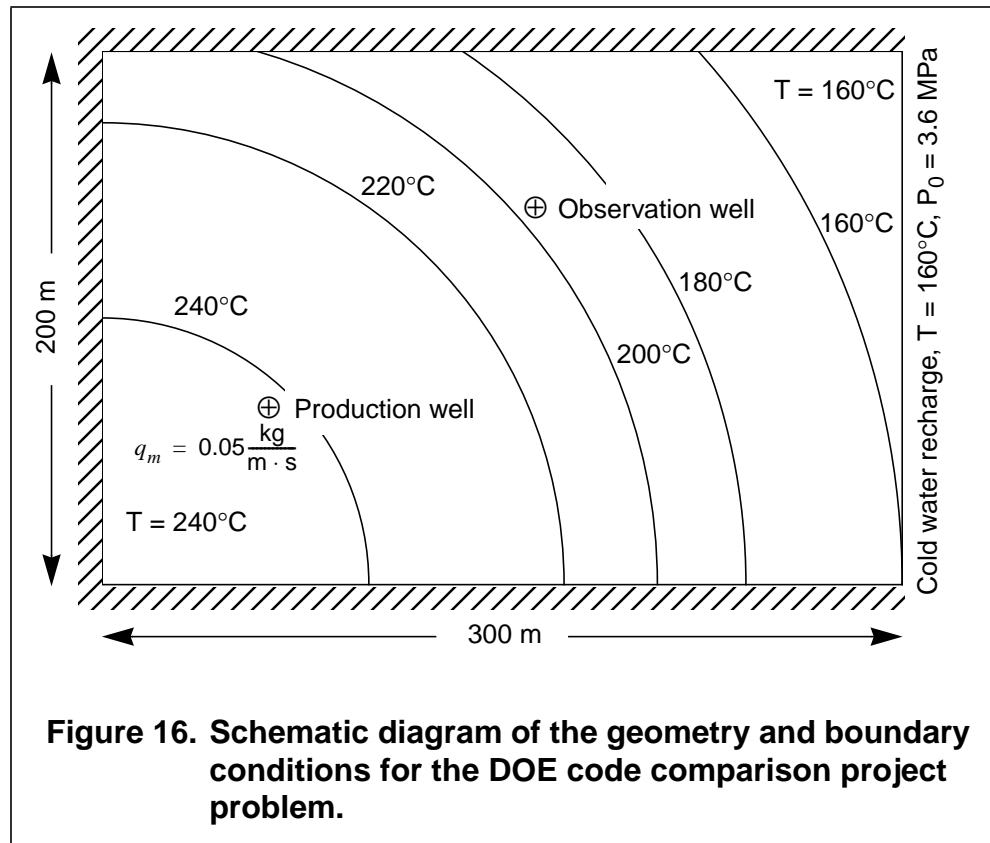
### 2.14.4 Summary of Test Cases

#### 2.14.4.1 DOE Code Comparison Project Problem Five

2.14.4.1.1 Function Tested. This test verifies that FEHM has correctly implemented heat and mass transfer and phase partitioning.

2.14.4.1.2 Test Scope. This test case is a verification test.

2.14.4.1.3 Requirements Tested. Requirements 2.2, “Finite-Element Coefficient Generation,” 2.3, “Formulate Transient Equations,” specifically Section 2.3.2 and Section 2.3.7, 2.4, “Apply Constitutive Relationships,” specifically Section 2.4.1 and Section 2.4.4, 2.5, “Compute Solution to Transient Equations,” 2.6, “Provide Input/Output Data Files,” and 2.7, “Provide Restart Capability,” specifically Section 2.7.2 and Section 2.7.3, of the FEHM RD are verified by this test.



2.14.4.1.4 Required Inputs. Problem input is provided in the following files:

- *doe.dat*: Basic input and geometry data (140 nodes, 117 elements)
- *doe.ini*: Initial temperature field, pressure, and saturation.

2.14.4.1.5 Expected Outputs. Values from FEHM for production well temperature and pressure, and pressure at the observation well versus time will be output and compared to the data from other codes. Values within 5% of those obtained by the other codes will be considered acceptable.

The required output file for this test is the:

- History data plot file (*doe.his*).

**Table XVI. Input Parameters for the DOE Code Comparison Project, Problem 5, Case A**

Parameter	Symbol	Value
Reservoir permeability	$k$	$2.5 \times 10^{-14} \text{ m}^2$
Reservoir porosity	$\phi$	0.35
Rock thermal conductivity	$\kappa_r$	$1 \frac{\text{W}}{\text{m} \cdot \text{K}}$
Rock density	$\rho_r$	$2563 \text{ kg/m}^3$
Rock specific heat	$C_r$	$1010 \frac{\text{J}}{\text{kg} \cdot \text{K}}$
Reservoir length	$x$	300 m
Reservoir thickness	$y$	200 m
Node spacing <sup>‡</sup>	$\Delta x, \Delta y$	25 m
Liquid residual saturation	$S_{lr}$	0.3
Gas residual saturation	$S_{vr}$	0.1
Reservoir discharge	$q_m$	$0.05 \frac{\text{kg}}{\text{m} \cdot \text{s}}$
Initial Pressure	$P_0$	3.6 MPa
Time step	$\Delta t$	30 - 60 days
Total elapsed time	$t$	10 years
Production well coordinates: $x = 62.5 \text{ m}, y = 62.5 \text{ m}$		
Observation well coordinates: $x = 162.5 \text{ m}, y = 137.5 \text{ m}$		
Initial temperature distribution: $[T \text{ in } ^\circ\text{C}, r \text{ in m ( } r = \sqrt{x^2 + y^2} \text{ )}]$ :		
$T(x, y, 0) = \begin{cases} 240 & r \leq 100 \\ 240 - 160\left(\frac{r-100}{200}\right)^2 + 80\left(\frac{r-100}{200}\right)^4 & 100 < r < 300 \\ 160 & r \geq 300 \end{cases}$		
Boundary conditions: At $x = 62.5 \text{ m}, y = 62.5 \text{ m}$ $q_m = 0.5 \frac{\text{kg}}{\text{m} \cdot \text{s}}$		
At $x = 300 \text{ m}, y = 0 - 200 \text{ m}$ $T = 160 ^\circ\text{C}, P = P_0 = 3.6 \text{ MPa}$		
At $x = 0 \text{ m}, y = 0 \text{ m}, y = 200 \text{ m}$ Impermeable, non-conductive		
<sup>‡</sup> For the FEHM simulation node spacing around the periphery is half the general spacing (12.5 m).		



## 2.15 Test of Heat Pipe

### 2.15.1 Purpose

The thermal hydrologic heat pipe problem tests several important processes in FEHM. These are:

- The air-water-heat subsurface flow;
- Unsaturated flow with high capillary forces;
- Air-water vapor diffusion process; and
- Finite difference and finite element grids.

### 2.15.2 Functional Description

The test suite consists of simulations of a thermal hydrologic heat pipe using both a standard coordinate grid definition and a finite difference model (fdm) grid definition. In addition to demonstrating that the heat and mass transfer problem has been correctly formulated, it will demonstrate that unsaturated flow with high capillary forces and the air-water vapor diffusion process are implemented correctly. It will also demonstrate that fdm grids have been correctly implemented.

### 2.15.3 Assumptions and Limitations

The problem consists of a small vertical column heated from below. This causes the liquid phase to rise in the column with the attendant increase in saturation in the top part of the grid. The increase in the water saturation forces the vapor phase downward. The geometry of the column is defined using both a standard coordinate grid (2-D) and an fdm grid description (3-D).

The output chosen for comparison was internodal mass flux of the gas and liquid phases at the top, middle, and bottom of the column. The mass fluxes are sensitive to all the processes listed above and most of the input quantities.

### 2.15.4 Summary of Test Cases

#### 2.15.4.1 Thermal Hydrologic Heat Pipe Problem

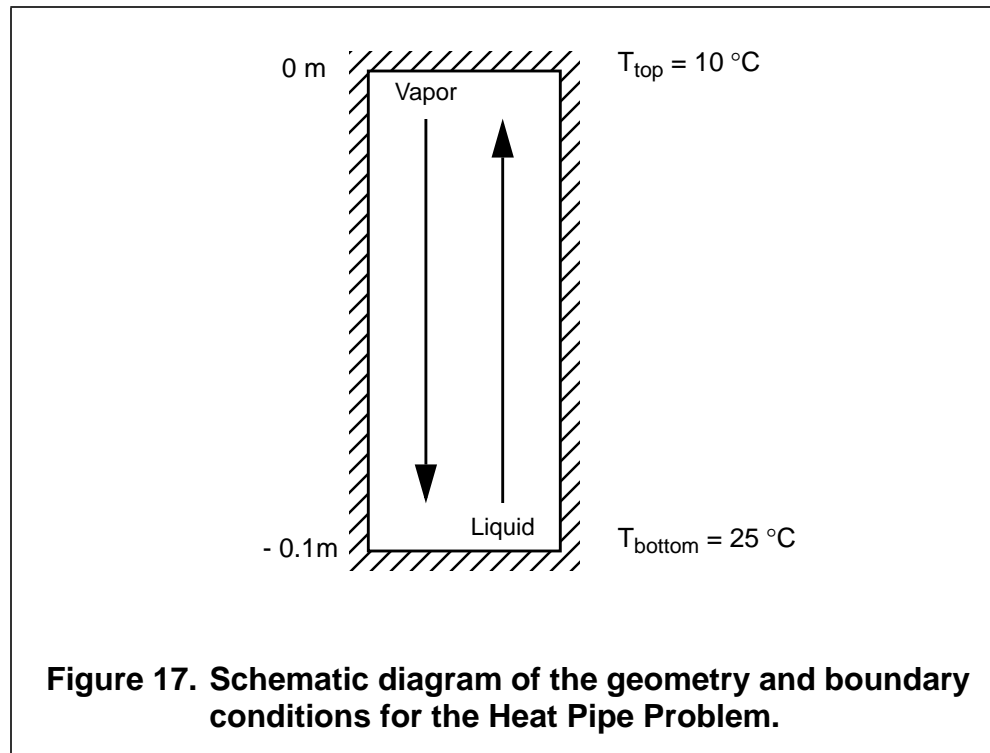
2.15.4.1.1Function Tested. This test verifies that FEHM has correctly implemented heat and mass transfer and phase partitioning.

2.15.4.1.2Test Scope. This test case is a verification test.

2.15.4.1.3Requirements Tested. Requirements 2.2, "Finite-Element Coefficient Generation," 2.3, "Formulate Transient Equations," specifically Section 2.3.2 and Section 2.3.3, 2.4, "Apply Constitutive Relationships," specifically Section 2.4.1, Section 2.4.2, and Section 2.4.4, 2.5, "Compute Solution to Transient Equations," and 2.6, "Provide Input/Output Data Files," of the FEHM RD are verified by this test.

2.15.4.1.4Required Inputs. Problem input is provided in the following files:

- *heat\_pipe\_fe.dat*: Basic input used with standard coordinate grid.
- *fe.grid*: Geometry data in standard coordinate format (102 nodes, 50 elements).



- *heat\_pipe\_fdm.dat*: Basic input used with fdm grid definition.
- *fdm.grid*: Geometry file containing fdm grid definition.

2.15.4.1.5 Expected Outputs. Values from FEHM for the steady state vapor and liquid mass flux will be output for both the standard coordinate and fdm grid definition runs and compared to each other. Values within 5% will be considered acceptable.

The required output files for this test are the:

- FEHM generalized summary output files (*heat\_pipe\_fe.out*, *heat\_pipe\_fdm.out*).

**Table XVII. Input Parameters for the Heat Pipe Problem**

Parameter	Symbol	Value
Reservoir permeability	$k$	$3.9 \times 10^{-14} \text{ m}^2$
Reservoir porosity	$\phi$	0.5
Rock thermal conductivity	$\kappa_r$	$0.6 \frac{\text{W}}{\text{m} \cdot \text{K}}$
Rock density	$\rho_r$	$1500 \text{ kg/m}^3$
Rock specific heat	$C_r$	$1100 \frac{\text{J}}{\text{kg} \cdot \text{K}}$
Coordinate Grid (2-D)		
Column width	$x$	2 m
Column height	$y$	0.1 m
Node spacing	$\Delta x$	2 m
	$\Delta y$	0.002 m
FDM Grid (3-D)		
Column width, depth	$x, y$	1 m
Column height	$z$	0.1 m
Node spacing	$\Delta x, \Delta y$	1 m
	$\Delta z$	0.002
Initial liquid saturation	$S_{l0}$	0.28
Liquid residual saturation	$S_{lr}$	0.0
Cutoff saturation	$S_{cutoff}$	0.01
van Genuchten model parameters		
Inverse of air entry pressure	$\alpha_G$	$3.6 \text{ m}^{-1}$
Power in formula	$n$	1.56
Initial Pressure	$P_0$	0.1 MPa
Time step	$\Delta t$	0.01 - 1608 days
Total elapsed time	$t$	10000 days
Top boundary temperature	$T_{top}$	10 °C
Bottom boundary temperature	$T_{bottom}$	25 °C
Initial temperature distribution: $T = 10. - 150. \times \text{height} \text{ (}^\circ\text{C)}$		

## 2.16 Test of Dry-Out of a Partially Saturated Medium

### 2.16.1 Purpose

Calculations of fluid flow in the presence of repository heat require the simultaneous solution of a heat and mass transfer system consisting of water, water vapor, and air. This test case exercises the code option that solves this type of flow and heat transport problem by passing air through a one-dimensional, partially saturated medium. The air evaporates water and removes it from the system. A dry-out zone progresses from the injection region through the flow path at a rate that can be predicted using an analytical solution.

### 2.16.2 Functional Description

The test suite consists of a simulation of the rate of movement of a dry region, starting at a condition of constant saturation throughout the flow path. Two cases are considered: a system without vapor pressure lowering, and one with vapor pressure lowering, which lowers the water-vapor-carrying capacity of the injected air.

### 2.16.3 Assumptions and Limitations

If dry air is injected into a partially saturated medium containing immobile liquid water, the water evaporates until the partial pressure of water vapor in the gas reaches its equilibrium vapor pressure. For a mass flow rate of air of  $\dot{m}_a$ , and assuming ideal gas mixture conditions, the corresponding rate of removal of water in the gas  $\dot{m}_w$  is given by

$$\dot{m}_w = \frac{M_w P_w \dot{m}_a}{M_a P_a}$$

where  $M_w$  and  $M_a$  are molecular weights and  $P_w$  and  $P_a$  are partial pressures, with the subscripts  $w$  and  $a$  referring to the water and air, respectively. Assuming that the vaporization of water into the flowing air occurs at a rapid rate, which reflects the assumption of rapid kinetics present in the FEHM code, a good approximation of dry-out can be obtained by assuming that the dry-out occurs as a sharp front. The rate of progression of this front can then be shown to be

$$r_{dry} = \frac{L \dot{m}_a M_w P_w}{\phi S V \rho_w M_a P_a}.$$

In this equation,  $L$  is the flow path length,  $V$  is the volume, and  $S$  is the liquid saturation. The problem is depicted in Fig. 18. Table XVI lists the input parameters used in this comparison. When vapor pressure lowering is included, the value of  $P_w$  in the equation is lower than it would be in the absence of this effect. The capillary pressure in these simulations is adjusted so that it is a constant value throughout the column, regardless of saturation. Its value is set using the linear capillary pressure model such that the water vapor pressure is lowered by a factor of 2.

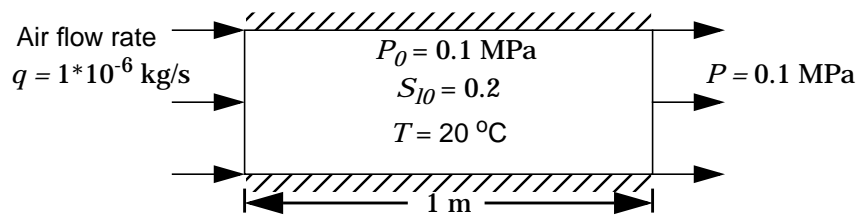


**Figure 18. Schematic drawing of the geometry and boundary conditions for the Dry-Out Simulations.**

**Table XVIII. Input Parameters for the Dry-Out Simulations**

Parameter	Symbol	Value
Air flow rate	$q$	$1.0 \cdot 10^{-6}$ kg/s
Volume of path	$V$	$1 \text{ m}^3$
Length of path	$L$	$1 \text{ m}$
Node spacing	$\Delta l$	$0.005 \text{ m}$
Porosity	$\phi$	$0.05$
Time step		
w/o vapor pressure lowering	$\Delta t$	$0.001 - 1.5 \text{ days}$
with vapor pressure lowering		$0.001 - 3 \text{ days}$
Total elapsed time		
w/o vapor pressure lowering	$t$	$500 \text{ days}$
with vapor pressure lowering		$1000 \text{ days}$
Total System Pressure	$P_0$	$0.1 \text{ MPa}$
Temperature (from which $P_w$ is computed)	$T$	$20 \text{ }^\circ\text{C}$
Initial water saturation	$S_{l0}$	$0.2$
Residual liquid saturation	$S_{lr}$	$0.3$
Residual vapor saturation	$S_{lv}$	$0.3$
Maximum liquid saturation	$S_{lmax}$	$1.0$
Maximum vapor saturation	$S_{vmax}$	$1.0$
Boundary conditions:	At $l = 0$ At $l = 1$	$q = 1 \cdot 10^{-6} \text{ kg/s}$ $P = 0.1 \text{ MPa}$

## 2.16.4 Summary of Test Cases

### 2.16.4.1 Dry-Out Without Vapor Pressure Lowering

2.16.4.1.1Function Tested. This test verifies that FEHM correctly simulates the dry-out of a partially saturated medium in the absence of vapor pressure lowering.

2.16.4.1.2Test Scope. This test case is a verification test.

2.16.4.1.3Requirements Tested. Requirements 2.2, “Finite-Element Coefficient Generation,” 2.3, “Formulate Transient Equations,” specifically Section 2.3.3 and Section 2.3.7, 2.4, “Apply Constitutive Relationships,” specifically Section 2.4.2 and Section 2.4.4, 2.5, “Compute Solution to Transient Equations,” and 2.6, “Provide Input/Output Data Files,” of the FEHM RD are verified by this test.

2.16.4.1.4Required Inputs. Problem input is provided in the following files:

- *dryout1.in*: Basic input data
  - *dryout.geom*: Geometry data. The grid consists of 201 x 2 nodes, thus simulating a one-dimensional flow system
- 2.16.4.1.5Expected Outputs. Values from FEHM for the position of the dry-out front at five different times should agree with the analytical solution. Position within 5% of the predicted value will be considered acceptable.

Required output files for this test are the:

- AVS contour data plot files for  $t = 100, 200, 300, 400$  and  $500$  days (*dryout1.10002\_sca\_node*, *dryout1.10003\_sca\_node*, *dryout1.10004\_sca\_node*, *dryout1.10005\_sca\_node*, *dryout1.10006\_sca\_node*).

### 2.16.4.2 Dry-Out With Vapor Pressure Lowering

2.16.4.2.1Function Tested. This test verifies that FEHM correctly simulates the dry-out of a partially saturated medium when vapor pressure lowering is included.

2.16.4.2.2Test Scope. This test case is a verification test.

2.16.4.2.3Requirements Tested. Requirements 2.2, “Finite-Element Coefficient Generation,” 2.3, “Formulate Transient Equations,” specifically Section 2.3.3 and Section 2.3.7, 2.4, “Apply Constitutive Relationships,” specifically Section 2.4.2 and Section 2.4.4, 2.5, “Compute Solution to Transient Equations,” and 2.6, “Provide Input/Output Data Files,” of the FEHM RD are verified by this test.

2.16.4.2.4Required Inputs. Problem input is provided in the following files:

- *dryout2.in*: Basic input data
- *dryout.geom*: Geometry data. The grid consists of 201 x 2 nodes, thus simulating a one-dimensional flow system

2.16.4.2.5Expected Outputs. Values from FEHM for the position of the dry-out front at five different times should agree with the analytical solution. Position within 5% of the predicted value will be considered acceptable.

Required output files for this test are the:

- AVS contour data plot files for  $t = 200, 400, 600, 800$  and  $1000$  days (*dryout2.10002\_sca\_node*, *dryout2.10003\_sca\_node*, *dryout2.10004\_sca\_node*, *dryout2.10005\_sca\_node*, *dryout2.10006\_sca\_node*).

## 2.17 Test of One Dimensional Reactive Solute Transport

### 2.17.1 Purpose

Tracers are used extensively to determine travel times and reservoir volumes. Reactive tracers can be used to infer reservoir properties such as temperature and geochemical composition. Reactive tracers will be used in the C-wells testing at Yucca Mountain. Of course, solute transport capabilities are also used to simulate radionuclide migration. A YMP code, SORBEQ (Robinson, 1993), has been developed and validated to model one dimensional reactive solute flow and adsorption. FEHM will be compared with SORBEQ on a one-dimensional solute problem with equilibrium sorption. This comparison will verify the species transport in one dimension, and since the codes use different numerical techniques (finite differences versus finite elements) this test suite provides an independent check of both codes.

### 2.17.2 Functional Description

The test suite consists of a simulation of solute transport for five independent species; a conservative solute, and species governed by the linear, Langmuir, Freundlich, and modified Freundlich isotherms.

### 2.17.3 Assumptions and Limitations

The problem is depicted in Fig. 19. Table XIX defines the input parameters used for FEHM and SORBEQ simulations. The adsorption parameters are given in Table XX. A fluid flow steady state is established by injecting fluid at a fixed flow rate at the inlet and applying a constant pressure boundary condition at the outlet. The solute transport simulation is executed assuming an initial concentration of zero everywhere in the column, and injecting fluid with a concentration of unity at the start of the solute transport phase of the simulation. For each solute the same dispersivity is assumed (0.033 m, equivalent to a dimensionless Peclet number  $L/\alpha$  of 30). The inlet concentration remains at unity for the entire simulation.

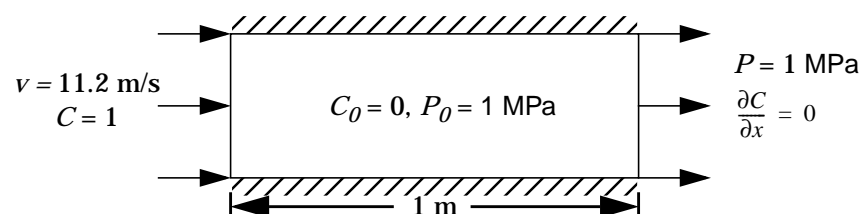


**Figure 19. Schematic drawing of the geometry and boundary conditions for the 1-D reactive tracer transport problem.**

### 2.17.4 Summary of Test Cases

#### 2.17.4.1 Reactive Tracer Transport

**2.17.4.1.1 Function Tested.** This test verifies that FEHM has correctly implemented reactive tracer transport.



**Table XIX. Input Parameters for the 1-D Reactive Tracer Transport Problem**

Parameter	Symbol	Value
Fluid Velocity	$v$	11.2 m/s
Flow Path Length	$L$	1 m
Node spacing	$\Delta l$	0.005 m
Dispersivity	$\alpha$	0.033 m
Porosity	$\phi$	0.3
Bulk Rock Density	$\rho_b$	2500 kg/m <sup>3</sup>
Time step (tracer)	$\Delta t$	0.09 - 0.43 s
Total elapsed time	$t$	100 s
Pressure	$P_0$	1.0 MPa
Initial concentration	$C_0$	0.0
Inlet concentration	$C_{in}$	1
Boundary conditions:		
At $l = 0$	$C = 1$	
At $l = 1$	$P = 1 \text{ MPa}, \frac{\partial C}{\partial x} = 0$	

**Table XX. Adsorption Parameters for the Reactive Tracer Transport Problem**

Adsorption Isotherm	$\alpha_1$	$\alpha_2$	$\beta$
Conservative	0.0	0.0	1.0
Linear	0.24	0.0	1.0
Langmuir	0.24	1.0	1.0
Freundlich	0.12	0.0	0.8
Modified Freundlich	0.48	1.0	0.8

2.17.4.1.2 Test Scope. This test case is a verification test.

2.17.4.1.3 Requirements Tested. Requirements 2.2, "Finite-Element Coefficient Generation," 2.3, "Formulate Transient Equations," specifically Section 2.3.4 and Section 2.3.7, 2.4, "Apply Constitutive Relationships," specifically Section 2.4.5, 2.5, "Compute Solution to Transient Equations," and 2.6, "Provide Input/Output Data Files," of the FEHM RD are verified by this test.

2.17.4.1.4 Required Inputs. Problem input is provided in the following file:

- *sorption.in*: Basic input and geometry data (402 nodes, 200 elements). A single simulation is performed that contains five noninteracting solutes with sorption parameters defined in Table XX.

2.17.4.1.5 Expected Outputs. Breakthrough curves (concentration at the outlet node for each species versus time) from FEHM will be output and compared to the SORBEQ results. When concentrations are close to zero, percent errors are misleading. Furthermore, considerable concentration errors result from only a small displacement of a breakthrough curve along the time axis because of the steep rise of the concentration-time curve for a typical case. Therefore, concentrations with percent errors less than 10% of the SORBEQ results and a root mean square error of the difference between the two simulations less than or equal to 0.01 when concentrations are greater than 0.1 will be considered acceptable.

The required output file for this test is the:

- Solute data plot file (*sorption.trc*).

## 2.18 Test of Henry's Law Species

### 2.18.1 Purpose

This set of verification runs tests the numerous combinations of effects possible for Henry's law solutes that may sorb or undergo chemical reaction. Two extremes for the one-dimensional flow field are employed: 1) air moving through a stagnant fluid phase, and 2) water moving through a stagnant air phase. The solute will partition into the stagnant fluid, resulting in a decrease in the overall solute transport velocity similar to that observed with equilibrium sorption.

### 2.18.2 Functional Description

The problem set has been divided into two segments. Segment 1 covers air moving through a stagnant fluid phase, and Segment 2 covers water moving through a stagnant air phase. The approach here is to check the results of a Henry's Law species against tests of a liquid- or vapor-only species under conditions designed to give similar breakthrough times.

### 2.18.3 Assumptions and Limitations

*Problem 1:* A Henry's law constant ( $K_H$ ) was chosen so that at any location half of the species resides in the vapor and half in the liquid. In the simulation, the tracer is exchanged between the flowing vapor and stagnant liquid. Therefore, this solute should behave identically to a linearly sorbing solute (see verification in Section 2.17 on page 80) with a sorption parameter that yields a velocity of one-half the conservative tracer velocity.

*Problems 2:* This run is similar to its counterpart in Segment 1, except that the water phase is moving. The breakthrough curves should agree closely with that obtained for a liquid-only species undergoing sorption.

The problem geometry is depicted in Fig. 20. Table XXI defines the input parameters and the adsorption, Henry's law, and reaction parameters are given in Table XXII. The problems are isothermal.

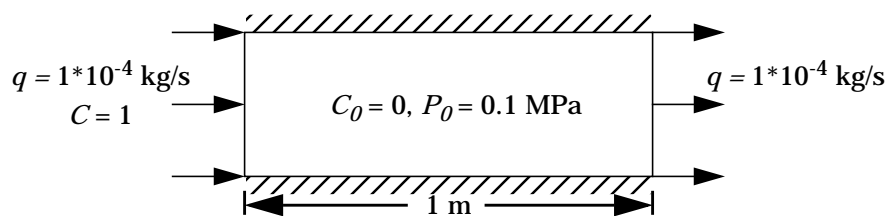


Figure 20. Schematic drawing of the geometry and boundary conditions for the Henry's Law species tests.

### 2.18.4 Summary of Test Cases

#### 2.18.4.1 Air Movement Through Stagnant Water

2.18.4.1.1 Function Tested. This test verifies that FEHM correctly simulates the transport of a species that partitions between a mobile air phase and immobile water.

**Table XXI. Input Parameters for the Henry's Law Species Tests**

Parameter	Symbol	Value
Flow rate (liquid flow rate for mobile-liquid case, air flow rate for mobile-air case)	$q$	$1.0 \cdot 10^{-4}$ kg/s
Flow Path Length	$L$	1 m
Node spacing	$\Delta l$	0.005 m
Dispersivity	$\alpha$	0.033 m
Porosity	$\phi$	0.05
Permeability		
Mobile air phase	$k$	$1 \cdot 10^{-11}$ m <sup>2</sup>
Mobile water phase		$1 \cdot 10^{-12}$ m <sup>2</sup>
Bulk Rock Density	$\rho_b$	2500 kg/m <sup>3</sup>
Time step (tracer)		
Mobile air phase	$\Delta t$	0.09 - 0.43 s
Mobile water phase		500 s
Total elapsed time (tracer)		
Mobile air phase	$t$	864 s
Mobile water phase		6 days
Pressure	$P_0$	0.1 MPa
Reference pressure	$P_{ref}$	0.1 MPa
Reference temperature	$T_{ref}$	20 °C
Initial water saturation		
Mobile air phase	$S_{l0}$	0.2
Mobile water phase		0.5
Residual liquid saturation		
Mobile air phase	$S_{lr}$	0.3
Mobile water phase		0.0
Residual vapor saturation		
Mobile air phase	$S_{lv}$	0.3
Mobile water phase		0.6
Maximum liquid saturation		
Mobile air phase	$S_{lmax}$	1.0
Mobile water phase		0.3
Maximum vapor saturation		
Mobile air phase	$S_{vmax}$	1.0
Mobile water phase		0.0

**Table XXI. Input Parameters for the Henry's Law Species Tests (Continued)**

Parameter	Symbol	Value
Initial concentration	$C_0$	0.0
Inlet concentration	$C_{in}$	1
Boundary conditions:	At $l = 0$ At $l = 1$	$C = 1, q = 1.0 \cdot 10^{-4} \text{ kg/s}$ $q = 1.0 \cdot 10^{-4} \text{ kg/s}$

**Table XXII. Adsorption, Henry's Law, and Reaction Parameters for the Henry's Law Species Tests**

Problem	$\alpha_1$	$\alpha_2$	$\beta$	$K_H \frac{\text{moles/kg water}}{\text{atm gas}}$
1 (both phases)	0.0	0.0	1.0	0.16514
2 (both phases)	0.0	0.0	1.0	4.145486e-2

2.18.4.1.2 Test Scope. This test case is a verification test.

2.18.4.1.3 Requirements Tested. Requirements 2.2, "Finite-Element Coefficient Generation," 2.3, "Formulate Transient Equations," specifically Section 2.3.4 and Section 2.3.7, 2.4, "Apply Constitutive Relationships," specifically Section 2.4.4 and Section 2.4.5, 2.5, "Compute Solution to Transient Equations," and 2.6, "Provide Input/Output Data Files," of the FEHM RD are verified by this test.

2.18.4.1.4 Required Inputs. Problem input is provided in the following files:

- *henry1.in*: Basic input data
- *henry.geom*: Geometry data. This two-dimensional grid contains 201 nodes in the flow direction, and 2 in the direction perpendicular to flow, making this effectively a one-dimensional simulation.

2.18.4.1.5 Expected Outputs. Values from FEHM for concentration versus time at the outlet node will be output and compared to the FEHM solution for a linearly sorbing solute with a retardation factor of 2. Concentrations within 0.01 of the sorbing solute solution, a root mean square error of the difference between the two simulations less than or equal to 0.01, and percent errors less than 10% when concentrations are greater than 0.1 will be considered acceptable.

The required output file for this test is the:

- Solute data plot file (*henry1.trc*).

#### 2.18.4.2 Water Movement Through Stagnant Air

2.18.4.2.1Function Tested. This test verifies that FEHM correctly simulates the transport of a species that partitions between a mobile water phase and immobile air.

2.18.4.2.2Test Scope. This test case is a verification test.

2.18.4.2.3Requirements Tested. Requirements 2.2, "Finite-Element Coefficient Generation," 2.3, "Formulate Transient Equations," specifically Section 2.3.4 and Section 2.3.7, 2.4, "Apply Constitutive Relationships," specifically Section 2.4.5, 2.5, "Compute Solution to Transient Equations," and 2.6, "Provide Input/Output Data Files," of the FEHM RD are verified by this test.

2.18.4.2.4Required Inputs. Problem input is provided in the following files:

- *henry2.in*: Basic input data
- *henry.geom*: Geometry data.

2.18.4.2.5Expected Outputs. Values from FEHM for concentration versus time at the outlet node will be output and compared to the FEHM solution for a linearly sorbing solute with a retardation factor of 2. Concentrations within 0.01 of the sorbing solute solution, a root mean square error of the difference between the two simulations less than or equal to 0.01, and percent errors less than 10% when concentrations are greater than 0.1 will be considered acceptable.

The required output file for this test is the:

- Solute data plot file (*henry2.trc*).

## 2.19 Test of Fracture Transport with Matrix Diffusion

### 2.19.1 Purpose

Matrix diffusion is an important process in the transport of contaminants in fractured porous media. Under certain limiting conditions, analytical solutions have been developed. The transport module of FEHM with equilibrium sorption can be tested in two dimensions against these analytical solutions to ensure that multi-dimensional transport problems with sorption are properly formulated. In addition, the generalized dual porosity model formulation can be tested against the same analytical solutions.

### 2.19.2 Functional Description

The test suite developed here consists of a two-dimensional grid with a permeability field set up to simulate one-dimensional flow in a fracture (a line of nodes along one edge of the model domain). Fluid in the surrounding matrix is stagnant. Tracers injected with the flowing fluid in the fracture can transport into the matrix via molecular diffusion. Sorption can occur either on the fracture, in the matrix, or both. The results for the breakthrough curve (concentration versus time at the outlet of the fracture) can be compared against analytical solutions to test the ability of the code to simulate solute transport with sorption.

The identical model setup will be used to test the Generalized Dual Porosity (GDPM) code option. For these tests, a one-dimensional grid with identical axial discretization will be used. Discretization in the secondary porosity will be set using the GDPM model option instead of as a two-dimensional, discrete-fracture grid. As in the discrete fracture model runs, a steady state flow field will be established with low matrix permeability, and then solute will be injected in the identical manner as in the other test cases. For this test problem, diffusion along the flow direction in the matrix, ignored in the GDPM formulation, should be negligible because of the long length scale of the model in the direction of flow, compared to the characteristic diffusional distance for this problem.. Therefore, the model results should be indistinguishable from the discrete fracture model runs.

### 2.19.3 Assumptions and Limitations

Tang et al. (1981) present an analytical solution for the case of one-dimensional axial dispersion in the fracture coupled to diffusion into an infinite medium [Equation 35 in Tang et al. (1981), revised for a fixed observation point a distance  $L$  from the inlet and no radioactive decay]:

$$\frac{C}{C_{in}} = \frac{2 \cdot \exp\left(\frac{L}{2\alpha}\right)}{\pi^{1/2}} \int_l^{\infty} \exp\left[-\xi^2 - \frac{L^2}{4\alpha^2\xi^2}\right] \operatorname{erfc}\left(\frac{Y}{2T}\right) d\xi$$

where  $\xi$  is the integration variable,  $l$ , the lower integration bound is given by

$$l = \frac{L}{2} \left( \frac{R_f}{\alpha v t} \right)^{1/2}$$

and the lumped parameters  $Y$ ,  $T$ , and  $A$  are given by

$$Y = \frac{R_f L \tau}{4 \alpha A \xi^2},$$

$$T = \sqrt{t - \frac{R_f L^2}{4 D \xi^2}},$$

and

$$A = \frac{b R_f}{\phi (R_m D_{mol})^{1/2}}.$$

In the above expressions,  $R_f$  is the retardation factor on the fracture,  $\tau$  is the mean residence time of fluid through the column,  $\alpha$  is the dispersivity,  $v$  is the fluid velocity,  $t$  is time,  $b$  is the half-width of the fracture aperture,  $\phi$  is the porosity of the matrix,  $R_m$  is the retardation factor in the matrix, and  $D_{mol}$  is the molecular diffusion coefficient of the solute. If we select a molecular diffusion coefficient such that the tracer has insufficient time to diffuse to the edge of the model domain on the opposite side of the fracture, then the solution of Tang et al. should be replicated by FEHM. For sorption, the analytical solution is given in terms of retardation factors for the fracture and matrix. In FEHM, the expression used to duplicate a retardation factor for a saturated medium is

$$R_f = 1 + \frac{\rho_b K_d}{\phi \rho_f}$$

where  $K_d$  is the sorption distribution coefficient. The problem geometry (symmetric about the fracture) is depicted in Fig. 21. Table XXIII lists the input parameters and conditions for this test suite while Table XXIV gives the sorption parameters. Separate cases are run with no sorption, sorption in the matrix, and sorption in both the fracture and matrix (flow occurs only in the fracture).



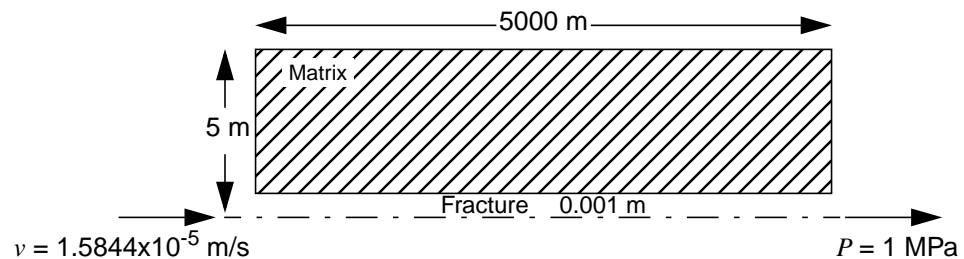


**Figure 21. Schematic drawing of the geometry and boundary conditions for the fracture transport problem.**

## 2.19.4 Summary of Test Cases

### 2.19.4.1 Transport with Matrix Diffusion, No Sorption

**2.19.4.1.1 Function Tested.** This test verifies that FEHM correctly simulates the transport system consisting of flow and dispersion in a fracture with diffusion into the rock matrix.

**2.19.4.1.2 Test Scope.** This test case is a verification test.

**2.19.4.1.3 Requirements Tested.** Requirements 2.2, "Finite-Element Coefficient Generation," 2.3, "Formulate Transient Equations," specifically Section 2.3.4 and Section 2.3.7, 2.4, "Apply Constitutive Relationships," specifically Section 2.4.5, 2.5, "Compute Solution to Transient Equations," and 2.6, "Provide Input/Output Data Files," of the FEHM RD are verified by this test.

**2.19.4.1.4 Required Inputs.** Problem input is provided in the following files:

- *tangtest1.in*: Basic input data.
- *tangtest.geom*: Coordinate and element information. The geometry is represented by a two-dimensional grid of 1590 nodes (53 in the direction of flow and 30 in the matrix). The node spacing in the matrix is small near the fracture where concentration gradients are largest.

**2.19.4.1.5 Expected Outputs.** Values from FEHM for concentration breakthrough curves will be output and compared to the analytical solution results. A root mean square error of the difference between the FEHM and Tang solution less than or equal to 0.01 for concentrations greater than 0.1 will be considered acceptable.

The required output file for this test is the:

- Solute data plot file (*tangtest1.trc*).

### 2.19.4.2 Transport with Matrix Diffusion, Sorption in the Matrix

**2.19.4.2.1 Function Tested.** This test verifies that FEHM correctly simulates the transport system consisting of flow and dispersion in a fracture with diffusion into the rock matrix, with sorption occurring in the matrix.

**Table XXIII. Input Parameters for the Fracture Transport with Matrix Diffusion Test Problem**

Parameter	Symbol	Value
Flow Path Length (x)	$L$	5000 m
Node spacing along flow path <sup>‡</sup>	$\Delta x$	100 m
Model width	$y$	5 m
Node spacings into the matrix	$\Delta y$	0.001 - 0.5 m
Fluid Density	$\rho_f$	1000 kg/m <sup>3</sup>
Bulk Rock Density	$\rho_b$	2700 kg/m <sup>3</sup>
Matrix Porosity	$\phi$	0.05
Pore Water Velocity	$v$	1.5844x10 <sup>-5</sup> m/s
Dispersivity in fracture	$\alpha$	500 m
Matrix Diffusion Coefficient	$D_{mol}$	1.5x10 <sup>-12</sup> m <sup>2</sup> /s
Time step (tracer)	$\Delta t$	0.001 - 5000 days
Total elapsed time	$t$	1500 years
Pressure	$P_0$	1.0 MPa
Initial concentration	$C_0$	0.0
Inlet concentration	$C_{in}$	1
Boundary conditions: At $l = 0$ m $q = v\rho_f\phi_f A_f = 7.922 \times 10^{-6}$ kg/s		
At $l = 5000$ m $P = 1$ MPa		
$\phi_f$ is the fracture porosity and $A_f$ is the cross-sectional area of the fracture.		

<sup>‡</sup>The node spacing at each edge is 1 m to accomodate boundary conditions.

2.19.4.2.2 Test Scope. This test case is a verification test.

2.19.4.2.3 Requirements Tested. Requirements 2.2, "Finite-Element Coefficient Generation," 2.3, "Formulate Transient Equations," specifically Section 2.3.4 and Section 2.3.7, 2.4, "Apply Constitutive Relationships," specifically Section 2.4.5, 2.5, "Compute Solution to Transient Equations," and 2.6, "Provide Input/Output Data Files," of the FEHM RD are verified by this test.

2.19.4.2.4 Required Inputs. Problem input is provided in the following files:

- *tangtest2.in*: Basic input data.

**Table XXIV. Adsorption Parameters for the Fracture Transport Problem**

Test		$\alpha_1$	$\alpha_2$	$\beta$	$R$
Transport with Matrix Diffusion, No Sorption	fracture	0.0	0.0	1.0	1.0
	matrix	0.0	0.0	1.0	1.0
Transport with Matrix Diffusion, Sorption (linear) in the Matrix	fracture	0.0	0.0	1.0	1.0
	matrix	$7.4074(10^{-2})$	0.0	1.0	5.0
Transport with Matrix Diffusion, Sorption in the Fracture and Matrix	fracture	8.88889	0.0	1.0	25.0
	matrix	$7.4074(10^{-2})$	0.0	1.0	5.0

- *tangtest.geom*: Coordinate and element information. The geometry is represented by a two-dimensional grid of 1590 nodes (53 in the direction of flow and 30 in the matrix). The node spacing in the matrix is small near the fracture where concentration gradients are largest.

2.19.4.2.5 Expected Outputs. Values from FEHM for concentration breakthrough curves will be output and compared to the analytical solution results. A root mean square error of the difference between the FEHM and Tang solution less than or equal to 0.01 for concentrations greater than 0.1 will be considered acceptable.

The required output file for this test is the:

- Solute data plot file (*tangtest2.trc*).

### 2.19.4.3 Transport with Matrix Diffusion, Sorption in the Fracture and Matrix

2.19.4.3.1 Function Tested. This test verifies that FEHM correctly simulates the transport system consisting of flow and dispersion in a fracture with diffusion into the rock matrix, with sorption occurring in the matrix and on the fracture.

2.19.4.3.2 Test Scope. This test case is a verification test.

2.19.4.3.3 Requirements Tested. Requirements 2.2, "Finite-Element Coefficient Generation," 2.3, "Formulate Transient Equations," specifically Section 2.3.4 and Section 2.3.7, 2.4, "Apply Constitutive Relationships," specifically Section 2.4.5, 2.5, "Compute Solution to Transient Equations," and 2.6, "Provide Input/Output Data Files," of the FEHM RD are verified by this test.

2.19.4.3.4 Required Inputs. Problem input is provided in the following files:

- *tangtest3.in*: Basic input data.
- *tangtest.geom*: Coordinate and element information. The geometry is represented by a two-dimensional grid of 1590 nodes (53 in the direction of flow and 30 in the matrix). The node spacing in the matrix is small near the fracture where concentration gradients are largest.

2.19.4.3.5Expected Outputs. Values from FEHM for concentration breakthrough curves will be output and compared to the analytical solution results. A root mean square error of the difference between the FEHM and Tang solution less than or equal to 0.01 for concentrations greater than 0.1 will be considered acceptable.

The required output file for this test is the:

- Solute data plot file (*tangtest3.trc*).

#### **2.19.4.4 Generalized Dual Porosity Option**

2.19.4.4.1Function Tested. This test verifies that FEHM correctly simulates the transport systems of Sections 2.19.4.1 and 2.19.4.2 using the Generalized Dual Porosity Model option.

2.19.4.4.2Test Scope. This test case is a verification test.

2.19.4.4.3Requirements Tested. Requirements 2.2, “Finite-Element Coefficient Generation,” 2.3, “Formulate Transient Equations,” specifically Section 2.3.4 and Section 2.3.7, 2.4, “Apply Constitutive Relationships,” specifically Section 2.4.5 and Section 2.4.8, 2.5, “Compute Solution to Transient Equations,” and 2.6, “Provide Input/Output Data Files,” of the FEHM RD are verified by this test.

2.19.4.4.4Required Inputs. Problem input is provided in the following files:

- *gdpm1.in*: Basic input data modeling transport with matrix diffusion and no sorption.
- *gdpm2.in*: Basic input data modeling transport with matrix diffusion and sorption in the matrix.
- *gdpm1dgrid.geom* and *gdpm1dgrid.stor*: Coordinate and element information. The geometry is represented by a one-dimensional model grid with node spacings equivalent to the discretization in the two-dimensional grid of this test suite (*tangtest.geom*). Note that although the X and Y coordinates have been interchanged, the identical problem is being modeled.

2.19.4.4.5Expected Outputs. Values from FEHM for concentration breakthrough curves will be output and compared to the analytical solution results. A root mean square error of the difference between the FEHM and Tang solution less than or equal to 0.01 for concentrations greater than 0.1 will be considered acceptable.

The required output files for this test are the:

- Solute data plot files (*gdpm1.trc*, *gdpm2.trc*).

## 2.20 Test of the Movement of a Dissolved Mineral Front

### 2.20.1 Purpose

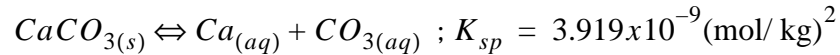
The ability of FEHM to model precipitation and dissolution reactions allows us to develop more sophisticated models to describe the rock-water interactions at the Yucca Mountain site. The analytical solution for a single, sharp-moving, equilibrium mineral front has been used to verify reactive transport models in the past (i.e., Engesgaard, 1991, Walsh et al., 1984). This analytical solution, which assumes no dispersion, is used to verify that FEHM is accurately predicting the velocity of a dissolved mineral front.

### 2.20.2 Functional Description

A one-dimensional transport simulation of calcite ( $\text{CaCO}_3(s)$ ) dissolution is tested. Profiles of concentration versus reactor length, at selected times, will be compared against the analytical solution.

### 2.20.3 Assumptions and Limitations

The precipitation and dissolution of calcite (a common mineral in many soils) are important processes which play a significant role in controlling the pH and alkalinity of groundwater. The dissolution reaction and the solubility product for this problem are:



Thus the transport system (illustrated in Fig. 22) consists of one equilibrium reaction with three species.

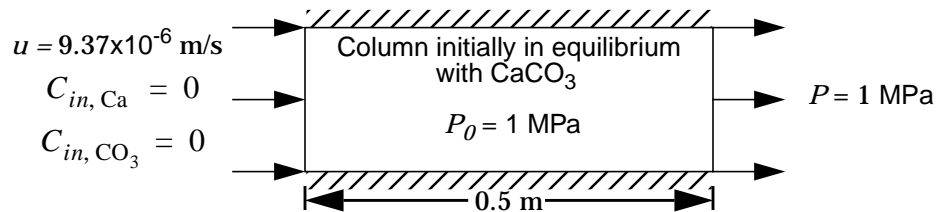


**Figure 22. Schematic drawing of the geometry and boundary conditions for the calcite dissolution problem.**

The analytical solution for a single dissolved mineral front (Fig. 23) is given by:

$$u_{\text{mineral}} = \frac{u \Delta C_{aq}}{\Delta C_{aq} + \frac{\rho_b}{\phi} \Delta C_s}$$

where  $u$  is the pore water velocity,  $u_{\text{mineral}}$  is the velocity of the mineral front,  $\rho_b$  is the bulk rock density,  $\phi$  is the porosity,  $\Delta C_s$  is the change in solid concentration across the front and  $\Delta C_{aq}$  is the change in aqueous

concentration across the front. A list of relevant input parameters and conditions is given in Table XXV.

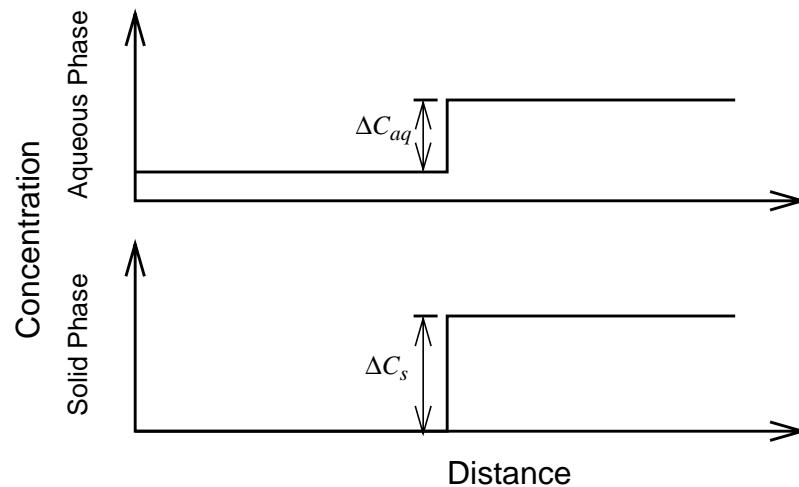


Figure 23. Aqueous and mineral front profiles modeled by the analytical solution.

## 2.20.4 Summary of Test Cases

### 2.20.4.1 Calcite Dissolution in a One-Dimensional System

2.20.4.1.1 Function Tested. This test verifies that FEHM correctly simulates the dissolution of a mineral.

2.20.4.1.2 Test Scope. This test case is a verification test.

2.20.4.1.3 Requirements Tested. Requirements 2.2, "Finite-Element Coefficient Generation," 2.3, "Formulate Transient Equations," specifically Section 2.3.4, 2.4, "Apply Constitutive Relationships," specifically Section 2.4.6, 2.5, "Compute Solution to Transient Equations," and 2.6, "Provide Input/Output Data Files," of the FEHM RD are verified by this test.

2.20.4.1.4 Required Inputs.

- *dissolution.in*: Basic input data.
- *dissolution.grid*: Coordinate and element information. (102 nodes, 50 elements to simulate a one-dimensional flow system).

2.20.4.1.5 Expected Outputs. Values from FEHM for the mean concentration of the mineral front will be compared to the analytical solution. Position within 5% of the predicted value will be considered acceptable.

The required output file for this test is the:

- AVS concentration contour data plot files for  $t = 20000$ ,  $60000$ , and  $100000$  s (*dissolution.10002\_con\_node*, *dissolution.10003\_con\_node*, *dissolution.10004\_con\_node*).

**Table XXV. Input Parameters for the Calcite Dissolution Problem**

Parameter	Symbol	Value
Reactor Length	$L$	0.5 m
Node spacing	$\Delta l$	0.01 m
Fluid Density	$\rho_f$	1000 kg/m <sup>3</sup>
Bulk Rock Density	$\rho_b$	1800 kg/m <sup>3</sup>
Porosity	$\phi$	0.32
Pore Water Velocity <sup>‡</sup>	$u$	9.37x10 <sup>-6</sup> m/s
Dispersivity	$\alpha$	0.0067 m
Time step	$\Delta t$	100 s
Total elapsed time	$t$	2.157 days
Pressure	$P_0$	1.0 MPa
CaCO <sub>3</sub> Initial Concentration	$C_{0, \text{CaCO}_3}$	2.0x10 <sup>-5</sup> mol/kg-solid
Ca Initial Concentration	$C_{0, \text{Ca}}$	6.26x10 <sup>-5</sup> mol/kg-water
CO <sub>3</sub> Initial Concentration	$C_{0, \text{CO}_3}$	6.26x10 <sup>-5</sup> mol/kg-water
Ca Inlet Concentration	$C_{in, \text{Ca}}$	0
CO <sub>3</sub> Inlet Concentration	$C_{in, \text{CO}_3}$	0
Boundary conditions:		
At $l = 0$		$u = 9.37 \times 10^{-6}$ m/s
		$C_{in, \text{Ca}} = 0, C_{in, \text{CO}_3} = 0$
At $l = 1$		$P = 1$ MPa
<sup>‡</sup> Flow rate $q = u \rho_f \phi / 2 \text{ nodes} = 0.0014992$ kg/s		

## 2.21 Test of Multi-Solute Transport with Chemical Reaction

### 2.21.1 Purpose

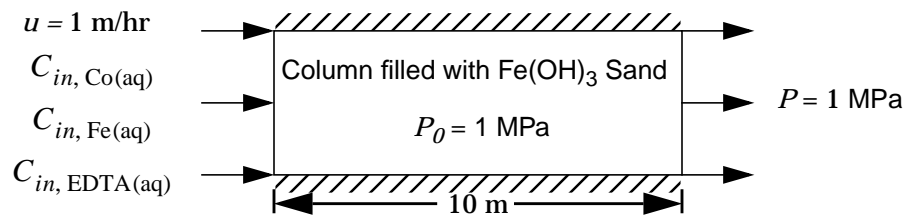
The coupled transport and chemical reaction of multiple species in solution is an important feature of FEHM that will allow us to incorporate more complex processes into radionuclide transport simulations, as well as to model rock-water interactions at the Yucca Mountain site. The most appropriate way to test this feature of the code is by comparison against a code that was designed specifically for such reactive transport simulations. The code we are using for this purpose is called PDREACT (Valocchi et al., 1994), a two-dimensional, isothermal, saturated-zone flow and transport code. This comparison will verify the species transport for a simple, one-dimensional saturated flow field for a complex, multiple interacting species simulation.

### 2.21.2 Functional Description

The suite of reactions described below are simulated for transport in a one-dimensional flow system. Concentration versus time breakthrough curves at the flow path exit and concentration of solid species at the exit versus time will be compared for the two codes.

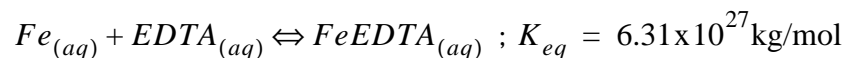
### 2.21.3 Assumptions and Limitations

The application of this test case is the transport of cobalt (Co) in groundwater. Radioactive cobalt is present in the subsurface at several DOE sites. Although its presence as a divalent cation implies that it should sorb strongly to most soils, its migration rate has been shown to be greater than expected due to complexation with EDTA, a decontaminating agent also found in the subsurface of these sites. Much experimental work has gone into studying the transport of Co as CoEDTA, a much less strongly sorbed species. Figure 24 illustrates the transport problem.

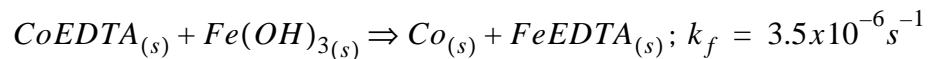
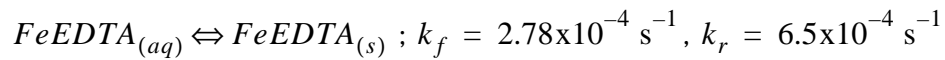
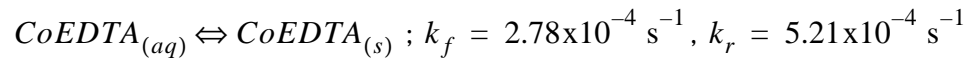
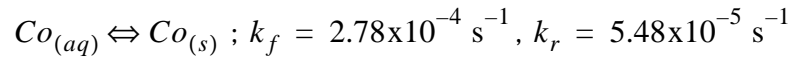


**Figure 24. Schematic drawing of the geometry and boundary conditions for the cobalt transport problem.**

The chemical reactions and equilibrium or rate constants used to perform this code comparison test are:







Thus the transport system consists of 8 species and six reactions, with reactions specified as either equilibrium or kinetically controlled.  $Fe(OH)_3$  is so prevalent in the sand that its concentration is assumed to be constant. In addition, it does not act as a true species in either simulation. A list of relevant input parameters and conditions for the code comparison are given in Table XXVI.

## 2.21.4 Summary of Test Cases

### 2.21.4.1 Cobalt Transport in a One-Dimensional Flow System

**2.21.4.1.1 Function Tested.** This test verifies that FEHM correctly simulates the reactive transport system consisting of both kinetic and equilibrium reactions, with both immobile and aqueous species.

**2.21.4.1.2 Test Scope.** This test case is a verification test.

**2.21.4.1.3 Requirements Tested.** Requirements 2.2, "Finite-Element Coefficient Generation," 2.3, "Formulate Transient Equations," specifically Section 2.3.4 and Section 2.3.7, 2.4, "Apply Constitutive Relationships," specifically Section 2.4.6, 2.5, "Compute Solution to Transient Equations," and 2.6, "Provide Input/Output Data Files," of the FEHM RD are verified by this test.

**2.21.4.1.4 Required Inputs.** Problem input is provided in the following file:

- *multi\_solute.in*: Basic input data, including the finite element grid [202 nodes, 100 elements (51 x 2 nodes to simulate a one-dimensional flow system)].

**2.21.4.1.5 Expected Outputs.** Values from FEHM for concentration breakthrough curves of aqueous species and concentration-time history at the outlet node for immobile (solid) species will be compared to the PDREACT results. Due to the low inlet concentrations, concentrations within 10% for all values that are greater than 10% of the peak value will be considered acceptable.

The required output file for this test is the:

- Solute data plot file (*multi\_solute.trc*).

**Table XXVI. Input Parameters for the Multi-Solute Reactive Transport Test Problem**

Parameter	Symbol	Value
Reactor Length	$L$	10 m
Node spacing	$\Delta l$	0.1 m
Fluid Density	$\rho_f$	1000 kg/m <sup>3</sup>
Bulk Rock Density	$\rho_b$	1500 kg/m <sup>3</sup>
Porosity	$\phi$	0.4
Pore Water Velocity	$u$	1 m/hr
Dispersivity	$\alpha$	0.05 m
Time step (tracer)	$\Delta t$	0.09 - 360 s
Total elapsed time	$t$	7.25 days
Pressure	$P_0$	1.0 MPa
Co Inlet Concentration	$C_{in, Co}$	3.1623x10 <sup>-5</sup> M
Fe Inlet Concentration	$C_{in, Fe}$	0 M
EDTA Inlet Concentration	$C_{in, EDTA}$	3.1623x10 <sup>-5</sup> M
Boundary conditions:	At $l = 0$ At $l = 1$	$u = 1$ m/hr $P = 1$ MPa
‡Flow rate $q = u\rho_f\phi/2$ nodes = 0.05556 kg/s		

## 2.22 Test of Three-Dimensional Radionuclide Transport

### 2.22.1 Purpose

A comparison will be made with TRACRN, (Travis and Birdsell, 1988) another YMP code, on a three dimensional, single phase liquid problem. The problem simulates the transport of a tracer undergoing radioactive decay, and thus is of particular interest to the Yucca Mountain Project. This comparison will verify the species transport in three dimensions. TRACRN has been compared against many known analytical solutions. While no three dimensional analytical solutions exist, a match between TRACRN and FEHM will give confidence that both are correct. Because the codes use different numerical techniques, the test provides a check for both codes.

### 2.22.2 Functional Description

The transport system described below consists of one aqueous species undergoing radioactive decay. Concentration-time histories at several locations in the model domain will be used to make the comparison.

### 2.22.3 Assumptions and Limitations

The radionuclide being simulated is Americium ( $^{243}\text{Am}$ ) which has a half life of 432 years. The model domain, depicted in Figure 25 is a cube (100 m on each side). Infiltration at a rate of  $10^{-4}$  kg/s occurs over a  $100\text{ m}^2$  region (four nodes) on the top of the box, and outflow is allowed over a  $900\text{ m}^2$  region (36 nodes) on the bottom. The inlet and outlet nodes are offset from each other in plan view so that flow will travel diagonally through the model domain. There is no flow on the remainder of the boundaries. The simulation is run in two parts. After a steady state flow field is established, a restart run that solves the transport of the radionuclide is carried out. The restart time for the transport simulation is set to 0 since the time required to establish a steady-state flow field has no relevance to the transport simulation. The  $^{243}\text{Am}$  is injected with the inlet fluid at a concentration of 1. A conservative tracer is also injected with the inlet fluid as an additional check between the two codes. The problem is isothermal. Table XXVII lists the input parameters and conditions for this test suite.

### 2.22.4 Summary of Test Cases

#### 2.22.4.1 Decay Chain Transport in a Three-Dimensional System

2.22.4.1.1 Function Tested. This test verifies that FEHM correctly simulates the reactive transport system consisting of a radionuclide decay in a three-dimensional flow system. A conservative tracer is also used to verify the three dimensional tracer transport. In addition, the restart capabilities of the code are verified.

2.22.4.1.2 Test Scope. This test case is a verification test.

2.22.4.1.3 Requirements Tested. Requirements 2.2, "Finite-Element Coefficient Generation," 2.3, "Formulate Transient Equations," specifically Section 2.3.4 and Section 2.3.7, 2.4, "Apply Constitutive Relationships," specifically Section 2.4.4 and Section 2.4.5, 2.5, "Compute Solution to Transient Equations,"

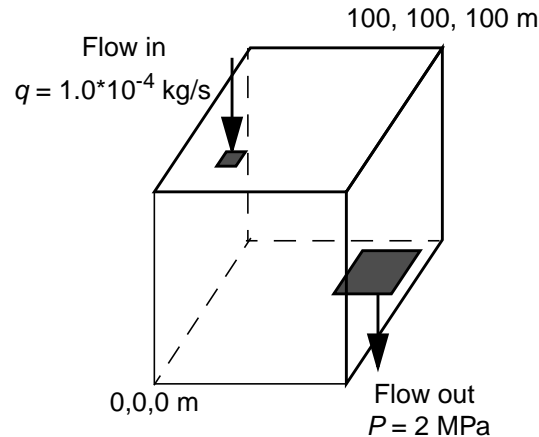


**Figure 25. Model domain and flow boundary conditions for the radionuclide transport test problem.**

2.6, "Provide Input/Output Data Files," and 2.7, "Provide Restart Capability," of the FEHM RD are verified by this test.

2.22.4.1.4 Required Inputs. Problem input is provided in the following files:

- *3d\_trac.gen\_ini.dat*: Basic input data for generating restart and coefficient storage files for the steady state flow field.
- *3d\_trac.grid*: Finite element grid, a structured, three-dimensional grid with 10,648 nodes (22x22x22), 9261 elements.
- *3d\_trac.dat*: Basic input data for transport portion of test run.
- *3d\_trac.ini*: Steady state flow initialization file (generated during first portion of test run).
- *3d\_trac.stor*: Coefficient storage file (generated during first portion of test run).

2.22.4.1.5 Expected Outputs. Values from FEHM for concentration-time histories at specified nodes will be compared to the TRACRN results. A root mean square error between FEHM and TRACRN concentrations, of less than or equal to 0.05, at concentrations greater than 10% of the peak value, will be considered acceptable.

The required output file for this test is the:

- Solute data plot file (*3d\_trac.trc*).

**Table XXVII. Input Parameters and Conditions for the Radionuclide Transport Test Problem**

Parameter	Symbol	Value
Reservoir dimensions	$x, y, z$	100 m
Node spacing <sup>‡</sup>	$\Delta x, \Delta y, \Delta z$	5 m
Bulk Rock Density	$\rho_b$	2700 kg/m <sup>3</sup>
Porosity	$\phi$	0.3
Infiltration rate	$q$	1.0*10 <sup>-4</sup> kg/s
Dispersivity	$\alpha$	5.0 m
Restart time	--	0. days
Time step (tracer)	$\Delta t$	2.74 - 10 years
Total elapsed time (tracer simulation)	$t$	5000 years
Pressure	$P_0$	1.0 MPa
Reference pressure	$P_{ref}$	0.1 MPa
Reference temperature	$T_{ref}$	20 °C
Initial water saturation	$S_{l0}$	1.0
Residual liquid saturation	$S_{lr}$	0.277
Maximum liquid saturation	$S_{lmax}$	1.0
van Genuchten model parameters		
Inverse of air entry pressure	$\alpha_G$	3.34 m <sup>-1</sup>
Power in formula	$n$	1.982
<sup>243</sup> Am Inlet Concentration	$C_{in, {}^{243}\text{Am}}$	1 M
Conservative Tracer Inlet Concentration	$C_{in, \text{Cons}}$	1 M
Boundary conditions:	At $x = 20 - 30$ m, $y = 20 - 30$ m, $z = 100$ m At $x = 60 - 90$ m $y = 60 - 90$ m, $z = 0$ m	$q = 1.0*10^{-4}$ kg/s  $P = 2$ MPa
<sup>‡</sup> For the FEHM simulation node spacing around the periphery is half the general spacing (2.5 m).		

## 2.23 Test of Streamline Particle Tracking Model

### 2.23.1 Purpose

Several test cases have been executed to confirm the accuracy of the streamline particle-tracking method by comparison with analytical solutions. Two dispersion models are available, the standard model and a more general model that allows for the longitudinal dispersivity to be different in vertical and horizontal directions (Lichtner et al. 2000). The model must be shown to obtain accurate breakthrough curves and in situ concentrations for advection, dispersion, and matrix diffusion. To test the standard dispersion model, the analytical solution developed by Leij et al. (1991) is used, which simulates longitudinal and transverse dispersion in a uniform flow field. This solution is solved using the computer code 3DADE (Software Activity Number SNL-1999094). For the combined dispersion and matrix diffusion case, the solution for diffusion into a semi-infinite matrix derived by Tang et al. (1981) will be used to test the behavior of the model under the limiting conditions of infinite fracture spacing. Because the analytical solutions use entirely different numerical techniques than the particle tracking method, the tests provide a rigorous check of the streamline particle tracking model. To test the general dispersion model, a comparison of the shape of the cloud of dispersed particles is made between theory and numerical results by tabulating the second moments of the particle locations (Lichtner et al. 2000).

An important question often encountered in environmental remedial work is “given the observed contaminant data, what could be the source location that would lead to the contaminant being observed at the measurement location?”. The reverse particle tracking capability has been developed to help answer this question. A test has been implemented which compares particle locations for a forward and reverse simulation.

The size of the capture zone of an extraction well depends on the pumping rate and the hydrologic properties of the reservoir. A situation can often arise where the size of the computational grid block exceeds the capture zone. In this case, not all the particles entering the grid block will be captured by the pumping well. The streamline particle tracking module accounts for this possibility by calculating the particle trajectory on a sub-grid scale using an approximate analytical solution (Zheng1994). This is tested by comparing the resultant particle paths for a coarse and fine grid.

The random walk method used for simulating dispersion in the particle tracking model includes a term which is proportional to the divergence of the dispersion tensor divided by the porosity (Lichtner et al. 2000). This term involves spatial derivatives of the fluid velocity. In situations where there are variations in porosity and permeability by several orders of magnitude, these have to be computed with care or large spurious jumps in the particle tracks can result. The implementation of this term is tested by comparing the resultant particle paths for a coarse and fine grid over a domain with a low porosity, low permeability block embedded in the center.

### 2.23.2 Functional Description

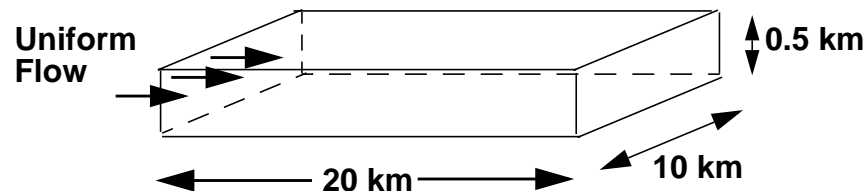
The test suite consists of four tests. The flow and transport system described below for the standard and generalized dispersion models consists of uniform flow and solute transport subject to longitudinal and transverse dispersion, and matrix diffusion. Travel time distributions at a

specified location in the model, and in situ concentration profiles at several locations in the model domain and second moments of particle locations at specified times will be used to make the comparison.

The reverse particle tracking capability is tested by comparing forward and reverse tracks for particles in the same flow fields. The particle capture model is tested by comparing particle tracks obtained on the same domain for two different grids. The divergence of the dispersion tensor is tested by comparing the resultant particle paths for a coarse and fine grid over a domain with a low porosity block embedded in the center.

### 2.23.3 Assumptions and Limitations

Test cases for the standard dispersion model with and without matrix diffusion in this suite are performed on a three-dimensional grid in which flow is aligned with the  $x$ -axis with an average pore velocity of 34 m/year. The grid dimensions are 10 km by 20 km in the horizontal directions and 500 m thick (Figure 26). In



Not to scale

**Figure 26. Model domain and flow boundary conditions for the streamline particle tracking standard dispersion model test problems.**

the first set of runs in this suite, the particles are inserted at the inlet within a single cell, and the breakthrough curve at a downstream location (15 km from the inlet) is recorded for the case of longitudinal dispersion with a dispersivity of 100 m, with and without matrix diffusion and sorption. For the test invoking both longitudinal and transverse dispersion, the same flow field will be used, but the solute will be input as a patch on the inlet face of the model. The dimensions of the patch will be 3,000 m in the  $y$ -direction and 12.5 m in the vertical direction, starting at the surface. Particle-tracking model runs, including both longitudinal and transverse dispersion, will be carried out with longitudinal dispersivity of 100 m and transverse dispersivity of 0.1 m (values typical of large-scale transport in porous media, after Gelhar, 1997). As the plume progresses downstream, spreading in the vertical direction should lower the maximum concentration of particles and allow the particles to migrate to greater depths than the original 12.5 m depth of the plume. At long times, at a constant solute injection concentration, the plume will approach a steady-state concentration distribution within the model.

The tests of the generalized dispersion model are performed on a three-dimensional grid with 10 equally spaced nodes in each direction with a spacing of 1 km. The fluid velocity for the cases using the Burnett and Frind and modified Burnett and Frind dispersion tensor is in the  $x$ - $z$  plane

at 45 degrees to the axis, with a magnitude of  $11.62 \times 10^{-11}$  m/s, and for the generalized axisymmetric dispersivity case is along the x-axis with a magnitude of  $8.22 \times 10^{-11}$  m/sec. In each case, 10000 particles are started in one corner of the model and the particle locations after  $6.94 \times 10^6$  days are recorded. The second moments of the location are calculated in each case.

The reverse particle tracking capability is tested by comparing forward and reverse tracks for particles in the same flow fields. The domain is a 200 m by 15 m by 20 m parallelepiped, fully saturated with water. A mesh with 17600 nodes is used, with a spacing varying between 2.5 m to 5.625 m in the x-direction, 1 m in the y-direction and 0.7279542 m in the z-direction. A constant head condition is applied on the right face of the model and a head varying linearly with x-direction is applied on the top surface of the model and the flow is allowed to equilibrate (Figure 27). This leads to streamlines starting at the top of the model and curving to the right as they move downward, exiting on the right face of the model. Ten particles are then started on the left near the top of the model and allowed to travel. Their exit locations are then recorded and used as the starting locations for the reverse tracking model.

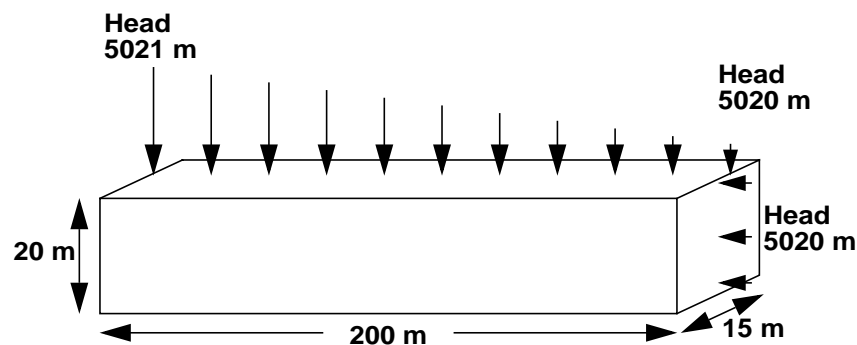


**Figure 27. Model domain and flow boundary conditions for the streamline particle tracking reverse tracking model test problems.**

The particle capture model is tested by comparing particle tracks obtained on the same domain for two different grids. The domain is a 1676 m by 1676 m by 15.24 m 3-dimensional parallelepiped, fully saturated with water. An extraction well is placed at the location  $x = 838$  m,  $y = 838$  m and going through the entire depth of the model in the z-direction. A uniform coarse mesh with 726 nodes is constructed with node spacing of 167.6 m in the x-direction, 167.6 m in the y-direction and 3.048 m in the z-direction. A finer mesh with 5766 nodes is constructed with node spacing varying from 220.28 m at the edge of the model to 2.289 m near the extraction well in the x and y directions, while remaining uniform at 3.048 m in the z direction. A steady state flow field from north to south is established in the model by applying uniform pressures at the north and south end of the model while extracting water from the well in the center. Then 12 particles are started



near the northern boundary and allowed to travel with the flow. Some of them are captured by the extraction well and some travel on to the southern boundary.

The divergence of the dispersion tensor model is tested by comparing particle tracks obtained on the same domain for two different grids. The domain is a 1000 m by 1000 m by 1000 m 3-dimensional cube with a 200 m by 200 m by 1000 m parallelepiped embedded in the center, fully saturated with water (Figure 28). A uniform coarse mesh with 1331 nodes is constructed with node spacing of 100 m in the x-direction, 100 m in the y-direction and 100 m in the z-direction. A finer mesh with 112211 nodes is constructed with node spacing of 10 m in the x-direction, 10 m in the y-direction and 100 m in the z-direction. A steady state flow field diagonally from bottom left corner to top right corner is established in the model by applying prescribed pressures at the left, right, front and back faces of the model. Then a particle is started near the bottom left boundary and allowed to travel with the flow.

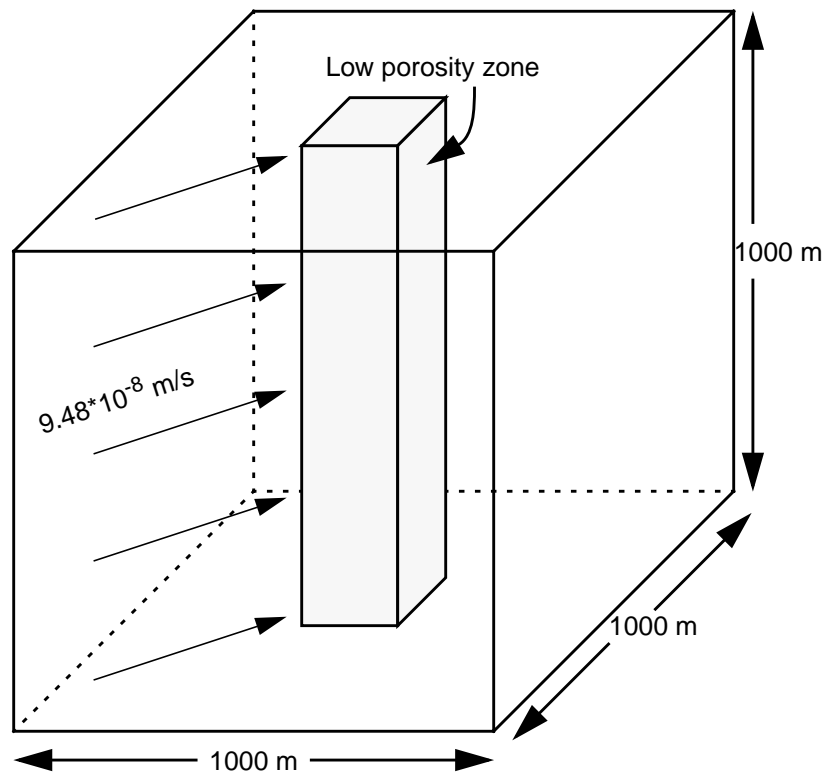


**Figure 28. Model domain and flow boundary conditions for the streamline particle tracking test of the divergence of the dispersion tensor model.**

Table XXVIII lists the input parameters and conditions for this test suite.

**Table XXVIII. Input Parameters and Conditions for the  
Streamline Particle Tracking Test Problems**

Parameter	Symbol	Value
Reservoir dimensions	$x$	20 km
Standard dispersion model	$y$	10 km
	$z$	0.5 km
Node spacing	$\Delta x, \Delta y$	400 m
Standard dispersion model	$\Delta z$	5 m
Reservoir dimensions	$x, y, z$	9 km
General dispersion model		
Node spacing	$\Delta x, \Delta y, \Delta z$	1 km
General dispersion model		
Reservoir dimensions	$x$	200 m
Reverse tracking model	$y$	15 m
	$z$	20 m
Node spacing	$\Delta x,$	2.5 - 5.625 m
Reverse tracking model	$\Delta y$	1 m
	$\Delta z$	0.7279542 m
Reservoir dimensions	$x, y$	1676 m
Particle capture model	$z$	15.24 m
Node spacing (particle capture model)		
Coarse grid	$\Delta x, \Delta y$	167.6 m
	$\Delta z$	3.048 m
Fine grid	$\Delta x, \Delta y$	2.89 - 220.28 m
	$\Delta z$	3.048 m
Reservoir dimensions	$x, y, z$	1000m
Divergence model		
Node spacing (divergence model)		
Coarse grid	$\Delta x, \Delta y, \Delta z$	100 m
Fine grid	$\Delta x, \Delta y$	10 m
	$\Delta z$	100 m
Bulk Rock Density	$\rho_b$	2530 kg/m <sup>3</sup>
Porosity		
Standard dispersion model		0.0283
General dispersion model		0.10
Reverse tracking model	$\phi$	0.35
Particle capture model		0.30
Divergence model, external domain		0.266
Divergence model, central parallelepiped		2.88*10 <sup>-5</sup>

**Table XXVIII. Input Parameters and Conditions for the  
Streamline Particle Tracking Test Problems**

Parameter	Symbol	Value
Reservoir permeability		
Standard dispersion model	$k$	$1.0 \times 10^{-12} \text{ m}^2$
General dispersion model		$1.0 \times 10^{-14} \text{ m}^2$
Reverse tracking model		$1.3 \times 10^{-14} \text{ m}^2$
Particle capture model		$4.0 \times 10^{-12} \text{ m}^2$
Divergence model		$5.0 \times 10^{-12} \text{ m}^2$
Longitudinal Dispersivity (standard dispersion model)	$\alpha_L$	
All tests except matrix diffusion		100 m
Matrix diffusion test		500 m
Transverse Dispersivity	$\alpha_T$	
Standard dispersion model (used only for In situ concentration profiles)		0.1 m
Dispersivity Coefficients (general model)		
Burnett and Frind Case	$\alpha_L$	3 m
	$\alpha_{TH}$	1 m
	$\alpha_{TV}$	0.1 m
Modified Burnett and Frind	$\alpha_{LH}$	3 m
	$\alpha_{LV}$	1 m
	$\alpha_{TH}$	1 m
	$\alpha_{TV}$	0.1 m
General Axisymmetric Case	$\alpha_1$	2 m
	$\alpha_2$	20 m
	$\alpha_3$	12 m
	$\alpha_4$	-4 m
Dispersivity Coefficients (divergence model)		
Longitudinal dispersivity	$\alpha_L$	3 m
Transverse dispersivity	$\alpha_T$	0.1 m
Particles Injected		
All dispersion tests except 2nd profile test	--	10000
2nd In situ concentration profile test		100000
Reverse tracking model		10
Particle capture model		12
Divergence model		1
Time step (particle)		
Breakthrough curve tests	$\Delta t$	2000 days
In situ concentration profile tests		333 days
General dispersion model		1267 years
Reverse tracking model		300 days
Particle capture model		1157 days
Divergence model		$1 \times 10^7$ days

**Table XXVIII. Input Parameters and Conditions for the  
Streamline Particle Tracking Test Problems**

Parameter	Symbol	Value
Total elapsed time		
No sorption test		1370 years
Sorption test		2500 years
Matrix diffusion test		3000 years
In situ concentration profile tests	$t$	960 years
General dispersion model		$2.74 \times 10^6$ years
Reverse tracking model		$1 \times 10^{14}$ years
Particle capture model		$3 \times 10^7$ years
Divergence model		$1 \times 10^9$ days
Restart time	--	0. days
Pumping rate		
Particle capture model	$q$	0.1639 kg/s
Pore Water Velocity		
Standard dispersion model	$u$	34 m/year
Pore Water velocity (general dispersion model)		
Burnett and Frind and Modified Burnett and Frind Cases	$v_x$	$8.22 \times 10^{-11}$ m/s
	$v_y$	0 m/s
	$v_z$	$8.22 \times 10^{-11}$ m/s
General Axisymmetric Case	$v_x$	$8.22 \times 10^{-11}$ m/s
	$v_y$	0 m/s
	$v_z$	0 m/s
Darcy velocity		
Divergence model	$u$	$9.48 \times 10^{-8}$ m/s
Pressure		
Dispersion models	$P_0$	2.2 MPa
Particle capture model		0.1 MPa
Inlet Pressure		
Standard dispersion model	$P_{in}$	2.3767 MPa
General dispersion model		2.0 MPa
Outlet Pressure		
Standard dispersion model	$P_{out}$	2.0 MPa
General dispersion model		2.045 MPa
Boundary conditions:		
Reverse tracking model		
At $x = 0 - 200$ m, $y = 0 - 15$ m, $z = 20$ m		$H = 5021 - 5020$ m
At $x = 200$ m, $y = 0 - 15$ m, $z = 0 - 20$ m		$H = 5020$ m
Particle capture model		
At $x = 0 - 1676$ m, $y = 0$ , $z = 0 - 15.24$ m		$P = 0.1146$ MPa
At $x = 0 - 1676$ m, $y = 1676$ m, $z = 0 - 15.24$ m		$P = 0.1$ MPa

---

**Table XXVIII. Input Parameters and Conditions for the  
Streamline Particle Tracking Test Problems**


---

Parameter	Symbol	Value
Divergence model		
At x = 0 m, y = 0 m, z = 0 - 1000 m	$P$	1.46 MPa
At x = 1000 m, y = 0 - 1000 m, z = 0 - 1000 m	$P$	1.44 MPa

---

## 2.23.4 Summary of Test Cases

### 2.23.4.1 Test of Breakthrough Curve, Conservative, Sorbing, and Matrix Diffusion Models

**2.23.4.1.1 Function Tested.** This test verifies that FEHM correctly simulates breakthrough curves of longitudinal dispersion with and without sorption and matrix diffusion using the streamline particle tracking model.

**2.23.4.1.2 Test Scope.** This test case is a verification test.

**2.23.4.1.3 Requirements Tested.** Requirements 2.2, "Finite-Element Coefficient Generation," 2.3, "Formulate Transient Equations," specifically Section 2.3.4, Section 2.3.6, and Section 2.3.7, 2.4, "Apply Constitutive Relationships," specifically Section 2.4.5, 2.5, "Compute Solution to Transient Equations," 2.6, "Provide Input/Output Data Files," and 2.7, "Provide Restart Capability," of the FEHM RD are verified by this test.

**2.23.4.1.4 Required Inputs.** Problem input is provided in the following files:

- *sptr\_long1.dat*: Basic input data for simulating longitudinal dispersion breakthrough curve, no sorption.
- *sptr\_long2.dat*: Basic input data for simulating longitudinal dispersion breakthrough curve with sorption.
- *sptr\_long3.dat*: Basic input data for simulating longitudinal dispersion breakthrough curve with matrix diffusion.
- *sptr.geom*: Finite element grid, a structured, three-dimensional mesh with 128,775 nodes, 120,000 elements.
- *valid1.stor*: Finite element coefficient storage file.
- *valid1.ini*: Steady state flow initialization file.

**2.23.4.1.5 Expected Outputs.** Values from FEHM for normalized concentration-time histories at a specified node 15 km downstream from the injection will be compared to the analytical solution result. A root mean square error between FEHM and the analytical solution, of less than or equal to 0.05, at concentrations greater than 10% of the peak value, will be considered acceptable.

The required output files for these tests are the:

- Streamline particle data output files (*sptr\_long1.sptr3*, *sptr\_long2.sptr3*, *sptr\_long3.sptr3*).

#### 2.23.4.2 Test of In Situ Concentration Profile, Longitudinal and Transverse Dispersion

2.23.4.2.1Function Tested. This test verifies that FEHM correctly simulates in situ concentrations assuming longitudinal and transverse dispersion using the streamline particle tracking model.

2.23.4.2.2Test Scope. This test case is a verification test.

2.23.4.2.3Requirements Tested. Requirements 2.2, "Finite-Element Coefficient Generation," 2.3, "Formulate Transient Equations," specifically Section 2.3.6 and Section 2.3.7, 2.4, "Apply Constitutive Relationships," specifically Section 2.4.5, 2.5, "Compute Solution to Transient Equations," 2.6, "Provide Input/Output Data Files," and 2.7, "Provide Restart Capability," of the FEHM RD are verified by this test.

2.23.4.2.4Required Inputs. Problem input is provided in the following files:

- *plume1.dat*: Basic input data for simulating 10,000 particle test of in situ concentration profiles.
- *plume2.dat*: Basic input data for simulating 100,000 particle test of in situ concentration profiles.
- *sptr.geom*: Finite element grid, a structured, three-dimensional mesh with 128,775 nodes, 120,000 elements.
- *valid1.stor*: Finite element coefficient storage file.
- *valid1.ini*: Steady state flow initialization file.

2.23.4.2.5Expected Outputs. Values from FEHM for normalized concentration profiles at specified nodes, 5 and 10 km downstream from the injection, will be compared to the analytical solution result. A root mean square error between FEHM and the analytical solution, of less than or equal to 0.10, at concentrations greater than 10% of the peak value, will be considered acceptable. A further check of the model will be to perform the same simulation with 100,000 particles, and visually verify that the agreement of model and analytical solution improves. Due to the long run times associated with injection of a larger number of particles, and the desire to perform the automated test runs in a reasonable period of time, this latter simulation will generally be performed outside the automated suite of test cases.

The required output files for these tests are the:

- Solute data plot files (*plume1.trc*, *plume2.trc*).

#### 2.23.4.3 Test of the Generalized Dispersion Tensor

2.23.4.3.1Function Tested. This test verifies that FEHM correctly simulates particle locations for dispersion using the Burnett and Frind tensor, the modified Burnett and Frind tensor, and the Generalized Axisymmetric dispersion tensor.

2.23.4.3.2Test Scope. This test case is a verification test.

2.23.4.3.3Requirements Tested. Requirements 2.2, "Finite-Element Coefficient Generation," 2.3, "Formulate Transient Equations," specifically Section 2.3.6 and Section 2.3.7, 2.4, "Apply

Constitutive Relationships,” specifically Section 2.4.5, 2.5, “Compute Solution to Transient Equations,” and 2.6, “Provide Input/Output Data Files,” of the FEHM RD are verified by this test.

**2.23.4.3.4 Required Inputs.** Problem input is provided in the following files:

- *tensorxz1.dat*: Basic input data for simulating Burnett and Frind dispersion tensor.
- *tensorxz2.dat*: Basic input data for simulating modified Burnett and Frind dispersion tensor.
- *tensorx.dat*: Basic input data for simulating General Axisymmetric dispersion tensor.
- *tensor.geom*: Finite element grid, a structured, three-dimensional grid with 1000 nodes (10x10x10), 729 elements.

**2.23.4.3.5 Expected Outputs.** Values from FEHM for particle locations are output in file \*.sptr1 for these cases. These values are post processed to obtain the expected values for the standard deviation (square root of second moment) at  $6.949 \times 10^8$  days. An error of less than or equal to 2 % of the theoretical value, given in Table XXIX will be considered acceptable.

---

**Table XXIX. Analytical Values for Standard Deviation at  $6.949 \times 10^8$  days**

---

Case	$\Delta x$ (m)	$\Delta y$ (m)	$\Delta z$ (m)
Burnett and Frind	147	88	147
Modified Burnett and Frind	133	118	133
Generalized Axisymmetric	516	329	140

---

The required output files for these tests are the:

- Streamline particle data output files (*tensorxz1.sptr1*, *tensorxz2.sptr1*, *tensorx.sptr1*).

## **2.23.4.4 Test of Reverse Tracking Model**

**2.23.4.4.1 Function Tested.** This test verifies that FEHM correctly simulates reverse tracking.

**2.23.4.4.2 Test Scope.** This test case is a verification test.

**2.23.4.4.3 Requirements Tested.** Requirements 2.2, “Finite-Element Coefficient Generation,” 2.3, “Formulate Transient Equations,” specifically Section 2.3.6 and Section 2.3.7, 2.5, “Compute Solution to Transient Equations,” 2.6, “Provide Input/Output Data Files,” and 2.7, “Provide Restart Capability,” of the FEHM RD are verified by this test.

**2.23.4.4.4 Required Inputs.** Problem input is provided in the following files:

- *forward.dat*: Basic input data for simulating forward particle tracking.

- *reverse.dat*: Basic input data for simulating reverse particle tracking.
- *forward.fin*: Steady state flow initialization file generated from forward simulation and then used by reverse simulation.
- *forward-reverse.geom*: Finite element grid, a structured, three-dimensional grid with 17600 nodes (50x15x22), 15435 elements.
- *right\_constant.boun*, *top.boun*: Flow macro data defining problem head boundary conditions.

2.23.4.4.5 Expected Outputs. Values from FEHM for particle locations are output in file \*.sptr1 for these cases. These values are post processed to compare the particle locations for the forward and reverse tracks [i.e. by inverting the order of positions (backwards in time) for the reverse tracking model]. A difference of less than or equal to 1 m between particle locations of the forward and reverse tracks will be considered acceptable.

The required output files for these tests are the:

- Streamline particle data output files (*forward.sptr1*, *reverse.sptr1*).

## 2.23.4.5 Test of Particle Capture Model

2.23.4.5.1 Function Tested. This test verifies that FEHM correctly simulates particle capture.

2.23.4.5.2 Test Scope. This test case is a verification test.

2.23.4.5.3 Requirements Tested. Requirements 2.2, "Finite-Element Coefficient Generation," 2.3, "Formulate Transient Equations," specifically Section 2.3.6 and Section 2.3.7, 2.5, "Compute Solution to Transient Equations," 2.6, "Provide Input/Output Data Files," and 2.7, "Provide Restart Capability," of the FEHM RD are verified by this test.

2.23.4.5.4 Required Inputs. Problem input is provided in the following files:

- *zheng1.dat*: Basic input data for simulating particle capture on a coarse grid.
- *zheng1.flow.ini*: Steady state flow initialization file.
- *zheng1.geom*: Finite element grid, a structured, three-dimensional grid with 726 nodes (11x11x6), 500 elements.
- *zheng2.dat*: Basic input data for simulating for simulating particle capture on a fine grid.
- *zheng2.flow.ini*: Steady state flow initialization file.
- *zheng2.geom*: Finite element grid, a structured, three-dimensional grid with 5766 nodes (31x31x6), 4500 elements.

2.23.4.5.5 Expected Outputs. Values from FEHM for particle locations are output in file \*.sptr1 for these cases. These values are post processed to compare the particle locations for the coarse and fine grid tracks in time. A difference of less than or equal to 17 m between particle locations of the coarse and fine grid tracks (~10 % of the coarse grid spacing) will be considered acceptable.



The required output files for these tests are the:

- Streamline particle data output files (*zheng1.sptr1*, *zheng2.sptr1*).

#### **2.23.4.6 Test of Divergence of Dispersion Tensor Model**

2.23.4.6.1 **Function Tested.** This test verifies that FEHM correctly simulates random walk particle transport.

2.23.4.6.2 **Test Scope.** This test case is a verification test.

2.23.4.6.3 **Requirements Tested.** Requirements 2.2, “Finite-Element Coefficient Generation,” 2.3, “Formulate Transient Equations,” specifically Section 2.3.6 and Section 2.3.7, 2.5, “Compute Solution to Transient Equations,” 2.6, “Provide Input/Output Data Files,” and 2.7, “Provide Restart Capability,” of the FEHM RD are verified by this test.

2.23.4.6.4 **Required Inputs.** Problem input is provided in the following files:

- *cube\_center\_coarse.dat*: Basic input data for simulating coarse mesh.
- *1331x100.geom*: Finite element grid, a structured, three-dimensional grid with 1331 nodes (11x11x11), 6000 elements.
- *cube\_center\_coarse.ini*: Flow field initialization file.
- *cube\_center\_fine.dat*: Basic input data for simulating fine mesh.
- *flow\_pres.macro*: Input for the “flow” macro for the fine mesh.
- *100x100x10.geom*: Finite element grid files, a structured, three-dimensional grid with 112211 nodes (101x101x11), 100000 elements.
- *100x100x10.stor*: Finite element coefficient storage file for the fine mesh.
- *cube\_center\_fine.ini*: Flow field initialization file.

2.23.4.6.5 **Expected Outputs.** Values from FEHM for particle locations are output in file \*.sptr1 for these cases. These values are post processed to compare the particle locations for the coarse and fine grid tracks in time. A difference of less than or equal to 50 m between particle locations of the coarse and fine grid tracks will be considered acceptable.

The required output files for these tests are the:

- Streamline particle data output files (*10cube\_center.sptr1*, *cube\_center.sptr1*).

## 2.24 Test of Cell-Based Particle Tracking Model

### 2.24.1 Purpose

Several test cases have been executed to confirm the accuracy of the cell-based particle-tracking method by comparison with analytical and other numerical solutions. The model must be shown to obtain accurate breakthrough curves for advection, dispersion, and matrix diffusion for a single continuum and dual permeability model formulation. To test the model for diffusion and dispersion, the analytical solution developed by Tang et al. (1981) is used, which simulates one-dimensional flow through a fracture and diffusion into a semi-infinite matrix. In addition, the transfer function approach for simulating matrix diffusion is tested by comparing the results to a discrete fracture model. These cases test the behavior of the model under the limiting conditions of infinite fracture spacing, finite fracture spacing and comparison to a numerical discrete fracture model. Decay chains must also be computed adequately using the multiple-species option. For these comparisons, a test case using the numerical model CHAIN (van Genuchten, 1985) was developed for comparison to the particle tracking model. Because the analytical and numerical solutions use entirely different techniques than the particle tracking method, the test provides a rigorous check of the cell-based particle tracking model. Finally, the PC interface between GoldSim (Golder Associates, 2002) and FEHM is tested for this decay-chain problem. In this case, GoldSim defines the input mass instead of it being a direct input to FEHM, but otherwise the problem is identical. A multispecies test using transfer functions is also included.

### 2.24.2 Functional Description

The test cases for this suite consist of three simulations that test the ability of the code to simulate single-species transport with advection, dispersion, sorption, and matrix diffusion; one test problem to test the transport of a decay chain consisting of four species; and a simulation in which the same decay chain problem is used to test the GoldSim-FEHM interface.

### 2.24.3 Assumptions and Limitations

The problem geometry is depicted in Fig. 29. Table XXX defines the input parameters used for FEHM particle tracking simulations. A fluid flow steady state is established by injecting fluid at a fixed flow rate at the inlet and applying a constant pressure boundary condition at the outlet. The solute transport simulation is executed by injecting particles either as a pulse or over a finite duration. For the single-species simulations, we assume each solute has the same dispersivity (0.033 m, equivalent to a dimensionless Peclet number  $L/\alpha$  of 30). The inlet concentration is assumed to be normalized to unity for the entire simulation.

For the dual permeability test cases, the problem geometry in which the particle tracking calculations are performed is a one-dimensional pathway with overlapping fracture and matrix continua. A series of test problems are run for this geometry, and the outlet mass flux versus time of solute is simulated in response to solute introduced as a step change in concentration at the inlet. The comparison model is an idealized discrete fracture model which captures concentration gradients in the matrix via the direct finite element solution of a two-dimensional grid. The structure of the discrete fracture model is such that all of the following flow conditions are tested: Flow in the fracture only, stagnant fluid in the

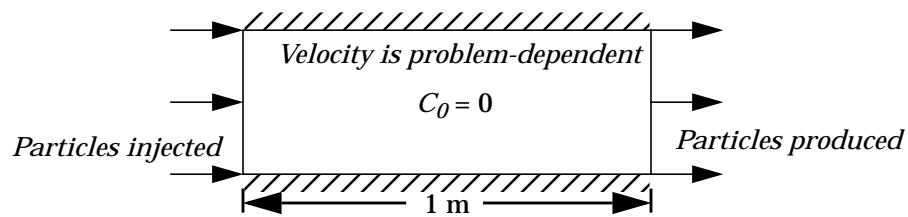


**Figure 29. Model domain and flow boundary conditions for the cell-based particle tracking test problems.**

matrix; parallel flow in the fracture and matrix, with no advective interchange between the media; a combination of these two systems in which a transition from fracture-dominated (90% fracture flow, 10% matrix flow) to more evenly distributed flow (60% fracture flow, 40% matrix flow) occurs at half way along the path. For cases being compared to a discrete fracture model, the discrete fracture simulations are performed with a qualified version of FEHM. To control the advective flux from fracture to matrix, the permeability at the interface between the fracture and matrix nodes is set to a low value, except for the case in which flow transitions from fracture to matrix. Transport of conservative, sorbing, diffusing, and nondiffusing solutes will ensure that the dual permeability particle tracking option is robust over a wide range of transport conditions. The one-dimensional grids and flow fields in the dual permeability particle tracking simulations will be constructed by hand and read into the test problem, based on an abstraction of the flow field from the discrete fracture model. This flow field will be read directly into FEHM for the particle tracking run. Because of the approximations involved, including the use of transfer functions that must be interpolated between, exact comparisons between model and data are not expected to be obtained. However, trends in the model output, and comparisons between the various transport parameter tests, should follow the same trends. That is, plateaus in the breakthrough curves and the mean arrival times at the outlet should be approximated. The multispecies test models two species which are the same. The final particle concentrations can be examined in the output file to determine that the two species have behaved basically the same.

For the multiple-species decay-chain simulation, the decay chain  $1 \rightarrow 2 \rightarrow 3 \rightarrow 4$  is simulated, with decay half lives of the species equaling 10,000, 3,000, 10,000, and 4,000 years, respectively. Particles for species 1 are injected at a constant rate from 0 to 5,000 years, and species 2, 3, and 4 are formed through the decay reactions, with no input at the inlet. The retardation factors for the four species are 1, 1, 1.9, and 1, respectively (i.e. only species 3 sorbs).

## 2.24.4 Summary of Test Cases

### 2.24.4.1 Test of Breakthrough Curve, Conservative, Sorbing, and Matrix Diffusion Models

**2.24.4.1.1 Function Tested.** This test verifies that FEHM correctly simulates breakthrough curves of longitudinal dispersion with

**Table XXX.Input Parameters and Conditions for the Cell-Based Particle Tracking Test Problems**

Parameter	Symbol	Value
Fluid Velocity		
No sorption & sorption tests	$v$	11.2 kg/s
Matrix diffusion test		5.8e-7 kg/s
Decay chain test		5.0e-10 kg/s
Flow Path Length	$x$	1 m
Node spacing	$\Delta x$	0.1 m
Dispersivity		
Other tests	$\alpha$	0.01
Decay chain test		0.005
Matrix Diffusion Coefficient		
Matrix diffusion test only	$D_{mol}$	1.0e-10 m <sup>2</sup> /s
Sorption Coefficient		
Sorption test	$K_D$	0.12 kg-fluid/kg-rock
Matrix diffusion test: matrix		0.18 kg-fluid/kg-rock
Decay chain test: 3rd species		0.108 kg-fluid/kg-rock
Retardation factor		
Matrix diffusion test: fracture	$R_f$	0.5
Porosity		
Other tests	$\phi$	0.3
Matrix diffusion test		0.001
Bulk Rock Density	$\rho_b$	2500 kg/m <sup>3</sup>
Restart time	--	0. days
Total elapsed time		
No sorption & sorption tests	$t$	2.0e-3 days
Matrix diffusion test		10 days
Decay chain test		25000 years
Pressure	$P_0$	1 MPa
Initial concentration	$C_0$	0
Particles Injected		
Other tests	--	100000
Decay chain test		1100100

and without sorption and matrix diffusion using the cell-based particle tracking model.

2.24.4.1.2 Test Scope. This test case is a verification test.

2.24.4.1.3Requirements Tested. Requirements 2.2, “Finite-Element Coefficient Generation,” 2.3, “Formulate Transient Equations,” specifically Section 2.3.4 and Section 2.3.7, 2.4, “Apply Constitutive Relationships,” specifically Section 2.4.5, 2.5, “Compute Solution to Transient Equations,” 2.6, “Provide Input/Output Data Files,” and 2.7, “Provide Restart Capability,” of the FEHM RD are verified by this test.

2.24.4.1.4Required Inputs. Problem input is provided in the following files:

- *cellbased1.dat*: Basic input data for simulating one-dimensional dispersion breakthrough curve, no sorption.
- *cellbased2.dat*: Basic input data for simulating one-dimensional dispersion breakthrough curve with sorption.
- *cellbased3.dat*: Basic input data for simulating one-dimensional dispersion breakthrough curve with matrix diffusion, sorption in the matrix, and sorption on the fracture surfaces.
- *oned24.geom*: Finite element grid file, a two-dimensional grid consisting of 12x2 nodes, which reduces to a one-dimensional flow and transport system when flow is injected and produced from each side of the grid.
- *flow\_field1.ini*, *flow\_field2.ini*, *flow\_field3.ini*: Steady state flow initialization files.

2.24.4.1.5Expected Outputs. Values for the breakthrough curve (distribution of travel times of particles) from FEHM at the outlet will be compared to the analytical solution result. A root mean square error between FEHM and the analytical solution, of less than or equal to 0.05, at concentrations greater than 10% of the peak value, will be considered acceptable.

The required output files for these tests are the:

- Restart data files (*cellbased1.fin*, *cellbased2.fin*, *cellbased3.fin*).

#### **2.24.4.2 Test of Breakthrough Curve, Dual Permeability Model with Advection, Sorption, and Fracture/Matrix Interchange**

2.24.4.2.1Function Tested. This test verifies that FEHM correctly implements the dual permeability particle tracking model using transfer function curves of transport generated using a discrete fracture model.

2.24.4.2.2Test Scope. This test case is a verification test.

2.24.4.2.3Requirements Tested. Requirements 2.2, “Finite-Element Coefficient Generation,” 2.3, “Formulate Transient Equations,” specifically Section 2.3.4 and Section 2.3.7, 2.4, “Apply Constitutive Relationships,” specifically Section 2.4.5, 2.5, “Compute Solution to Transient Equations,” 2.6, “Provide Input/Output Data Files,” and 2.7, “Provide Restart Capability,” of the FEHM RD are verified by this test.

2.24.4.2.4Required Inputs. Problem input is provided in the following files:

- *dkmf1t1.dat*: Input data for flow field 1, diffusion, no matrix sorption.
- Other files associated with this run: Three particle tracking macro files for this test case are used: *f1t1.ptrk*, *f1t1free.ptrk*, *f1t1freesvd.ptrk*. These files in turn use the following transfer function files: *pfracture3.dat*, *pfracture\_free.dat*, *pfracture\_freesvd.dat*. Grid files: *1d\_dkm.grid*, *1d\_dkm.stor*. Flow field: *flow1.ini*.
- *dkmf1t2.dat*: Input data for flow field 1, diffusion, matrix sorption. The particle tracking and transfer function files for this test are *f1t2.ptrk* and *pfracture3.dat*. Grid files: *1d\_dkm.grid*, *1d\_dkm.stor*. Flow field: *flow1.ini*.
- *dkmf2t1.dat*: Input data for flow field 2, diffusion, no sorption, parallel flow in fracture and matrix. The particle tracking and transfer function files for this test are *f2t1reg.ptrk* and *uz\_la\_tfcures.in*. Grid files: *1d\_dkm2.grid*, *1d\_dkm2.stor*. Flow field: *flow2.ini*.
- *dkmf3t1.dat*: Input data for flow field 3, no diffusion, no sorption, parallel flow in fracture and matrix, abrupt change of flow fraction in fracture half way down the flow path. The particle tracking and transfer function files for this test are *f3t1free.ptrk* and *uz\_la\_tfcures.in*. Grid files: *1d\_dkm2.grid*, *1d\_dkm2.stor*. Flow field: *flow3.ini*.

2.24.4.2.5 Expected Outputs. Breakthrough curves from the dual permeability particle tracking model (the final simulation particle arrival times from FEHM) will be visually compared to the discrete fracture model results, the Sudicky and Frind analytical solution (flow field 1), or examined to ensure proper breakthrough of the correct proportions of mass for the no diffusion case (*dkmf3t1.dat*). The particle tracking model is an abstraction intended to capture the main features of the distribution of arrival times of a solute, so a direct comparison with numerical criteria to assess the goodness of agreement with the discrete fracture model is inappropriate. Instead, visual comparisons will be performed to ensure that the model captures the key features of the discrete fracture model over the range of the verification suite. For example, in simulations for which a plateau in breakthrough occurs (*dkmf3t1.dat*), followed by a rise at later times, the particle tracking model should capture the plateau, and approximate the arrival times of the various rises in the breakthrough curve. Comparisons between sorbing and conservative transport runs should qualitatively agree, and mean arrival times of curves without distinct plateaus should also agree.

The required output files for these tests are the:

- Restart data files (*dkmf1t1.fin*, *dkmf1t1free.fin*, *dkmf1t1freesvd.fin*, *dkmf1t2.fin*, *dkmf2t1.fin*, *dkmf3t1.fin*) and final postprocessed breakthrough curve files (*dkmf1t1.output*, *dkmf1t1free.output*, *dkmf1t1freesvd.output*, *dkmf1t2.output*, *dkmf2t1reg.output*, *dkmf3t1freesvd.output*).

#### 2.24.4.3 Test of Breakthrough Curves for Decay-Chain Case, Sorption of Intermediate Species

2.24.4.3.1 Function Tested. This case ensures that the decay-chain option of the multiple-species particle-tracking model properly accounts for radioactive decay chains for a mixed case of conservative and sorbing radionuclides.

2.24.4.3.2 Test Scope. This test case is a verification test.

2.24.4.3.3 Requirements Tested. Requirements 2.2, "Finite-Element Coefficient Generation," 2.3, "Formulate Transient Equations," specifically Section 2.3.4 and Section 2.3.7, 2.4, "Apply Constitutive Relationships," specifically Section 2.4.5, 2.5, "Compute Solution to Transient Equations," 2.6, "Provide Input/Output Data Files," and 2.7, "Provide Restart Capability," of the FEHM RD are verified by this test.

2.24.4.3.4 Required Inputs. Problem input is provided in the following files:

- *chain.in*: Basic input data for simulating one-dimensional decay-chain breakthrough curve.
- *chain.mptr*: mptr input macro data for simulating decay-chain breakthrough curve.
- *chain.geom*: Finite element grid file, a two-dimensional grid consisting of 201x2 nodes, which reduces to a one-dimensional flow and transport system when flow is injected and produced from each side of the grid.
- *chain.ini*: Steady state flow initialization file.

2.24.4.3.5 Expected Outputs. Values for the breakthrough curves (distribution of travel times of particles) of the four species from FEHM at the outlet will be compared to the computer code CHAIN. A root mean square error between FEHM and CHAIN, of less than or equal to 0.05, at concentrations greater than 10 % of the peak value, will be considered acceptable.

The required output file for this test is the:

- Output data file (*chain.out*).

#### 2.24.4.4 Test of GoldSim/FEHM Interface for Breakthrough Curves for Decay-Chain Case

2.24.4.4.1 Function Tested. This case ensures that the GoldSim/FEHM Interface properly passes radionuclide mass back and forth, and that GoldSim properly invokes FEHM to perform the transport calculations. A test problem identical to that discussed in the previous section (the four-species decay chain problem) will be used for this test.

2.24.4.4.2 Test Scope. This test case is a verification test.

2.24.4.4.3 Requirements Tested. Requirements 2.2, "Finite-Element Coefficient Generation," 2.3, "Formulate Transient Equations," specifically Section 2.3.4 and Section 2.3.7, 2.4, "Apply Constitutive Relationships," specifically Section 2.4.5, 2.5, "Compute Solution to Transient Equations," 2.6, "Provide Input/Output Data Files," and 2.7, "Provide Restart Capability," of the FEHM RD are verified by this test.

2.24.4.4.4 Required Inputs. Problem input is provided in the following files:

- *goldsimchain.gsm*: GoldSim model file for performing the transport calculation.
- *chain\_gsm.files*: File that specifies FEHM input and output file names to be used for the simulation. This file must be renamed to *fehmn.files* prior to the GoldSim run.
- *chain\_gsm.in*: Basic input data for simulating one-dimensional decay-chain breakthrough curve.
- *chain\_gsm.mptr*: mptr input macro for simulating decay-chain breakthrough curve.
- *chain.geom*: Finite element grid file, a two-dimensional grid consisting of 201x2 nodes, which reduces to a one-dimensional flow and transport system when flow is injected and produced from each side of the grid.
- *chain\_gsm.ini*: Steady state mass flux initialization file.
- *fehmn.gold*: File that specifies number of input and output parameters passed between GoldSim and FEHM.
- *fehmn\_real.bat*: Batch file that is executed during GoldSim initialization of FEHM (note the file has no commands for this simulation).
- *fehmn\_ts0.bat*: Batch file that is executed during first GoldSim time step (note the file has no commands for this simulation).

2.24.4.4.5 Expected Outputs. Because the GoldSim model cannot be run as part of the automated suite of test runs, automated numerical comparisons are not possible. Instead, values for the cumulative breakthrough with time of the four species from GoldSim will be compared visually to the results of the previous test case (see Figure 30). The test will be considered acceptable if there are no systematic differences between the GoldSim output and the results of either FEHM, produced in the previous test case, or the CHAIN code.

#### **2.24.4.5 Test of Breakthrough Curve, Dual Permeability Model with Fracture/Matrix Interchange for Multiple Species**

2.24.4.5.1 Function Tested. This test verifies that FEHM correctly implements the dual permeability particle tracking model using transfer function curves of transport generated using a discrete fracture model.

2.24.4.5.2 Test Scope. This test case is a verification test.

2.24.4.5.3 Requirements Tested. Requirements 2.2, “Finite-Element Coefficient Generation,” 2.3, “Formulate Transient Equations,” specifically Section 2.3.4 and Section 2.3.7, 2.4, “Apply Constitutive Relationships,” specifically Section 2.4.5, 2.5, “Compute Solution to Transient Equations,” 2.6, “Provide Input/Output Data Files,” and 2.7, “Provide Restart Capability,” of the FEHM RD are verified by this test.



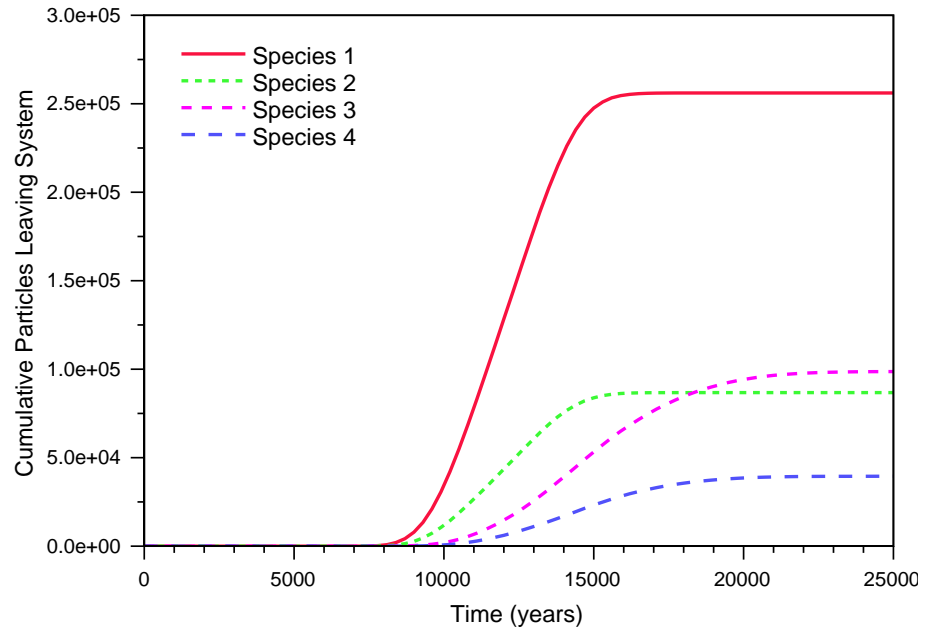


**Figure 30. FEHM solution for cumulative breakthrough concentration versus time.**

2.24.4.5.4 Required Inputs. Problem input is provided in the following files:

- *fehm\_test\_mptr.dat*: Basic input data for simulating multispecies breakthrough curve.
- *fehm\_amr\_base.dpd*: Dual permeability macro input.
- *fehm\_amr\_base.rock*: rock macro input.
- *fehm\_test\_mptr.mptr*: mptr input macro data for simulating multispecies breakthrough curve.
- *fehm.grid*: Grid file.
- *fehm.stor*: Coefficient storage file.
- *fehm.zone*, *fehm.zone2*: zone macro input.
- *glaqma.ini*: Steady state flow initialization file.
- *uz\_la\_tfcurves.in*: Transfer function file.

2.24.4.5.5 Expected Outputs. Breakthrough curves from the dual permeability particle tracking model (the final simulation particle arrival times from FEHM) will be examined to ensure proper breakthrough of the correct proportions of mass for the multispecies test. The number of particles that have left the system, remain in the system, and decayed should be within 10% of each other for both species at the final time step.

The required output file for this test is the:

- Output data files (*fehm\_test\_mptr.out*).

### 3.0 INSTRUCTIONS for EXECUTION of TEST CASES

The following instructions apply to execution of any of the test problems described in Sections 2.2 to 2.24. Prior to execution of the selected test problem the user should know the following:

- Location of the FEHM executable;
- Location and names of the test input files;
- Location where test output should be written, and which output files are required for validation of results.

The example shown in Figure 31 illustrates execution of the Avdonin problem with a 400 node domain (Section 2.11 Test of Heat and Mass Transfer in Porous Media) using the interactive terminal interface. For purposes of this example the executable is found at /home/fehm/bin/xfehm\_v2.21sun, the verification input is located in /home/fehm/verification/avdonin/input, and the output will be written to /home/fehm/verification/avdonin/output. Filename responses for the example assume the problem is being executed from the test directory /home/fehm/verification/avdonin. Note that user responses have been italicized for emphasis and <cr> represents a carriage return.

```
seismo2% /home/fehm/bin/xfehm_v2.21sun

version  FEHM V2.21sun 03-08-12 QA:QA    08/18/2003  11:37:55

**** Default names for I/O files ****

control file           : fehm.files
input file             : filen.*
geometry data file     : filen.*
zone data file         : filen.*
output file            : filen.out
read file (if it exists) : filen.ini
write file (if it exists) : filen.fin
history plot file      : filen.his
tracer history plot file : filen.trc
contour plot file      : filen.con
dual or dpdp contour plot file : filen.dp
stiffness matrix data read/write file : filen.stor
input check file       : filen.chk

**** where ****

"filen.*" may be 100 characters maximum. If a name is not entered
when prompted for, a default file name is used. "fehm.dat" is the
default used for the input file name.

**** note ****

A save file and input check file are always written, if you do not
provide a name for these files, the following defaults will be used:
fehm.files, fehm.chk
```

**Figure 31. Illustration of code execution and terminal output for the Avdonin test problem .**

```

Enter name for iocntl -- default file name: not using
[(name/na or not using), RETURN = DEFAULT]
<cr>

Enter name for inpt -- default file name: fehmn.dat
[(name/na or not using), RETURN = DEFAULT]
input/avdonin.in

Do you want all file names of the form input/avdonin.* ? [(y/n), RETURN = y] **
* Note: If "y" incoor and inzone will equal inpt ***
n

Enter name for incoor -- default file name: input/avdonin.in
[(name/na or not using), RETURN = DEFAULT]
input/avdonin.geom.400

Enter name for inzone -- default file name: input/avdonin.in
[(name/na or not using), RETURN = DEFAULT]
na

Enter name for iout -- default file name: input/avdonin.out
[(name/na or not using), RETURN = DEFAULT]
output/avdonin400.out

Enter name for iread -- default file name: input/avdonin.ini
[(name/na or not using), RETURN = DEFAULT]
na

Enter name for isave -- default file name: input/avdonin.fin
[(name/na or not using), RETURN = DEFAULT]
na

Enter name for ishis -- default file name: input/avdonin.his
[(name/na or not using), RETURN = DEFAULT]
output/avdonin400.his

Enter name for istrc -- default file name: input/avdonin.trc
[(name/na or not using), RETURN = DEFAULT]
na

Enter name for iscon -- default file name: input/avdonin.con
[(name/na or not using), RETURN = DEFAULT]
na

Enter name for iscon1 -- default file name: input/avdonin.dp
[(name/na or not using), RETURN = DEFAULT]
na

```

**Figure 31. Illustration of code execution and terminal output for the Avdonin test problem (Continued).**

```

Enter name for isstor -- default file name: input/avdonin.stor
[(name/na or not using), RETURN = DEFAULT]
na

Enter name for ischk -- default file name: input/avdonin.chk
[(name/na or not using), RETURN = DEFAULT]
na

tty output -- show all reference nodes, selected reference nodes, or none:
[(all/some/none), RETURN = none]
none

user subroutine number (provided to subroutine USER before every time step):
[RETURN = none]
none

Not using tty output

File purpose - Variable - Unit number - File name

control      - iocntl  - 0 - not using
input        - inpt   - 11 - input/avdonin.in
geometry     - incoor  - 12 - input/avdonin.geom.400
zone         - inzone  - 11 - input/avdonin.in
output       - iout    - 14 - output/avdonin400.out
initial state - iread   - 0 - not using
final state  - isave   - 0 - not using
time history - ishis   - 17 - output/avdonin400.his
time his.(tr) - istrc  - 0 - not using
contour plot - iscon   - 0 - not using
con plot (dp) - iscon1 - 0 - not using
fe coef stor - isstor  - 0 - not using
input check  - ischk   - 0 - not using
Value provided to subroutine user: not using

If data is OK enter yes to continue, no to restart terminal input,
or stop to end program: [(yes/no/stop), RETURN = yes]
yes

```

**Figure 31. Illustration of code execution and terminal output for the Avdonin test problem (Continued).**

The Appendix describes an automated test scheme that can be used to sequentially execute the tests described in Sections 2.1 to 2.24.

## 4.0 REFERENCES

- Auer, L. H., N. D. Rosenberg, K. H. Birdsell, and E. M. Whitney, "The Effects of Barometric Pumping on Contaminant Transport," *Journal of Contaminant Hydrology* **24**, 145-166 (1996). TIC:254769
- Bear, J., *Dynamics of Fluids in Porous Media*, American Elsevier, New York, NY, 764 pp (1972). TIC:217356
- Bejan, A., *Convection Heat Transfer*, 2nd Edition, Wiley, NY, 1995. TIC:24140
- Carslaw, H. S., and J. C. Jaeger, *Conduction of Heat in Solids*, 2nd Edition, Clarendon Press (1959). TIC:206085
- Engesgaard, P., "Geochemical Modelling of Contaminant Transport in Groundwater," Ph.D. Thesis, Technical University of Denmark, 65-67 (1991). TIC:254776
- Faust, C. R., and J. W. Mercer, "An Analysis of Finite-Difference and Finite-Element Techniques for Geothermal Reservoir Simulation," Society of Petroleum Engineers of AIME, SPE 5742 (1976). TIC:254777
- Gelhar, L.W., *Perspectives on Field-Scale Application of Stochastic Subsurface Hydrology. Subsurface Flow and Transport: A Stochastic Approach*, Dagan, G., and Neuman, S.P., eds., 157-176, Cambridge University Press, New York, New York (1997). TIC:247805
- Golder Associates, "User's Guide GoldSim Graphical Simulation Environment", Version 7.40, Golder Associates Inc., Redmond, Washington (2002). MOL.20030130.0347, TIC:235624
- Harr, L., J. Gallagher, and G. S. Kell, *NBS/NRC Steam Tables, Thermodynamics, and Transport Properties and Computer Programs for Vapor and Liquid States of Water*, Hemisphere Press (1984). TIC:241793
- Ho, C. K., "Assessing Alternative Conceptual Models of Fracture Flow," in *Proceedings of the TOUGH Workshop '95*, Lawrence Berkeley Laboratory, Berkeley, CA, March 20-22 (1995). MOL.19960610.0017, TIC:216504
- Leij, F. J., T. H. Skaggs, and M. T. van Genuchten, "Analytical Solutions for Solute Transport in Three-Dimensional Semi-Infinite Porous Media," *Water Resources Research*, **27** (10), 2719-2733. Washington, D.C.: American Geophysical Union (1991). TIC:238367
- Lichtner, P. C., S. Kelkar, and B. Robinson, "New Form of Dispersion Tensor for Axisymmetric Porous Media with Implementation in Particle Tracking," *Water Resources Research*, **38**, (8), 21-1 to 21-16. Washington, D.C.: American Geophysical Union (2002). 163821, TIC:254597
- Matthews, C. S., and D. G. Russell, *Pressure Buildup and Flow Tests in Wells*, Society of Petroleum Engineers of AIME, 10-11 (1967). NNA.19890713.0201
- Moench, A. F., "Double-Porosity Models for a Fissured Groundwater Reservoir with Fracture Skin," *Water Resources Research* **20**, 831-846 (1984). HQS.19880517.2762
- Molloy, M. W., "Geothermal Reservoir Engineering Code Comparison Project," *Proceedings Special Panel on Geothermal Model Intercomparison Study at the Sixth Workshop on Geothermal Reservoir Engineering*, Stanford University (1980). TIC:249211
- Nilson, R. H., E. W. Peterson, K. H. Lie, N. R. Burkgard, and J. R. Hears, "Atmospheric Pumping; a Mechanism Causing Vertical Transport of Contaminated Gases through Fractured Permeable Media," *H. Geophys. Res.* **96** (B13), 21933-21948 (1991). TIC:234195

Pritchett, J. W., "The DOE Code Comparison Study: Summary of Results for Problem 5," *Sixth Workshop on Geothermal Reservoir Engineering*, Stanford University (1980). TIC:249211

Pruess, K., "TOUGH2 A General Purpose Numerical Simulator for Multiphase Fluid and Heat Flow," Lawrence Berkeley Laboratories, LBL-29400 (1991). NNA.19940202.0088

Ramey, H. J., "Wellbore Heat Transmission," *JPT*, 427-435 (April 1962). TIC254773

Robinson, B., "The SORBEQ Application," Los Alamos documents SORBEQ SRS, SORBEQ MMS, SORBEQ VVP, SORBEQ VVR, ECD-20 (1993). MOL.19980116.0400

Shan, C., R. W. Falta, and I. Javandel, "Analytical Solutions of Steady State Gas Flow to a Soil Vapor Extraction Well in the Unsaturated Zone," *Water Resources Research* **28** (4), 1105-1120 (1992). TIC:254767

Software Installation Test Plan for the FEHM Application Version 2.21, 10086-ITP-2.21-00.

Software Requirements Document for the FEHM Application Version 2.21, 10086-RD-2.21-00.

Stauffer, P., Auer, L.H., Rosenberg, N.D., Compressible gas in porous media: a finite amplitude analysis of natural convection, *Int. J. Heat Mass Transfer* **40**(7), 1585-1589 (1997). TIC:231352

Tang, D. H., E. O. Frind, and E. A. Sudicky, "Contaminant Transport in Fractured Porous Media: An Analytical Solution for a Single Fracture," *Water Resources Research* **17**(3), 555-564 (1981). NNA.19900711.0084

Theis, C. V., "The Relation Between the Lowering of the Piezometric Surface and the Rate and Duration of the Discharge of a Well using Ground-Water Storage," *EOS Trans. AGU* **16**, 519-524 (1935). TIC:223158

Thomas, L. K., and R. G. Pierson, "Three Dimensional Reservoir Simulation," *SPEJ* **18**, 151-161 (1978). NNA.19910806.0013

Toronyi, R. M., and S. M. Farouq Ali, "Two-Phase Two-Dimensional Simulation of a Geothermal Reservoir and Wellbore System," *SPEJ* **17**, 171-183 (1977). NNA.19910806.0014

Travis, B. J., and K. H. Birdsell, "TRACRN 1.0: A Model of Flow and Transport in Porous Media for the Yucca Mountains Project -- Model Description and Users Manual," LA-UR-88-3986 (Nov. 1988). TIC:236523

van Genuchten, M. T. 1985. "Convective-Dispersive Transport of Solutes Involved in Sequential First-Order Decay Reactions," *Computers in Geosciences* **11** (2), 129-147, Pergamon Press, New York, New York (1985). TIC:245188

Valocchi, A. J., and D.E. Pastor, "PDREACT, Version 1.1, Description and User's Guide," Dept. of CE, University of Illinois, DRAFT (May 1994). TIC:254784

Walsh, M. P., S. L. Bryant, R. S. Schechter, and L. W. Lake, "Precipitation and Dissolution of Solids Attending Flow Through Porous Media," *Amer. Inst. Chem. Engng. J.* **30**, 317-328 (1984). TIC:224164

Warren, J. E., and P. J. Root, "The Behavior of Naturally Fractured Reservoirs," *SPEJ* **3**, 245-255 (1963). TIC:233671

Weeks, E. P., "Field Determination of Vertical Permeability to Air in the Unsaturated Zone," U. S. Geol. Surv., Prof. Pap. No. 1051 (1978). TIC:218986

Wilson, M. L., ed., "Total-System Performance Assessment for Yucca Mountain - SNL Second Iteration (TSPA-1993)," Sandia National Laboratories Report SAND93-2675 (1994). TIC:102773

Zheng, C., "Analysis of Particle Tracking Errors Associated with Spatial Discretization", *Ground Water* **32** (5), 821- 828 (1994). TIC:226463

Zyvoloski, G. A., and Z. V. Dash, "Software Verification Report FEHMN Version 1.0," LA-UR-91-609 (1991). NNA.19910806.0018

Zyvoloski, G. A., Z. V. Dash, and S. M. Kelkar, "FEHMN 1.0: Finite Element Heat and Mass Transfer Code," LA-12062-MS, Rev. 1 (1992). NNA.19910625.0038

Zyvoloski, G. A., B. A. Robinson, and Z. V. Dash, *FEHM Application*, SC-194 (1999). MOL.19990810.0029

Zyvoloski, G. A., B. A. Robinson, Z. V. Dash, and L. L. Trease, "User's Manual for the FEHM Application - A Finite Element Heat- and Mass-Transfer Code," LA-13306-M (1997). TIC:235999

## APPENDIX: FEHM VALIDATION SCRIPTS

### A. Description of Scripts

A series of *cshell* scripts were developed to automate the validation operations for FEHM Version 1.0 (Zyvoloski, et al. 1997). For FEHM Version 2.0 they were updated to use the Perl programming language so they could be implemented on both UNIX/Linux and Windows platforms (see Table XXXI). A primary script, **FEHM V&V Script for Execution of Comparison Tests (FEHM\_VVSECT.pl)**, controls the FEHM verification runs then generates a comparison of results via supporting comparison test scripts (i.e. **compproblem.pl**) and a summary report. An execution log is generated when the primary script is run. A listing of the **FEHM\_VVSECT.pl** script for UNIX/Linux and an example of a specific run comparison script are given in Appendix Sections F and G. There are minor variations between the versions of the UNIX/Linux and Windows scripts (**FEHM\_VVSECT.pl**, **FEHM\_VVSECT\_PC.pl**) due to the need for auxiliary date programs on Windows, and differences in usage of system calls. The problem comparison scripts, however, are identical for both platforms. Subsidiary programs, **COMPARE**, **COMPARET**, **SUMMARIZE**, and others used for generating the numerical comparisons and summaries, are also described in Table XXXI.

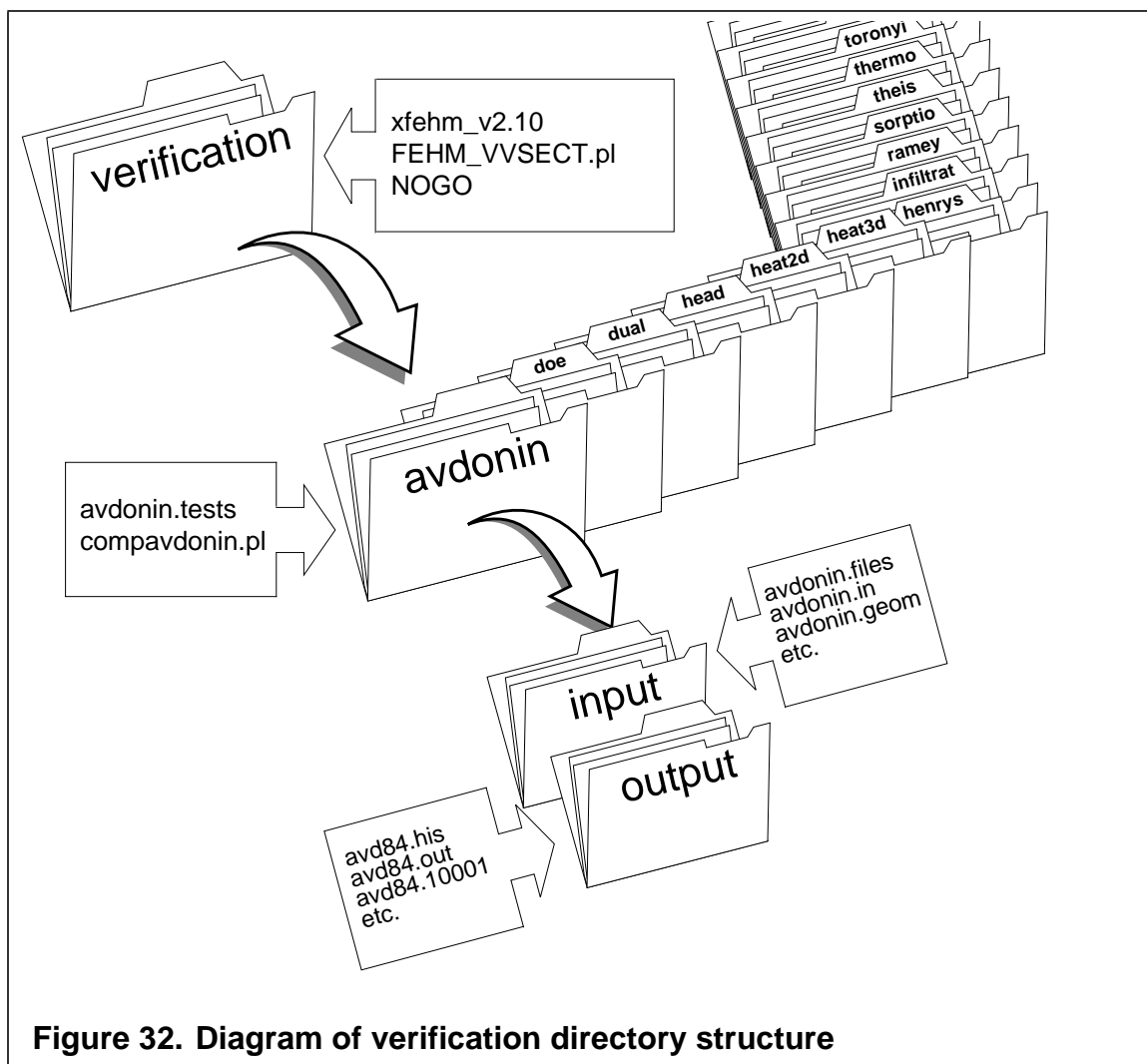
Table XXXI. Scripts and Support Programs for Verification Operations	
Script/Program Name	Description
FEHM_VVSECT.pl or FEHM_VVSECT_PC.pl	Executes all verification test problems and generates comparison of results and summary usage: <b>FEHM_VVSECT.pl [machine_descriptor]</b>
compproblem.pl	Problem specific script for <b>COMPARE</b> and <b>SUMMARIZE</b> input/output setup and execution usage: <b>compproblem.pl COMPARE SUMMARIZE date COMPARET</b>
COMPARE	Program that reads <b>FEHM</b> results and generates a numeric comparison with analytical or alternate code solutions.
COMPARET	Program that reads thermodynamic results and generates a numeric comparison with steam table data.
COMPSAT	Program that uses FEHM saturation function to generate saturation values for comparison with steam table data.
COMPOTHER	Program that uses FEHM thermodynamic routine to generate thermodynamic values (compressibility, density, enthalpy, viscosity) for comparison with steam table data.
SUMMARIZE	Program that reads results from <b>COMPARE</b> and <b>COMPARET</b> and outputs the results for related groups of tests in a single table.
DATESTRING	Generate a date string in yymmdd format for naming execution log and summary report files on Windows platforms.*
DATE_TIME	Generate the date and time for informational output to execution log on Windows platforms.*
* Note: For UNIX the builtin "date" function is used to generate these values.	



Table XXXI. Scripts and Support Programs for Verification Operations	
Script/Program Name	Description
BTC	Program used to post-processes “.trc” file to extract an in situ concentration profile from the streamline particle tracking simulation.
COMPARE_DIVFC	Program used to post-process “.spt1” files to compare particle positions for the fine and coarse grid tracks of the divergence of dispersion tensor problem.
COMPARE_FC	Program used to post-process “.spt1” files to compare particle positions for the fine and coarse grid tracks of the particle capture problem.
COMPARE_FR	Program used to post-process “.spt1” files to compare particle positions for the forward and reverse tracks of the reverse tracking problem.
flux_out.pl	Script used to post-process “.out” file to extract internode flux at steady state for the heat pipe problem.
massgen.pl	Script used to post-process “.out” file to extract mass fraction of solute remaining in the system from the barometric transport simulation.
MOMENTS2	Program used to post-process “.spt1” file to calculate first and second moments of x, y, z from the streamline particle tracking simulation using the generalized dispersion tensor.
PROCESS	Program used to post-process “.fin” file to extract a breakthrough concentration profile from the cellbased particle tracking simulation.
sppart.pl	Script used to post-process “.out” file to extract particles leaving zone from the decay-chain simulation.
VECTOR_MAG	Program used to post-process “_vec_node” file to compute volume flux magnitudes for the convection simulations.
water_budget.pl	Script used to post-process “.out” files to extract steady state water budget for the water table simulations.
WT	Program used to post-process AVS files to compute water table level for the water table simulations.

The problems are setup in a directory tree file structure. The root/verification directory contains the primary script (**FEHM\_VVSECT.pl**) with a subdirectory for each test problem. The execution log and summary report are written to the root directory (see Appendix Sections H and I for examples). Each problem directory contains the problem specific comparison (**compproblem.pl**) script, an input and output subdirectory, and other files as needed (Fig. 32).

The following problems are currently run by the **FEHM\_VVSECT.pl** script [the section numbers correspond to the problem and result descriptions found in the FEHM VTP (this document) and VTP Attachment 1: avdonin (2.11), barometric (2.9), cellbased (2.24), chain (2.24), convection (2.12), dissolution (2.20), divergence (2.23), doe (2.14), dryout (2.16), dual (2.10), fracture\_transport (2.19), head (2.4), heat2d (2.2), heat3d (2.2), heat\_pipe (2.15), henrys\_law (2.18), infiltration (2.7), mptr\_test (2.24), multi\_solute (2.21), particle\_capture (2.23), ramey (2.3), reverse\_tracking (2.23), sorption (2.17), streamline (2.23), tensor (2.23), theis (2.5), toronyi (2.13), thermodynamics (2.1), transferf (2.24), transport3D (2.22), vapor\_extraction (2.8), and



**Figure 32. Diagram of verification directory structure**

water\_table (2.6). As additional test problems are developed they will be incorporated into the test environment. The thermodynamics tests (2.1) are generally run independently since the functions need only be retested if the polynomial coefficients are modified. Also, any errors introduced to the routines containing the thermodynamic functions would result in errors in the other tests.

It should be noted that the barometric transport problem (2.9), cellbased particle tracking problems (2.24), convection problems (2.12), heat pipe problem (2.15), streamline particle tracking problems (2.23), and the water table problem (2.6) require post-processing of FEHM output for generation of data for comparisons. For the barometric transport problem this is done using the multiple simulations option of the code (thus providing a check for that option), while the post-processing for the other problems is executed from the problem comparison scripts.

## B. Installation

Instructions for installing FEHM and executing the installation test are provided in the Software Installation Test Plan for the FEHM Application Version 2.21 (FEHM ITP). The following describes only the verification test environment.

Files needed to setup the verification environment are contained in a tar file called VERIFICATION.tar for UNIX/Linux, and in a Winzip archive called VERIFICATION.zip for Windows\*. See Appendix Section J for a listing of files in the archive. A directory should be created and the files installed there, i.e. for UNIX,

```
% mkdir VERIFICATION
```

```
% cd VERIFICATION
```

```
% tar xvf Installation_directory/VERIFICATION.tar
```

where *Installation\_directory* is the location of the VERIFICATION.tar file. Auxiliary programs (COMPARE and SUMMARIZE), are also installed in this directory, but may be moved/installed elsewhere if desired.

On Windows the Winzip archive will automatically extract the files into FEHM\Verification and the auxiliary programs (COMPARE, SUMMARIZE, DATESTRING and DATE\_TIME) into FEHM\bin on the specified drive, i.e., C:. They may also be moved to different locations if desired.

\*Please check distribution media for exact names of archive files and executables. Version and/or platform identifiers are often included in the names to further identify the products and UNIX/Linux archives are often compressed to reduce size (i.e., VERIFICATION\_V2.21sun.tar.gz).

## C. Customization of Scripts for Local Environment

The primary script (Appendix Section F) requires customization for the local environment. Items to be customized are:

- Location and name of the FEHM executable (1);
- Name of the verification directory (2); and
- Locations and names of the auxiliary programs (4);

Optionally, the following may be modified so only a subset of the tests are run:

- List of test problems to be executed (3); and
- List of test problems to be checked and summarized (5).

Note that the referenced numbers [(1) - (5)] refer to the annotations on the **FEHM\_VVSECT.pl** script listing, and are used to identify the lines where the customizations should be made.

## D. Using the Validation Scripts

To run the verification tests the user should change to the verification directory. This directory should contain a subdirectory for each verification problem to be run and each problem subdirectory should contain an input and output subdirectory.

To run all verification test problems on UNIX/Linux use **FEHM\_VVSECT.pl**,

```
% ./FEHM_VVSECT.pl      -or-      perl FEHM_VVSECT.pl
```

(Note that the second form is used when “perl” is not installed in /usr/bin.)

or for Windows use **FEHM\_VVSECT\_PC.pl** from an MS\_DOS prompt,

```
C:\FEHM\Verification FEHM_VVSECT_PC.pl
```

Note that the operating system of the test platform is automatically determined via a system call during script execution and output to log and summary files. To further identify the environment in which the tests are being run a descriptor may be added to the command line when the script is invoked,

```
% ./FEHM_VVSECT.pl “Sun Ultra-2 (Fujitsu compiler)”
```

or

```
C:\FEHM\Verification FEHM_VVSECT_PC.pl Dell Pentium III
```

The descriptor may be quoted or not depending on characters included in the text string, and whether they have special meaning to the Perl interpreter.

The execution directory will contain a log of the runs and result comparisons in files called VERIFICATION.*date* and SUMMARY\_RPT.*date* where *date* is the date of execution in yymmdd format. (See Appendix Sections G and I for examples of these files.) It should be noted that if a log file or summary file with the current date or identifier already exists in the execution directory it will be renamed, i.e., VERIFICATION.*date*.old or SUMMARY\_RPT.*date*.old. If the backup files already exist, they will be overwritten.

To run selected problems instead of the complete test suite, the test problem list must be modified as noted above in Appendix Section C.

It should also be noted that during test script execution, problem identifiers are written to the terminal as the programs are executed. Any errors that result from program execution will be output to the screen, while script errors will be written to the log file.

## E. Assumptions and Limitations

The validation scripts were developed on a Sun-4 architecture and have been tested on Sun and PC Windows and Linux systems, but should also work on other standard UNIX workstations. The examples provided below were run on a Sun. The scripts require that Perl Version 5.\* be installed on the system where the tests are being executed. For more information on Perl and/or to obtain a copy visit [www.perl.com](http://www.perl.com).

Note that disk requirements for the complete test suite are approximately ~0.5 GB and when executed on a Sun Blade 1000 workstation with a 750 MHz processor run time was approximately ~3 hours.

**F. FEHM\_VVSECT.pl****FEHM\_VVSECT Script for UNIX Platform**

```

#!/usr/bin/perl -w
#   FEHM_VVSECT
#   FEHM V&V Script for Execution of Comparison Tests

# Define executable and file locations
(1) $XFEHM = "/home/fehm/bin/xfehm_v2.21";

# Verify that XFEHM is executable
(-x $XFEHM) || die "$XFEHM does not exist or is not an executable file.";

# Define file path
(2) $VER_DIR = "/home/fehm/FEHM_V2.21/VERIFICATION";
(-d $VER_DIR) || die "$VER_DIR is not a directory or does not exist.";
# Change into the verification directory to execute the tests
chdir $VER_DIR;

# Define system on which tests are being executed
$osname = `uname -s`;
chomp ($osname);
$osnum = `uname -r`;
$i = 0;
$ex_string = "Tests executed on ";
if ($ARGV[0]) {
    while ($ARGV[$i]) {
        $ex_string = $ex_string."$ARGV[$i] ";
        $i++;
    }
} else {
    $ex_string = $ex_string."system ";
}
$ex_string = $ex_string."running $osname $osnum";

# Get the date and open the log file, if an old file exists save it
$date = `date +%y%m%d`;
chomp ($date);
$logfile = "VERIFICATION.$date";

if (-e $logfile) {
    rename ("logfile", "$logfile.old") || die "Can't rename old log file";
}

open (LOGFILE, ">$logfile") || die "Cannot open the log file";

# Execute FEHM with no input to determine version being tested
system ("touch fehmn.dat; $XFEHM < NOGO > fehmn.version");
open (VERSION, "fehmn.version") || die "Cannot get program version";

```

**FEHM\_VVSECT Script for UNIX Platform (Continued)**

```

while (<VERSION>) {
  if (/version/) {
    ($dum, $dum, $prog, $num, $did) = split (/ +/);
    $version = "$prog $num $did";
    last;
  }
}
unlink <fehmn.*>;

$date_time = `date`;
print LOGFILE "$version: Verification started $date_time";
print LOGFILE "$ex_string\n";

```

```

# Define and Execute FEHM verification problems
# Note: If the initialization files for streamline need to be regenerated
# "streamline.init" should be included in the list below and streamline.files
# should be updated to reflect the location of the recomputed initialization files.

```

- (3) @problem = qw(avdonin baro\_trans baro\_vel cellbased.init cellbased chain convection dissolution div\_coarse div\_fine doe dryout dual forward reverse fracture\_transport gdpm heat2d heat3d heat3d.finv heat\_pipe henrys\_law infiltration multi\_solute particle\_capture ramey sorption streamline tensor theis toronyi transferf1 transferf2 transferf3 mptr\_test transport3D.init transport3D vapor\_extraction water\_table);

```

foreach $p (@problem) {
  $problem_dir = "$VER_DIR/$p";
  print LOGFILE "***** BEGIN $p *****\n";
  if (-d $problem_dir) {
    do_run();
  } else {
    print LOGFILE "Problem directory for $p does not exist\n";
  }
  print LOGFILE "***** END $p *****\n";
}

```

```

print LOGFILE "Checking Results for the FEHM Application Verification Runs\n\n";

```

```

# Run problem comparisons and summarize results
# Define verification executables

```

- (4) \$COMPARE = "/home/fehm/bin/COMPARE";  
\$COMPARET = "/home/fehm/bin/COMPARET";  
\$SUMMARIZE = "/home/fehm/bin/SUMMARIZE";

```

# Verify that verification executables exist / can be executed
(-x $COMPARE) || die "$COMPARE does not exist or is not an executable file.";
(-x $COMPARET) || die "$COMPARET does not exist or is not an executable file.";
(-x $SUMMARIZE) || die "$SUMMARIZE does not exist or is not an executable file.";

```

```

# Open the report file, if an old file exists save it
$rptfile = "SUMMARY_RPT.$date";

```

**FEHM\_VVSECT Script for UNIX Platform (Continued)**

```

if (-e $rptfile) {
    rename ("$rptfile", "$rptfile.old") || die "Can't rename old report file";
}

open (RPTFILE, ">$rptfile") || die "Cannot open the report file";
print RPTFILE "SUMMARY of COMPARISON TESTS for $version run $date\n";
print RPTFILE "-----\n\n";

#Note: barometric checks both velocity and transport cases
#Note: gdpm is included in fracture_transport for verification checks
#Note: heat3d.finv is included in heat3d for verification checks
#Note: reverse_tracking checks the forward and reverse streamline particle tracking
#Note: *.init runs are not checked as they only provide a background flow field

(5) @problem = qw(avdonin barometric cellbased transferf convection dissolution doe dryout dual
fracture_transport head heat2d heat3d heat_pipe henrys_law infiltration multi_solute ramey sorption
streamline tensor reverse_tracking particle_capture divergence theis thermodynamics toronyi
transport3D vapor_extraction water_table);
foreach $p (@problem) {
    $problem_dir = "$VER_DIR/$p";
    print LOGFILE "***** BEGIN $p CHECK *****\n";
    if (-d $problem_dir) {
        print RPTFILE "***** \U$p\E *****\n";
        do_check();
        do_summary();
    } else {
        print LOGFILE "Problem directory for $p does not exist\n";
    }
    print LOGFILE "***** END $p CHECK *****\n\n";
}
print RPTFILE "NOTE: $ex_string";

$date_time = `date`;
print LOGFILE "$version: Verification ended $date_time";

print "FEHM_VVSECT Completed\n";

sub do_run {
# If a multiple simulation file exists for this test
    if (-e "$problem_dir/input/$p.msim") {
        open (INLIST, "$problem_dir/input/$p.msim") || die "Can't open $p msim file" ;
        open(OUTLIST, ">$problem_dir/fehm.$p.msim") || die "Can't open output file" ;
        while (<INLIST>) {
            print OUTLIST $_;
        }
        close(INLIST) || die "Can't close input file list" ;
        close(OUTLIST) || die "Can't close output file" ;
    }
# If there is more than one test case for this problem
    if (-e "$problem_dir/$p.tests") {
        multi_test();
    } else {

```

**FEHM\_VVSECT Script for UNIX Platform (Continued)**

```
# There is a single test case for this problem
    one_test();
}

sub one_test {
    chdir $problem_dir;
    open (INLIST, "$problem_dir/input/$p.files") || die "Can't open $p file list" ;
    open(OUTLIST, ">fehm.files") || die "Can't open output file" ;
    print LOGFILE "\tRunning $p problem\n";
    while (<INLIST>) {
        print OUTLIST $_;
    }
    close(INLIST) || die "Can't close input file list" ;
    close(OUTLIST) || die "Can't close output file" ;

    system("$XFEHM");
    unlink <fehm.*>;
    chdir $VER_DIR;
}

sub multi_test {
    open (VARS, "$problem_dir/$p.tests") || die "Can't open test configuration file";
    @vars = <VARS>;
    chomp (@vars);
    $i = 3;
    chdir $problem_dir;
    while ($vars[$i]) {
        open (INLIST, "$problem_dir/input/$p.files") || die "Can't open $p file list" ;
        open(OUTLIST, ">fehm.files") || die "Can't open output file" ;
        print LOGFILE "\tRunning $vars[0] problem: $vars[$i]\n";
        while (<INLIST>) {
            s/$vars[2]/$vars[$i]/;
            print OUTLIST $_;
        }
        $i++;
        close(INLIST) || die "Can't close input file list" ;
        close(OUTLIST) || die "Can't close output file" ;
        system("$XFEHM");
    }
    unlink <fehm.*>;
    chdir $VER_DIR;
}

sub do_check {
    print LOGFILE "\tVerifying $p results\n";
    chdir $problem_dir;
    system("perl comp$p.pl $COMPARE $$SUMMARIZE $date");
}
```



**FEHM\_VVSECT Script for UNIX Platform (Continued)**

```
sub do_summary {  
    $sumfile = "$problem_dir/summary.$date";  
    if (-e $sumfile) {  
        open (SUMFILE, "$sumfile") || print RPTFILE "\tUnable to open $p summary file\n";  
        while (<SUMFILE>) {  
            print RPTFILE $_;  
        }  
    } else {  
        print RPTFILE "\tUnable to summarize $p results\n";  
    }  
}
```

## G. Example of Run Comparison Script

### compavdonin.pl Script

```
#!/usr/bin/perl -w
# Comparisons for avdonin problem

$COMPARE = $ARGV[0];
$SUMMARIZE = $ARGV[1];
$date = $ARGV[2];

(-x $COMPARE) || die "$COMPARE does not exist or is not an executable file." ;
(-x $SUMMARIZE) || die "$SUMMARIZE does not exist or is not an executable file." ;

$sumfile = "summary.$date";
if (-e $sumfile) {
    rename ("$sumfile", "$sumfile.old") || die "Can't rename old summary file" ;
}

@type = qw(history contour);
@geom = (84, 400, 800);

foreach $t (@type) {
    foreach $g (@geom) {
        open (INFILE, "input/avdonin.comparein.$t") || die "Can't open avdonin.comparein.$t" ;
        open (OUTFILE, ">comparein") || die "Can't open comparein" ;
        while (<INFILE>) {
            s/base/$g/;
            print OUTFILE $_;
        }
        close (INFILE) || die "Can't close input file" ;
        close (OUTFILE) || die "Can't close output file" ;
        system("$COMPARE");
    }
    open (INFILE, "input/avdonin.summary") || die "Can't open avdonin.summary" ;
    open (OUTFILE, ">summarize") || die "Can't open summarize" ;
    if ($t eq "history") {
        $param = "time";
    } else {
        $param = "pos";
    }
    while (<INFILE>) {
        s/param/$param/;
        print OUTFILE $_;
    }
    close (INFILE) || die "Can't close input file" ;
    close (OUTFILE) || die "Can't close output file" ;
    system("$SUMMARIZE >> summary.$date");
}
unlink <comparein*>;
unlink <"summarize">;
```

## H. Execution Log

### Example of Execution Log

FEHM V2.21sun 03-08-12: Verification started Tue Aug 12 12:30:34 MDT 2003  
Tests executed on system running SunOS 5.9

```
***** BEGIN avdonin *****
Running avdonin problem: 84
Running avdonin problem: 400
Running avdonin problem: 800
***** END avdonin *****
```

```
***** BEGIN baro_trans *****
Running baro_trans problem
***** END baro_trans *****
```

- 
- 
- 

```
***** BEGIN water_table *****
Running water_table problem: uz
Running water_table problem: wtsi
***** END water_table *****
```

Checking Results for the FEHM Application Verification Runs

```
***** BEGIN avdonin CHECK *****
Verifying avdonin results
***** END avdonin CHECK *****
```

```
***** BEGIN barometric CHECK *****
Verifying barometric results
***** END barometric CHECK *****
```

- 
- 
- 

```
***** BEGIN water_table CHECK *****
Verifying water_table results
***** END water_table CHECK *****
```

FEHM V2.21sun 03-08-12: Verification ended Tue Aug 12 15:10:59 MDT 2003

## **I. Summary Report**

**Example of Summary Report**

SUMMARY of COMPARISON TESTS for FEHM V2.21sun 03-08-12 run 030812

## \*\*\*\*\* AVDONIN \*\*\*\*\*

Avdonin Radial Heat and Mass Transfer Problem

Comparison of Model and Analytical Solution for Temperature vs Time

At R coordinate (m) 37.5000

Test Case	Maximum Error	Maximum % Error	RMS Error
84 nodes	1.2560	0.7744	2.162E-04
400 nodes	0.4036	0.2470	6.951E-05
800 nodes	0.3892	0.2380	6.744E-05

Avdonin Radial Heat and Mass Transfer Problem

Comparison of Model and Analytical Solution for Temperature vs Position

At Time 0.100000E+10

Test Case	Maximum Error	Maximum % Error	RMS Error
84 nodes	0.5233	0.3239	1.746E-04
400 nodes	0.2818	0.1745	3.417E-05
800 nodes	0.2819	0.1746	2.214E-05

## \*\*\*\*\* BAROMETRIC \*\*\*\*\*

Barometric Pumping Test - effects on pore-scale velocity

Comparison of Model and Analytical Solution for Velocity vs Depth during cycle

Test Case	Maximum Error	Maximum % Error	RMS Error
Time 1.75 days	3.215E-08	32.0900	7.023E-03
Time 3.5 days	1.677E-07	49.0200	3.685E-03
Time 5.25 days	1.738E-08	39.8200	4.340E-03
Time 7 days	1.750E-07	48.0100	3.552E-03

•

•

•

## \*\*\*\*\* WATER\_TABLE \*\*\*\*\*

Water Table Problem

Comparison of Water Table Position for UZ and WTSI Models

At Value 0.500000

Test Case	Maximum Error	Maximum % Error	RMS Error
Saturation 0.5	107.0000	24.9000	8.053E-03

Total Water in System (kg)

UZ Model	WTSI Model	Difference	% of UZ Total
1.801870e+09	1.808240e+09	-6.370000e+06	0.3535

NOTE: Tests executed on system running SunOS 5.9

**J. List of Files in the Verification Archive**

Note that files listed below are grouped by problem (see list in Appendix Section A).

COMPARE	chain.in	compare_divfc.in
COMPARET	chain.ini	cube_center_coarse.dat
DATESTRING (Windows)	chain.mptr	cube_center_coarse.ini
DATE_TIME (Windows)	CHAIN.out	cube_center_fine.dat
FEHM_VVSECT.pl (UNIX)	chain1.analyt	cube_center_fine.ini
FEHM_VVSECT_PC.pl (Windows)	chain2.analyt	div_coarse.files
NOGO	chain3.analyt	div_fine.files
SUMMARIZE	chain4.analyt	flow_pres.macro
empty.txt (Windows only)	compcellbased.pl	compdoe.pl
avdonin.comparein.contour	flow_field1.dat	doe.comparein.pressures
avdonin.comparein.history	flow_field2.dat	doe.comparein.temperatures
avdonin.files	flow_field3.dat	doe.dat
avdonin.geom.400	oned24.geom	doe.files
avdonin.geom.800	PROCESS	doe.in
avdonin.geom.84	process.dat	doe.summary
avdonin.in	sppart.pl	doe_code1.pressures
avdonin.summary	tang_ptrk1.analyt	doe_code1.temperatures
avdonin.tests	tang_ptrk2.analyt	doe_code2.pressures
avdoninout.analyt_pos	tang_ptrk3.analyt	doe_code2.temperatures
avdoninout.analyt_time	compconvection.pl	doe_code3.pressures
compavdonin.pl	convection.tests	doe_code3.temperatures
	conv2d_air.dat	doe_code4.pressures
auer_MFR.analyt	conv2d_air_check.10001_sca_head	doe_code4.temperatures
auer_vel.analyt	conv2d_air_check.10002_sca_node	doe_code5.pressures
baro.grid	conv2d_air_check.magni_sca_node	doe_code5.temperatures
baro_trans.files	conv2d_water.dat	doe_code6.pressures
baro_trans.msim	conv2d_water_check.10001_sca_head	doe_code6.temperatures
baro_trans0.in	conv2d_water_check.10002_sca_node	
baro_trans1.in	conv2d_water_check.magni_sca_node	compdryout.pl
baro_trans2.in	convection.comparein.magnitude	dryout.analyt2
baro_vel.files	convection.comparein.temperature	dryout.analyt3
baro_vel.in	convection.files	dryout.analyt4
barometric.comparein.contour	convection.summary	dryout.analyt5
barometric.comparein.mfr	vector.files	dryout.analyt6
barometric.files	VECTOR_MAG	dryout.comparein
barometric.summary		dryout.files
compbarometric.pl	compdissolution.pl	dryout.geom
massgen.pl	dissolution.analyt2	dryout.summary
	dissolution.analyt3	dryout.tests
cellbased.init.tests	dissolution.analyt4	dryout1.in
cellbased.tests	dissolution.comparein	dryout2.in
cellbased.comparein	dissolution.files	
cellbased.files	dissolution.grid	compdual.pl
cellbased.init.files	dissolution.in	dual.files
cellbased.summary	dissolution.summary	dual.geom
cellbased1.dat		dual.summary
cellbased2.dat	COMPARE_DIVFC	dual.tests
cellbased3.dat	compdivergence.pl	dual1.comparein
chain.comparein	100x100x10.geom	dual1.in
chain.files	100x100x10.stor	dual1_out.analyt
chain.geom	1331x100.geom	dual2.comparein

dual2.in  
 dual2\_out.analyt  
 dual3.comparein  
 dual3.in  
 dual3\_out.analyt  
 compfracture\_transport.pl  
 fracture\_transport.files  
 fracture\_transport.tests  
 gdpm.comparein  
 gdpm.files  
 gdpm.tests  
 gdpm1.in  
 gdpm1dgrid.geom  
 gdpm1dgrid.stor  
 gdpm2.in  
 tang1.analyt  
 tang1g.analyt  
 tang2.analyt  
 tang2g.analyt  
 tang3.analyt  
 tangtest.comparein  
 tangtest.geom  
 tangtest.summary  
 tangtest1.in  
 tangtest2.in  
 tangtest3.in  
 comphead.pl  
 head.comparein  
 head.dat  
 head.files  
 head.summary  
 head.tests  
 head3D.grid  
 headd.comparein  
 pres.dat  
 compheat2d.pl  
 heat2d.comparein.contour  
 heat2d.comparein.history  
 heat2d.files  
 heat2d.geom.2d\_mix  
 heat2d.geom.2d\_quad  
 heat2d.geom.2d\_ref  
 heat2d.geom.2d\_tri  
 heat2d.in  
 heat2d.summary  
 heat2d.tests  
 heat2din.analyt  
 heat2dout.analyt\_pos  
 heat2dout.analyt\_time  
 compheat3d.pl  
 heat3d.comparein.contour  
 heat3d.comparein.history

heat3d.files  
 heat3d.finv.files  
 heat3d.finv.in  
 heat3d.finv.tests  
 heat3d.geom.3d\_mix  
 heat3d.geom.3d\_quad  
 heat3d.geom.3d\_ref  
 heat3d.geom.3d\_tets  
 heat3d.geom.3d\_tri  
 heat3d.in  
 heat3d.summary  
 heat3d.tests  
 heat3din.analyt  
 heat3dout.analyt\_pos  
 heat3dout.analyt\_time  
 compheat\_pipe.pl  
 fdm.grid  
 fe.grid  
 fluxout.pl  
 heat\_pipe.comparein  
 heat\_pipe.files  
 heat\_pipe.summary  
 heat\_pipe.tests  
 heat\_pipe\_fdm.dat  
 heat\_pipe\_fe.dat  
 comphenrys\_law.pl  
 henry.geom  
 henry1.comparein  
 henry1.in  
 henry1\_out.analyt  
 henry2.comparein  
 henry2.in  
 henry2\_out.analyt  
 henrys.summary  
 henrys\_law.files  
 henrys\_law.tests  
 compinfiltration.pl  
 infiltration.comparein.dpm  
 infiltration.comparein.ecm  
 infiltration.dpm.in  
 infiltration.ecm.in  
 infiltration.files  
 infiltration.geom  
 infiltration.summary  
 infiltration.tests  
 infiltration.tough2.ecm  
 infiltration.tough2.fracture  
 infiltration.tough2.matrix  
 fehm\_amr\_base.dpd  
 fehm\_amr\_base.rock  
 fehm\_test\_mptr.dat  
 fehm\_test\_mptr.mptr

fehmn.grid  
 fehmn.stor.gz  
 fehmn.zone  
 fehmn.zone2  
 glaqma.ini.gz  
 mptr\_test.files  
 mptr\_test.msim  
 uz\_la\_tfcures.in.gz  
 compmulti\_solute.pl  
 multi.pdreact\_CoEDTA\_aq.out  
 multi.pdreact\_CoEDTA\_s.out  
 multi.pdreact\_Co\_aq.out  
 multi.pdreact\_Co\_s.out  
 multi.pdreact\_EDTA\_aq.out  
 multi.pdreact\_FeEDTA\_aq.out  
 multi.pdreact\_FeEDTA\_s.out  
 multi.pdreact\_Fe\_aq.out  
 multi\_solute.comparein  
 multi\_solute.files  
 multi\_solute.in  
 multi\_solute.summary  
 COMPARE\_FC  
 compparticle\_capture.pl  
 particle\_capture.tests  
 compare\_fine\_coarse.in  
 particle\_capture.files  
 zheng1.dat  
 zheng1.flow.ini  
 zheng1.geom  
 zheng2.dat  
 zheng2.flow.ini  
 zheng2.geom  
 compramey.pl  
 ramey.comparein.contour  
 ramey.comparein.history  
 ramey.files  
 ramey.geom  
 ramey.in  
 ramey.summary  
 rameyout.analyt\_pos  
 rameyout.analyt\_time  
 compsorption.pl  
 sorbeq\_out.cons  
 sorbeq\_out.fr  
 sorbeq\_out.lang  
 sorbeq\_out.lin  
 sorbeq\_out.mfr  
 sorption.comparein  
 sorption.files  
 sorption.in  
 sorption.summary

COMPARE\_FR  
compreverse\_tracking.pl  
compare\_forward\_revers.in  
forward-reverse.geom  
forward.dat  
forward.files  
forward.stor  
freverse.dat  
reverse.files  
right\_constant.boun  
top.boun

BTC  
btc\_plume1\_10000.files  
btc\_plume1\_4800.files  
btc\_plume2\_10000.files  
btc\_plume2\_4800.files  
compstreamline.pl  
plume.comparein  
plume1.dat  
plume10000.analyt  
plume2.dat  
plume4800.analyt  
sptr.geom  
sptr1.analyt  
sptr2.analyt  
sptr3.analyt  
sptr\_longd1.dat  
sptr\_longd2.dat  
sptr\_longd3.dat  
streamline.comparein  
streamline.files  
streamline.init.files  
streamline.summary  
streamline.tests  
valid1.dat  
valid1.ini  
valid1.stor

comptensor.pl  
MOMENTS2  
tensor.files  
tensor.geom  
tensor.pl  
tensor.tests  
tensorx.dat  
tensorxz1.dat  
tensorxz2.dat

comptheis.pl  
theis.comparein.contour  
theis.comparein.history  
theis.files  
theis.in  
theis.summary  
theisout.analyt\_pos  
theisout.analyt\_time

comptoronyi.pl  
toronyi.comparein  
toronyi.files  
toronyi.in  
toronyi.saturation

COMPSAT  
COMPETHER  
compthermodynamics.pl  
thermo.comparein.compress  
thermo.comparein.press  
thermo.comparein.temp  
thermo.compress\_data.liq  
thermo.compress\_data.vap  
thermo.saturation\_data  
thermo.steam\_table\_data.liq  
thermo.steam\_table\_data.vap  
thermodynamics.comparein  
thermodynamics.summary

1d\_dkm.grid  
1d\_dkm.stor  
1d\_dkm2.grid  
1d\_dkm2.stor  
comptransferf.pl  
dkmf1t1.dat  
dkmf1t1free.dat  
dkmf1t1freesvd.dat  
dkmf1t2.dat  
dkmf2t1.dat  
dkmf3t1.dat  
f1t1.ptrk  
f1t1free.ptrk  
f1t1freesvd.ptrk  
f1t2.ptrk  
f2t1reg.ptrk  
f3t1free.ptrk  
flow1.ini  
flow2.ini

flow3.ini  
pfraction3.dat  
pfraction\_free.dat  
pfraction\_freesvd.dat  
transferf1.files  
transferf1.tests  
transferf2.files  
transferf2.msim  
transferf3.files  
transferf3.msim  
uz\_la\_tfcurves.in.gz

3d\_trac.comparein  
3d\_trac.dat  
3d\_trac.grid  
3d\_trac.init.dat  
3d\_trac.summary  
3d\_tracr3d\_am.out  
3d\_tracr3d\_cons.out  
comptransport3D.pl  
transport3D.files  
transport3D.init.files

compvapor\_extraction.pl  
vapextract.comparein  
vapextract.geom  
vapextract.summary  
vapextract\_aniso.in  
vapextract\_iso.in  
vapextractout\_aniso.analyt  
vapextractout\_iso.analyt  
vapor\_extraction.files  
vapor\_extraction.tests

2d\_heter\_uz.dat  
2d\_heter\_wtsi.dat  
compwater\_table.pl  
fdm\_2d\_heter\_100\_17.grid  
water\_budget.pl  
water\_table.comparein  
water\_table.files  
water\_table.summary  
water\_table.tests  
WT  
wt.in